



DEGREE PROJECT IN ELECTRICAL ENGINEERING,  
SECOND CYCLE, 30 CREDITS  
*STOCKHOLM, SWEDEN 2020*

# **Multi-resolution encoding and optimization for next generation video compression**

**VIGNESH V MENON**

arXiv:2301.12191v1 [cs.MM] 28 Jan 2023



# **Multi-resolution encoding and optimization for next generation video compression**

VIGNESH V MENON

MSc Information and Network Engineering

Date: October 16, 2020

Supervisor: Jonatan Samuelsson

Examiner: Markus Flierl

School of Electrical Engineering and Computer Science

Host company: Divideon AB

Swedish title: Kodning och optimering med flera upplösningar för nästa generations videokomprimering



## Abstract

Multi-encoding implies encoding the same content in multiple spatial resolutions and multiple bitrates. This work evaluates the encoder analysis correlations across 2160p, 1080p, and 540p encodings of the same video for conventional ABR bitrates. A multi-resolution tier multi-ABR encoding scheme is modeled and evaluated, which significantly improves the computational efficiency of conventional ABR encoding. Video content is first encoded at the lower resolution with the associated median bitrate, and encoder analysis decisions, such as motion vectors and CU block structure, are then used in the other encodes in the same resolution tier. The analysis is then extrapolated and refined to be used in higher-resolution encodes. The scheme is validated using x265 HEVC video encoder. The proposed multi-resolution tier multi-bitrate encoding scheme achieves overall speed-ups of up to 2.5x, compared to the conventional single-instance encoding approach. Furthermore, this speed-up is achieved without substantial losses in coding efficiency.

SIMD Vector units in CPUs have become the de-facto standard for accelerating media and other kernels that exhibit parallelism. This work also demonstrates the impact of hardware-aware optimizations on the encoding speeds of the next-generation video codecs. The work is evaluated using the Arowana XVC encoder.

## Sammanfattning

Att komprimera samma videosekvens i olika upplösningar och vid olika bithastighet kan kallas "multi-encoding". Denna uppsats utvärderar komprimeringsanalys vid upplösning 2160p, 1080p och 540p av samma videosekvens med bithastighet anpassad för adaptiv videoströmning. En komprimeringsmetod med tre nivåer som ger en signifikant förbättring i beräkningsprestanda har modellerats och utvärderats. Videosekvenserna komprimeras först vid lägsta upplösningen och kodningsval såsom rörelsevektorer och blockstruktur används sedan vid komprimering i samma upplösning och även i högre upplösning genom extrapolation. Modellen har validerats genom att använda x265 HEVC-kodaren. Den föreslagna modellen med tre nivåer ger en sammanlagd uppsnabbning om 2.5x i genomsnitt, jämfört med konventionell komprimering. Uppsnabbningen åstadkoms utan substantiell förlust i kodningseffektivitet.

Moderna processorers SIMD instruktioner har blivit de-facto standard för acceleration av mediaprocessering och liknande beräkningar som kan utnyttja parallelism. Denna uppsats påvisar också effekten av hårdvaruoptimering för uppsnabbning av nästa generations video codecs. Arbetet är utfört i videokodaren Arowana XVC.

# Contents

<b>1</b>	<b>Introduction</b>	<b>2</b>
1.1	Introduction to video compression . . . . .	2
1.2	Introduction to Single Instruction Multiple Data . . . . .	3
1.3	Report Structure . . . . .	4
<b>2</b>	<b>HEVC Adaptive Bitrate Streaming</b>	<b>6</b>
2.1	HEVC Background . . . . .	6
2.2	x265 Background . . . . .	8
2.3	ABR Streaming Background . . . . .	8
2.4	Related Work . . . . .	11
<b>3</b>	<b>XVC and Intel SIMD Background</b>	<b>13</b>
3.1	XVC video codec . . . . .	13
3.2	Single Instruction Multiple Data extension . . . . .	14
3.2.1	Intel Streaming SIMD Extensions 4 . . . . .	15
3.2.2	Intel Advanced Vector Extensions 2 . . . . .	15
3.3	Related Work . . . . .	16
<b>4</b>	<b>Analysis Sharing Methods in x265</b>	<b>17</b>
4.1	Testing method . . . . .	17
4.2	Intra resolution analysis sharing in x265 . . . . .	19
4.2.1	State of the art method . . . . .	19
4.2.2	Proposed method . . . . .	20
4.3	Inter-resolution analysis sharing in x265 . . . . .	21
<b>5</b>	<b>Intel SIMD optimization methods for XVC Encoding</b>	<b>24</b>
5.1	SIMD implementation methods . . . . .	24
5.2	NASM Assembler support . . . . .	25
5.3	Accelerating Arowana XVC Encoding with Intel SIMD . . . . .	25
5.4	Selecting the kernels to Accelerate . . . . .	25
5.4.1	Cost functions . . . . .	26
5.4.2	SIMD implementation of cost functions . . . . .	27
5.5	Method to evaluate cycle-count improvements . . . . .	32

<b>6</b>	<b>Results and Discussion</b>	<b>33</b>
6.1	State of the art Intra-resolution analysis sharing in x265 . . . . .	33
6.2	Proposed Intra resolution analysis sharing in x265 . . . . .	34
6.3	Inter-resolution analysis sharing in x265 . . . . .	36
6.4	State of the art multi-encoding scheme . . . . .	38
6.5	Proposed multi-encoding scheme . . . . .	38
6.6	Improvement in XVC encoding with SIMD optimization . . . . .	40
<b>7</b>	<b>Conclusions and Future Directions</b>	<b>42</b>
7.1	Conclusions . . . . .	42
7.2	Future Directions . . . . .	43
	<b>Bibliography</b>	<b>44</b>
<b>A</b>	<b>x265 CLI Options</b>	<b>47</b>
A.1	Preview of x265 encoder analysis share modes . . . . .	47
A.2	Preview of x265 encoder analysis refinement modes . . . . .	48
<b>B</b>	<b>SSE4 SIMD optimization</b>	<b>50</b>
<b>C</b>	<b>AVX2 SIMD optimization</b>	<b>58</b>

# List of Figures

2.1	HEVC Encoder block diagram [10] . . . . .	7
2.2	Context-Aware Encoding [5] . . . . .	11
2.3	Multi-rate implementation proposed in [16], [17] . . . . .	12
2.4	Multi-rate implementation proposed in [18] . . . . .	12
3.1	Performance benefit for x264 and x265 from Intel® Advanced Vector Extensions 2 for 1080p encoding with main profile using an Intel® Core™ i7-4500U Processor [28] . . . . .	16
4.1	Intra resolution analysis sharing across $W \times H$ resolution encode for CQP representation with lowest QP as master representation . . . . .	19
4.2	Intra resolution analysis sharing across $W \times H$ resolution encode for CQP representation with median QP as master representation . . . . .	21
4.3	Average encode time for all representations in intra-resolution analysis sharing for 1080p videos . . . . .	22
4.4	Inter resolution analysis sharing for CQP representation . . . . .	23
5.1	Cycle-count gains of the Intel® Streaming SIMD Extensions 4 kernels over the corresponding C++ kernels . . . . .	26
5.2	Cycle-count gains of the Intel® Advanced Vector Extensions 2 kernels over the corresponding C++ kernels . . . . .	26
6.1	Intra resolution analysis sharing across $W \times H$ resolution encode for ABR representation with the state of the art method ( $B_1 > B_2 > B_3 > B_4 > B_5$ ) . . . . .	33
6.2	Intra resolution analysis sharing across $W \times H$ resolution encode for ABR representation with the proposed method ( $B_1 > B_2 > B_3 > B_4 > B_5$ ) . . . . .	34
6.3	Comparison of BD-Rate for cVBR stand-alone encoding for the state-of-the-art method and the proposed method . . . . .	35
6.4	Comparison of BD-PSNR for cVBR stand-alone encoding for the state-of-the-art method and the proposed method . . . . .	35
6.5	Inter resolution analysis sharing for ABR representation ( $B_1 > B_2 > B_3 > B_4 > B_5$ ) . . . . .	36
6.6	Comparison of BD-Rate for cVBR stand-alone encoding for inter-resolution with analysis refinement and without refinement . . . . .	37

6.7	Comparison of BD-PSNR for cVBR stand-alone encoding for inter-resolution with analysis refinement and without refinement . . . . .	38
6.8	Representation of the state-of-the-art encoder analysis sharing across the resolutions and bitrates . . . . .	39
6.9	Representation of the proposed encoder analysis sharing across the resolutions and bitrates . . . . .	39
6.10	XVC encoding speedup for CrowdRun video for Arowana XVC presets (GOP length=2 seconds) . . . . .	40
6.11	XVC encoding speedup for BasketballDrive video for Arowana XVC presets (GOP length=2 seconds) . . . . .	41
6.12	XVC encoding speedup for DucksTakeOff video for Arowana XVC presets (GOP length=2 seconds) . . . . .	41

# List of Tables

2.1	Fixed Bitrate Encoding ladder proposed by Apple in Apple Tech Note TN2224 [5] . . . . .	9
2.2	Per-Title Encoding proposed by Netflix [5] . . . . .	10
3.1	SIMD extensions to general purpose processors [24] . . . . .	15
4.1	Videos used to validate the methods used . . . . .	17
4.2	QP considered for CQP mode test for various resolutions . . . . .	18
4.3	cVBR bitrates considered for various resolutions . . . . .	18
4.4	System configurations for Testing . . . . .	19
4.5	Measure of speedup and compression efficiency for intra-resolution analysis sharing with lowest QP (highest quality) representation as master encode	20
4.6	Measure of speedup and compression efficiency for intra-resolution analysis sharing with median QP representation as master encode . . . . .	21
4.7	Average improvement of BD-Rate for intra-resolution analysis sharing with median quality representation as master encode . . . . .	22
4.8	Measure of speedup and BD-Rate for 1080p inter-resolution analysis sharing with 540p representation as the master encode and analysis reuse level 10 . . . . .	22
5.1	Speedups of SAD kernels with SSE4 and AVX2 optimizations . . . . .	28
5.2	Speedups of SATD kernels with SSE4 and AVX2 optimizations . . . . .	32
6.1	Measure of speedup and BD-Rate for ABR intra resolution analysis sharing with the state-of-the-art method . . . . .	34
6.2	Measure of speedup and BD-Rate for ABR intra resolution analysis sharing with the proposed method . . . . .	35
6.3	Measure of speedup and BD-Rate for 1080p and 2160p ABR inter-resolution analysis sharing with 540p median bitrate representation and 1080p median bitrate representation as master encode respectively . . . . .	36
6.4	Measure of speedup and BD-Rate for 1080p and 2160p ABR inter-resolution analysis sharing with refinement with 540p median bitrate representation and 1080p median bitrate representation as master encode respectively . .	37

A.1	x265 analysis reuse levels and their respective descriptions [29] . . . . .	47
A.2	Intra refinement techniques in x265 [29] . . . . .	48
A.3	Inter refinement techniques in x265 [29] . . . . .	49
A.4	Motion vector refinement techniques in x265 [29] . . . . .	49

# List of abbreviations

**AAC** Advanced Audio Coding

**ABR** Adaptive bitrate

**AMP** Advanced Motion Prediction

**AVC** Advanced Video Coding

**AVX** Advanced Vector Extensions

**AVX2** Advanced Vector Extensions 2

**AVX512** Advanced Vector Extensions 512

**BD-PSNR** Bjøntegaard Delta Peak Signal to Noise Ratio

**BD-Rate** Bjøntegaard Delta Rate

**CABAC** Context-Adaptive Binary Arithmetic Coding

**CB** Coding Block

**CPU** Central Processing Unit

**CQP** Constant Quantization Parameter

**CTB** Coding Tree Block

**CTU** Coding Tree Unit

**CU** Coding Unit

**cVBR** Capped Variable Bitrate

**DVD** Digital Versatile Disc

**FMA** Fused Multiply-Accumulate

**HDR** High Dynamic Range

**HEVC** High Efficiency Video Coding

**HTTP** Hypertext Transfer Protocol

**IEC** International Electrotechnical Commission

**ISA** Instruction Set Architecture

**ISO** International Organization for Standardization

**ITU-T** International Telecommunication Union- Telecommunications standardization

**JCTVC** Joint Collaborative Team on Video Coding

**JVET** Joint Video Exploratory Team

**MPEG** Moving Picture Experts Group

**MV** Motion Vector

**PU** Prediction Unit

**QP** Quantization Parameter

**R-D** Rate-Distortion

**RDO** Rate-Distortion Optimization

**RQT** Residual QuadTree

**SIMD** Single Instruction Multiple Data

**SSE** Streaming SIMD Extensions

**SSE2** Streaming SIMD Extensions 2

**SSE4** Streaming SIMD Extensions 4

**SSSE3** Supplemental Streaming SIMD Extensions 3

**TB** Transform Block

**UHD** Ultra High Definition

**VCEG** Video Coding Experts Group

**VOD** Video On Demand

# Acknowledgements

I am deeply indebted to my supervisor **Mr. Jonatan Samuelsson**, CEO, Divideon, and my examiner **Dr. Markus Flierl**, Electrical Engineering and Computer Science, KTH Royal Institute of Technology, Sweden, for their continual support, ardent motivation, and enduring guidance throughout my project tenure.

I further extend my gratitude to Dr. Sundararaman Gopalan, Mrs. Gayathri N, Department of Electronics and Communication, Amrita School of Engineering Amritapuri Campus, India, my close friends who had worked with me closely in MulticoreWare Inc namely Kalyan Goswami, Praveen Tiwari, Santhoshini Sekar, Bhavna Hariharan and Kavitha Sampath for their belief in me and helping me in growing my learning curve.

Finally, I express my gratefulness to my parents, my uncle Dr. Venugopalan P, my aunt Mrs. Jyothi PM, and my sister Aishwarya for their love, encouragement, and support. I also acknowledge the support and motivation of my three dear friends in Stockholm- Anubhab Ghosh, Prajit T Rajendran and Shreya K Chari.

# Chapter 1

## Introduction

There is a tremendous increase in video content on streaming services over the last few years. The figure on the right shows the application-wise global internet traffic, where 62 % comprises video streaming. According to The Global Internet Phenomena Report from Sandvine, video plays in March 2020 have doubled compared to the end of February 2020 during the COVID-19 pandemic [1]. Hundreds of millions of subscribers and transactional VOD users are part of the internet traffic. The amount of available live linear and on-demand assets in UHD [2] is significantly growing. E.g., more than 250 cinematic titles are now available from major studios in UHD HDR, and it is noteworthy that FIFA World Cup 2018 was streamed live in UHD HDR [3]. The situation calls for effective video compression schemes to reduce the global network load.



Global internet traffic.  
Source: Sandvine [1]

### 1.1 Introduction to video compression

Video encoding refers to the process of converting raw video into a digital format that's compatible with many devices. This is for compatibility and efficiency with a desired set of applications and hardware such as for DVD/Blu-ray, mobile, video streaming, or general video editing. The encoding process transforms the video and audio data into a file and compresses according to the chosen encoding standard's specifications.

To shrink a video into a more manageable size, content distributors use a video compression technology called a *codec*. Codecs allow us to compress a bulky video for delivery and storage tightly. Codecs apply algorithms to the video and create a facsimile of it. The video is shrunk down for storage and transmission and later decompressed for viewing. Streaming employs both audio and video codecs. H.264, also known as AVC, is the most common video codec. AAC is the most common audio codec.

Once compressed, the components of a stream are packaged into a wrapper or file format. These files contain the audio codec, video codec, closed captioning, and associated metadata. Common containers include .mp4, .mov, .ts, and .wmv. Containers can often input multiple types of codecs. That said, not all playback platforms accept all containers and codecs. That's why multi-format encoding is crucial when streaming to many devices.

In current world of video compression, UHD and HDR content calls for using the HEVC video compression standard [4]. Other codecs are being developed to mitigate the royalty issues associated with HEVC- XVC codec is one of them. As the codecs developed for UHD video content comprises a significant amount of computations to achieve the desired compression efficiency, there is always scope for optimization of the encoding pipeline to achieve the best trade-off between computational speed, compression efficiency and visual quality.

On the other hand, the adaptive streaming approach [5] is nearly universally used over the last several years to reach heterogeneous devices on non-provisioned networks (such as the Internet). The key property of adaptive streaming from the standpoint of this project is that the same video content is made available to the player in different bitrates and resolutions (“bitrate ladder”). Encoding all steps of a bitrate ladder for 10-bit HEVC content requires a significant amount of computational resources – e.g. sub-1 frames per second (fps) encoding speeds are very common for high-quality offline encoding. Section 2.1 and Section 2.3 provide a more detailed introduction and background study to HEVC as well as to ABR streaming, respectively.

## 1.2 Introduction to Single Instruction Multiple Data

Over the years, tremendous advancements have been seen in computer architecture. This field also has a huge influence in the areas of video coding, especially in SIMD instructions deployment. The category of a parallel computer in Flynn's taxonomy constitutes SIMD. Computers that perform the same operation simultaneously on multiple data points are described here. They also have multiple processing elements. The development of software only MPEG-1 with general-purpose processors that can do real-time decoding is the reason for the introduction of SIMD extensions [6][7]. Adjustment of the volume of digital audio and contrast in a digital image are the common applications of SIMD extensions.

SIMD instructions are also utilized in modern CPU designs for enhancing multimedia use performance. Increasing the efficiency of video coding and standardization are other use cases of SIMD capabilities. This minimizes the effort in the elimination of sample dependencies and definition of computation precision.

ISAs, along with their micro-architectures, are getting more diversified in recent years. There is also an increase in complexity, like the inclusion of multiple instruction sets for SIMD ISAs. In addition, instructions have various performance features even after using the same ISA. Video codecs these days have the significant capability for the acceleration of SIMD, which intensifies the need for more investigation on the effect of these accelerations on video encoders. AVX512, which is the new SIMD extension released by Intel, are 512-bit extensions to the previous 256-bit Vector Extensions SIMD instructions for x86 ISA. AVX512 can accumulate eight 64-bit integers, eight double-precision, sixteen 32-bit integers, or sixteen single-precision floating point numbers within 512-bit vectors. This is around four times of SSE and twice the amount of data points AVX/ AVX2 can compute with one instruction.

This project aims to focus on the SIMD impact on video codec- XVC. The research tries to estimate the dependency of the complexity of the codec on the performance benefits achieved from SIMD extensions. The scope of research and analysis in this project is limited to Intel AVX2 SIMD and Intel SSE4 instructions, along with their potential benefits in the encoder speeds.

### 1.3 Report Structure

Chapter 2 gives brief insights on the background of HEVC ABR streaming. Section 2.1 gives details on the background of HEVC- its establishment as a leading video codec and some key technical details. Section 2.2 gives a brief background of x265, an open source HEVC encoder used in this work to evaluate the encoding approaches. Section 2.3 describes the ABR streaming terminology- its development and some key concepts. Section 2.4 mentions some of the previous works in the domain of this work, which are used in the literature study of this work.

Chapter 3 gives brief insights on the XVC video codec and Intel SIMD optimization. Section 3.1 discusses the background of XVC video codec, while Section 3.2 explains the background of SIMD extensions. Section 3.2.1 and Section 3.2.2 introduce Intel SSE4 and AVX2 SIMD extensions. Section 3.3 presents some of the literature referred to for this project.

Chapter 4 gives brief insights on the methods used in this project for multi-resolution and multi-rate analysis sharing in x265. Section 4.1 shows how the various methods considered in this project are tested. Section 4.2 explains the methods used in intra-resolution

analysis sharing where Section 4.2.1 details the state of the art method while Section 4.2.2 describes the proposed method. Section 4.3 shows the details of the method used in Inter resolution analysis sharing.

Chapter 5 presents the work carried out to understand the impact of SIMD parallelism in media processing. Section 5.1 shows various methods used for SIMD implementation and motivates the choice of the hand-written assembly method. Section 5.2 explains about NASM assembler used for compiling hand-written assembly code in this project. Section 5.3 shows the CPU cycle count improvements for kernels accelerated with Intel SSE4 and AVX2 SIMD. Section 5.4 mentions how the functions to be optimized are chosen, Section 5.4.1 and Section 5.4.2 describing the implementation of encoder cost functions and the resulting CPU cycle count improvements. Section 5.5 explains the method used to evaluate the CPU cycle count improvements for each optimized function.

Chapter 6 evaluates the methods described in Section 4 in the real time streaming scenarios. Section 6.1 shows the state-of-the-art intra-resolution analysis sharing method in cVBR mode and discusses the associated results. Section 6.2 discusses the proposed intra-resolution analysis sharing method in cVBR mode and its improvement over the state-of-the-art intra-resolution analysis sharing method. Section 6.3 explains the inter-resolution analysis sharing method in cVBR, the need for analysis refinement, and the associated results. Section 6.4 and Section 6.5 discuss state-of-the-art and the proposed multi-encoder structure with the scheme for encoder analysis sharing and the associated results, respectively. Section 6.6 discusses the improvements of the Arowana XVC encoding speeds utilizing the SIMD extensions.

Chapter 7 concludes the project report and summarises the key findings during the project. Section 7.1 discusses the conclusions and Section 7.2 discusses the future directions of this work which haven't been explored as part of this project respectively.

# Chapter 2

## HEVC Adaptive Bitrate Streaming

This chapter gives brief insights into the background of HEVC ABR streaming. Section 2.1 gives details on the background of HEVC- its establishment as a leading video codec and some key technical details. Section 2.2 gives a brief background of x265, an open source HEVC encoder used in this work to evaluate the encoding approaches. Section 2.3 describes the ABR streaming terminology- its development and some key concepts. Section 2.4 mentions some of the previous works in the domain of this work, which are used in the literature study of this work.

### 2.1 HEVC Background

HEVC was finally endorsed as an encoding standard as the successor of the hugely popular AVC standard by the JCTVC [4]. Its inception was carried out over 2.5 years, and the first version was finalized in 2013 [8]. The JCTVC was created originally by a collaboration of ITU-T VCEG and ISO IEC MPEG working on the HEVC standard. The final HEVC specification was approved as part of the Recommendation H.265 by ITU-T and as MPEG.H Part 2 by ISO IEC. The most recent version of HEVC in use is its 7th version [9]. HEVC development emphasized performing efficient encoding of high-resolution videos, which leads to a significant coding gain while encoding UHD (4K or 2160p resolution) videos [2]. This is accomplished in the HEVC standard by incorporating tools for increasing coding efficiency.

The basic processing units in HEVC are created by partitioning each video frame into square-shaped CTBs. CTBs come in varying sizes such as 16x16, 32x32 or 64x64. A more complex structure called CTU is created by combining the CTB with associated syntax elements: one luma and two corresponding chroma. By increasing the size of the CTU we can obtain a better coding efficiency at high resolutions at the cost of an increase in computational complexity. HEVC uses a hierarchical quad-tree partitioning structure which splits the CTU into one more of coding units or CUs of varying sizes between 8x8 and 64x64. In addition, it is also possible to subdivide the CUs into smaller blocks along

coding tree boundaries for intra-picture (spatial) and inter-picture (temporal motion compensated) predictions. If the candidate block is present in the same frame, it is termed intra-predicted, whereas if it is from a different frame, it is said to be inter-predicted. Intra-predicted blocks can be represented as a combination of a prediction block and a mode denoting the angle of prediction. The modes used in intra-prediction are DC, planar and angular modes. They represent various angles from the predicted block. On the other hand, inter-predicted blocks can be represented as a combination of the reference block (block used for prediction) and the MV, which represents the delta difference between the reference block and the current block. The block with a net zero MV uses the merge mode, and the others use the AMP mode. In the special case where there is no residual, ie. the predicted block is identical to the source, we use the skip mode- a special case of the merge mode. To provide the prediction data, a minimum of one PU is defined for each CU. The prediction mode selected indicates whether the CU (comprising of the CB, single luma, and two chroma) is coded in the intra-picture prediction mode or the inter-picture prediction mode. TBs can be formed by partitioning a CB in size varying from 4x4 to 32x32 to perform transform coding of the prediction residuals. Each CTB thus acts as a root node of the coding tree, and the coding block acts as the leaf of the coding tree. The coding block is a root of the transform or RQT.

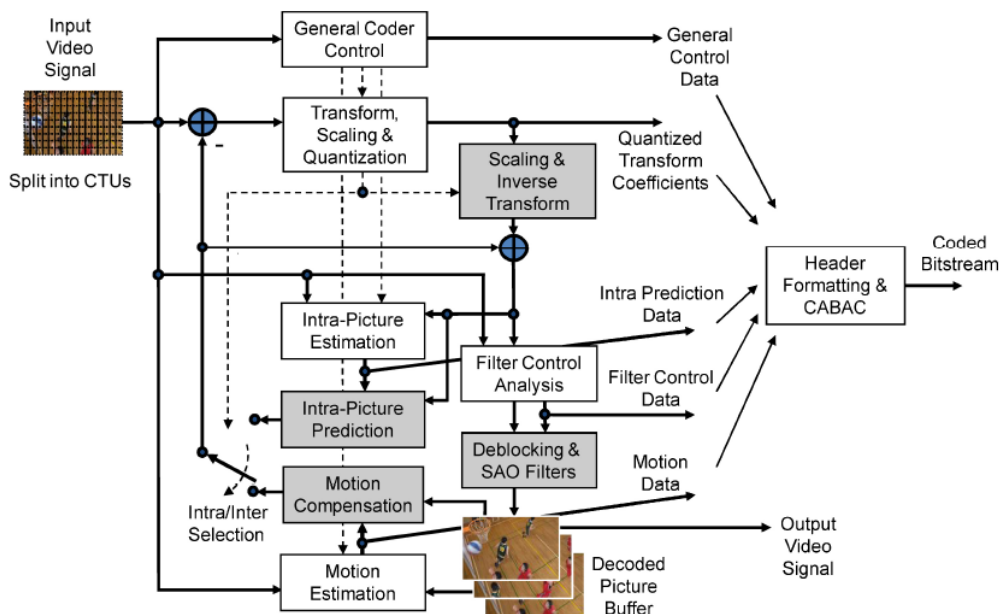


Figure 2.1: HEVC Encoder block diagram [10]

RDO [11] is used in intra or inter-picture prediction, including the quad-tree and RQT partitioning. RDO aims to ensure that distortion is minimized at the pre-set target bit rate or that the bit rate is minimized at a target quality level for distortion pre-set. In a high-resolution video, efficient encoding would require many block-splitting decisions and, thereby, a large number of RDO calculations. This translates to a higher drain on

computational resources. Reducing the overall computational complexity of encoding is thus essential in providing a high quality UHD visual experience to a large audience economically.

After the finalization of the HEVC standard in 2013, various open-source implementations for video encoding into the H.265/MPEG-HEVC compression format have come to the fore- x265 is one of them. The background on x265 is explained in Section 2.2.

## 2.2 x265 Background

The x265 is an open-source HEVC encoder that compresses raw video in compliance with the HEVC standard [4]. This encoder is integrated into several open-source frameworks, including VLC, HandBrake [12], and FFMpeg [13] and is the de-facto open-source video encoder for HEVC. The x265 encoder has assembly optimizations for several platforms, including Intel architecture, ARM, and PowerPC. The x265 encoder employs techniques for inter-frame and intra-frame parallelism to deal with the increased complexity of HEVC encoding. For inter-frame parallelism, x265 encodes multiple frames in parallel by using system-level software threads. For intra-frame parallelism, x265 relies on the Wave-front Parallel Processing (WPP) tool exposed by the HEVC standard. This feature enables encoding rows of CTUs of a given frame in parallel while ensuring that the blocks required for intra-prediction from the previous row are completed before the given block starts to encode; as per the standard, this translates to ensuring that the next CTU on the previous row completes before starting the encode of a CTU on the current row. The combination of these features gives a tremendous boost in speed with no loss in efficiency compared to the publicly available reference encoder, HM.

## 2.3 ABR Streaming Background

ABR is a technology that allows streaming files efficiently over HTTP networks. The user's video player is offered multiple files on the same content in different sizes, and the client selects the most appropriate file for playback on the device. The design focuses on improving streaming by delivering the right content in all circumstances based on the specific device and network condition, which decreases the need for re-buffering. ABR streaming makes it possible for video players to select the best available video segment or chunk to play, depending on the available bitrate and device capability.

The ABR Ladder is an array of segments of differing quality and resolution, which are available in the streaming server. If the bitrate increases, the video player logic chooses a file of larger size with better quality, analogous to climbing up the ladder. If the bitrate decreases, the video player switches back to a lower-quality file, analogous to climbing down the ladder. ABR streaming improves previous streaming models by adjusting the

stream to choose the most suitable bitrate and changing the transport conditions based on the current situation. This makes it extremely useful for streaming on mobile networks. ABR streaming uses dynamic tracking of parameters such as CPU, memory capacity, and network conditions and subsequently delivers video quality to match.

ABR is supported by most modern video players. The video player logic on the user's device can choose among all the segments available in the video's manifest file, which are adjusted to increase the bitrates. The video player selects the best match based on the available bandwidth on the user's device at a particular moment. The player initially requests the lowest bit rate segments that are on offer. If the video player determines that the download speed is higher than the bitrate capability of the current segment, it will send a request for the next higher bitrate segment. This process continues until the current bitrate segment and the available bandwidth is matched appropriately. The video player will continue requesting segments at this selected bandwidth as long as the bandwidth remains at a similar level. If this process works smoothly, the user would have a smooth viewing experience in different network conditions.

Network Type	Dimensions	Frame rate	Total Bi-rate	Audio bi-rate	Key Frame
Cell	480x320	N/A	64	64	N/A
Cell	416x234	10-12	264	64	30-64
Cell	480x270	10-12	464	64	90
WiFi	640x360	29.97	664	64	90
WiFi	640x360	29.97	1264	64	90
WiFi	960x540	29.97	1864	64	90
WiFi	960x540	29.97	2564	64	90
WiFi	1280x720	29.97	4564	64	90
WiFi	1280x720	29.97	6564	64	90
WiFi	1920x1080	29.97	8564	64	90

Table 2.1: Fixed Bitrate Encoding ladder proposed by Apple in Apple Tech Note TN2224 [5]

Apple proposed a Fixed Bitrate Encoding ladder in 2010, shown in Table 2.1. Here, a video file would be encoded into variants of ten distinct qualities, ranging from an audio-only stream at 64 kbps to a 1080p audio/video stream at 8564 kbps. The Apple dimension numbers reported for cell phones are for portrait review, whereas those reported for Wi-Fi are for landscape view.

Netflix refined the technique of ABR Ladder analysis with Per-Title Encoding in 2015. In this particular approach by Netflix, each video is encoded in multiple resolutions. The data rates identify the appropriate rungs that provide the best quality at each data rate,

respectively, as shown in Table 2.2. This ensured that a content provider could customize two parameters- the number of rungs in a ladder, and the related resolution based on the requirements for each specific video, as shown below. This strategy provided potential savings in encoding and storage.

Resolution	Fixed Bitrate ladder (kbps)	Per-title Ladder (kbps)
320x240	235	150
384x288	375	200
512x384	560	290
512x384	750	NA
640x480	1050	NA
720x480	1750	440
720x480	NA	590
1280x720	2350	830
1280x720	3000	1150
1920x1080	4300	1470
1920x1080	5800	2150
1920x1080	NA	3840

Table 2.2: Per-Title Encoding proposed by Netflix [5]

Context-Aware Encoding (CAE) started gaining traction around 2018. It expanded encoding considerations also to include devices. Using Context-Aware Encoding, a content provider could offer separate encoding parameters for each device type and deliver content to various device types, from smartphones to home theatres. The aim is to decrease the playback bandwidth while maintaining the same experience. This reduction in playback bandwidth can be quite substantial. The Context-Aware Ladder shown in Figure 2.2 can offer the same quality as the Fixed Bitrate Ladder by using lower bitrates or higher resolutions for each variant, thereby improving playback performance and cost efficiency, and with half the number of variants. If encoding is aimed at saving the overall bandwidth, one important factor would be the location where the content will be consumed. The traditional encoding approach involves creating typical settings for each video in a library. For situations wherein the video will be streamed to multiple devices, such as mobile devices on cellular data networks and wired set-top boxes, it is advisable to have multiple encoding schemes, one for each type of device expected. Context-Aware Encoding ensures that content providers can fine-tune parameters on a per-show or a per-scene encoding basis.

The critical aspect of adaptive streaming relevant to this work is that multiple representations are needed for a broader reach. This work proposes a method to decrease the computational redundancy in encoding the same video content at multiple resolutions and bitrates for adaptive streaming distribution.

Bitrate (kbps)	Fixed Bitrate Ladder	Context-Aware Ladder
0	270p @ 450kbps	288p @ 450kbps
	360p @ 700kbps	
1000	360p @ 900kbps	432p @ 777kbps
	540p @ 1200kbps	
	540p @ 1700kbps	
2000		720p @ 2500kbps
	720p @ 2500kbps	
3000	1080p @ 3500kbps	1080p @ 2366kbps
	1080p @ 3800kbps	
4000		

Figure 2.2: Context-Aware Encoding [5]

## 2.4 Related Work

The work [14] proposes an approach wherein the highest bitrate/ quality representation is encoded with unmodified HEVC. The dependent representations are then encoded based on the CU depth information. Since CUs typically tend to have higher depth values (smaller CU size) in higher quality by observation, we only search CUs for which their depth levels are smaller or equal to that of the co-located CU in the reference representation. Using this approach, larger depths are skipped in the search, and we can save a considerable amount of time.

Following this idea, [15] discusses a similar approach using representations with different resolutions. Since the CTUs in different resolutions encompass different corresponding areas, they do not match with each other. Thus, a novel matching algorithm is proposed here with the objective to obtain block structure information from high-resolution representation with an arbitrary down-sampling ratio. This information is subsequently used to skip unnecessary depth searches at the lower resolutions. The two methods mentioned above are combined to introduce an efficient multi-rate encoding method in the work discussed in [16]. Here, in addition to the CTU depth values, additional information from the reference representation- namely prediction mode, intra mode, and motion vectors are used to accelerate encoding of lower quality and lower resolution representations.

The approaches discussed above, make use of re-utilization of high-resolution results at the lower “dependent” or derived resolutions. This re-utilization results in a lesser usage requirement of computational resources as encoding low-resolution content is inherently faster. The work [17] proposed an approach with sharing analysis information across representations in x265 - but here, all representations are restricted to the same resolution.

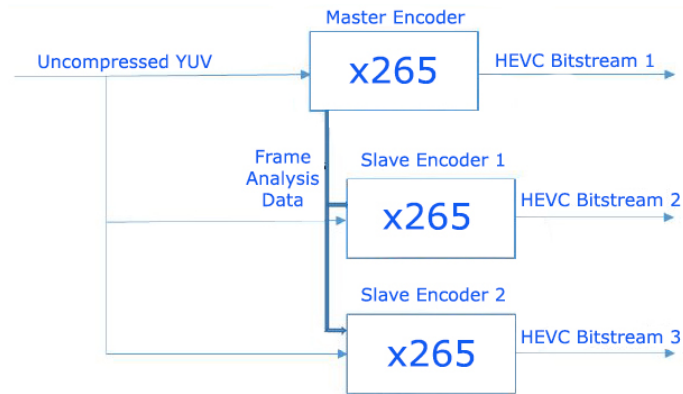


Figure 2.3: Multi-rate implementation proposed in [16], [17]

[18] introduces a novel implementation of the x265-based intelligent framework for multi-resolution encoding. Using such a framework, the relevant information related to the encoding decisions, such as a quad-tree structure, prediction modes, etc., which are made during the encode, can be shared from the lower resolution encode to the higher resolution encode. This makes the higher-resolution encoding process by up to two times faster.

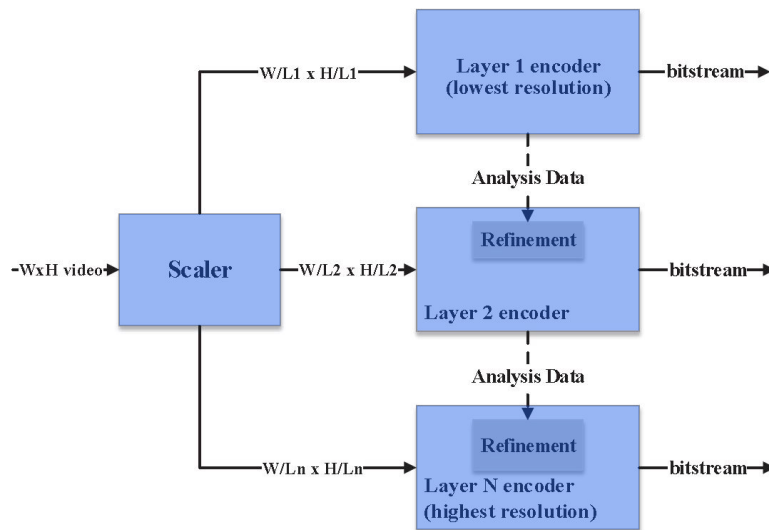


Figure 2.4: Multi-rate implementation proposed in [18]

# Chapter 3

## XVC and Intel SIMD Background

This chapter gives brief insights on the XVC video codec and Intel SIMD optimization. Section 3.1 discusses the background of XVC video codec, while Section 3.2 explains the background of SIMD extensions. Section 3.2.1 and Section 3.2.2 introduce Intel SSE4 and AVX2 SIMD extensions. Section 3.3 presents some of the literature referred to for this project.

### 3.1 XVC video codec

The video codec named XVC is developed by the software video compression company named Divideon AB and the first version of it was released in September 2017 [19]. It has been developed mainly based on known technology that has been included in AVC [20] or HEVC [4], or that has been evaluated in the context of the JVET [21]. The XVC video codec almost offers a middle-way between the existing options represented by HEVC and AV1 [22]. It is a block-based codec using intra and inter-predictions that operates on raw pictures of YUV pixel samples into a pre-defined standard bit-stream. Each picture in a video sequence is divided into rectangular blocks of samples of sizes up to 64x64 samples, which are predicted from samples in the same picture (intra-prediction) or samples in previously coded pictures (inter-prediction). Residuals are transformed using non-square transforms, and the coded symbols are compressed using a CABAC coder. Block boundaries are filtered using a deblocking filter.

In general, XVC is more similar to HEVC, but there are several clear differences. One of the most significant differences is that XVC uses non-square coding units for which both prediction and transform are applied. Thus, XVC does not contain separate trees of prediction units and transform units, as is the case with HEVC. It includes extensions to technologies in HEVC in several areas, for example, 67 intra-prediction modes instead of 35. Still, there is also a significant number of new coding tools for which there is no corresponding technology in HEVC, such as:

- Adaptive motion vector precision – where the precision of the MVs are signaled to

allow for more efficient signaling of long and integer MVs.

- Affine motion prediction – where individual MVs are calculated and applied for each 4x4 sub-block of a CU which makes it possible better to represent non-translational motions such as rotation and zoom.
- Cross component prediction – where chroma samples are predicted from luma samples using a linear model.
- Transform selection – where different transforms with different characteristics are evaluated to determine which transform most efficiently represents the residual of a specific CU.
- Local illumination compensation – where a linear model accounts for local offsets of sample values when predicting from reference pictures, particularly useful for representing changes in lighting conditions of an object or a scene.

The XVC codec has been tested with several open-source applications, including Exo-Player, FFmpeg, and VLC. These integrations have made it possible to use XVC on various devices and platforms, including Android, iOS, Windows, and Linux.

## 3.2 Single Instruction Multiple Data extension

SIMD is a class of parallel computers in Flynn's taxonomy [23]. Program with SIMD can simultaneously perform the same operation for multiple data elements. This is data-level parallelism, not concurrency, which means multiple data elements are being processed simultaneously, but only one operation is performed. The program, which can potentially run in data-level parallelism, can be significantly accelerated by SIMD.

The concept of SIMD was introduced in the early 1970s, known as a "vector" of data with single instructions, but it is separated from SIMD now. Afterward, the SIMD was introduced in modern SIMD machines which has many limited-functionality processors. Then the domain of SIMD CPU changed from desktop-computer to supercomputer. Since the desktop computer started to become performance efficient to support real-time gaming and audio/ video processing during the 1990s, the SIMD extensions went back to the desktop CPUs again.

Although SIMD is quite fit for accelerating programs, there are still some limitations for using SIMD in real-world applications.

- Not all programs can be accelerated by SIMD since not all programs can be vectorized easily. Some programs can be vectorized partially, but there would be a performance bottleneck due to the serial execution of non-vectorized functions.

SIMD ISA	Base ISA	Vendor	Year	SIMD Registers
MMX	x86	Intel	1996	8x64b
3DNow!	x86	AMD	1998	8x64b
SSE	x86/x86-64	Intel	1999	8/16x28b
SSE2	x86/x86-64	Intel	2000	8/16x28b
SSE3	x86/x86-64	Intel	2004	8/16x28b
SSSE3	x86/x86-64	Intel	2006	8/16x128b
SSE4	x86/x86-64	Intel	2007	8/16x128b
AVX	x86/x86-64	Intel	2011	16x256b
XOP	x86/x86-64	AMD	2011	8/16x128b
AVX2	x86/x86-64	Intel	2013	16x256b
AVX-512	x86/x86-64	Intel	2016	32x512b

Table 3.1: SIMD extensions to general purpose processors [24]

- SIMD are also limited for loading and storing data since all of the SIMD ISAs have different vector widths.
- Usually, using SIMD to accelerate the program needs a lot of human effort as the length of intrinsic code, or handwritten assembly code, is significantly longer than C or C++ code.
- Some SIMD ISAs are more complicated to be used than others because of, for example, the restrictions on data alignment, not all processors supporting all the SIMD ISAs. Investigating the influence of a new SIMD for a program still needs a lot of human effort.

### 3.2.1 Intel Streaming SIMD Extensions 4

Intel SSE4 is a SIMD CPU instruction set which was announced at the Fall 2006 Intel Developer Forum fully compatible with software written for previous generations of Intel 64 and IA-32 architecture microprocessors. All existing software would continue to run correctly without modification on microprocessors that incorporate SSE4, as well as in the presence of existing and new applications that incorporate SSE4. Intel SSE4 consists of 54 instructions. In some Intel documentation, a subset consisting of 47 instructions is referred to as SSE4.1. Additionally, SSE4.2, a second subset consisting of the seven remaining instructions.

### 3.2.2 Intel Advanced Vector Extensions 2

AVX2 expands most of the already introduced integer commands in SSE4 to 256 bits and introduces FMA operations. Intel first supported them with the Haswell processor, which

was introduced in 2013. AVX2 uses 16 YMM registers to perform SIMD. Each YMM register can hold and do simultaneous operations on eight 32-bit single-precision floating point numbers or four 64-bit double-precision floating point numbers. The SSE instructions are still utilized to operate on the lower 128 bits of the YMM registers. AVX2 introduces a three-operand SIMD instruction format, where the destination register is distinct from the two source operands.

### 3.3 Related Work

The trend of optimizing programs by SIMD extensions is quite common recently to leverage the existing CPU architectures. For Intel CPU architectures, different generations of SIMD extensions such as SSE2, SSSE3, SSE4.1 and AVX2 have been used to accelerate different video codecs such as MPEG-2, MPEG-4 Part 2. Recently H.264/AVC and HEVC have been optimized by the SIMD instructions. A detailed summary of works reporting SIMD optimization for codecs before H.264/AVC can be found in [25]. H.264/AVC also benefits greatly from SIMD accelerating, including luma and chroma interpolation filters, inverse transform, and deblocking filter acceleration. For instance, Zhou et al. [26], and Chen et al. [27] have reported that accelerating H.264/AVC by SSE2 can speedup the application ranging from 2.0 to 4.0. One of my previous works was accelerating x265 HEVC encoder by AVX512 SIMD extensions targeting Intel Core i9, and Intel® Xeon® Scalable Processors [28]. Figure 3.1 shows the measure of encoder speedup in x264 and x265 encoders using Intel® AVX2 SIMD optimization. This motivates the x86 optimization of a more complex Arowana XVC encoder for better performance benefits.

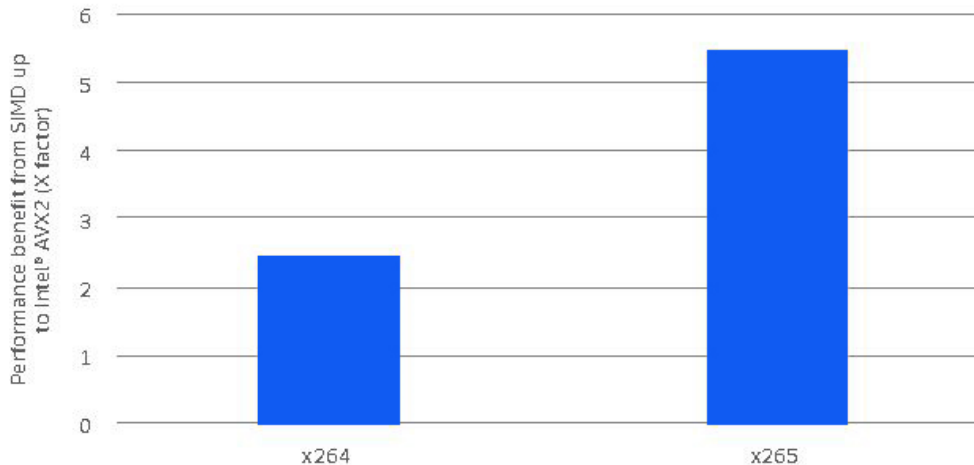


Figure 3.1: Performance benefit for x264 and x265 from Intel® Advanced Vector Extensions 2 for 1080p encoding with main profile using an Intel® Core™ i7-4500U Processor [28]

# Chapter 4

## Analysis Sharing Methods in x265

This chapter gives a brief insight into the methods used in this work for multi-resolution multi-rate analysis sharing in x265. Section 4.1 illustrates how the various approaches considered in this work are tested. Section 4.2 explains the methods used in intra-resolution analysis sharing where Section 4.2.1 details the state of the art method while Section 4.2.2 describes the proposed method. Section 4.3 shows the details of the method used in Inter resolution analysis sharing.

### 4.1 Testing method

The evaluation of the methods used was performed on different types of sequences with varying content. In the report, I mention the results obtained using well-known short sequences mentioned in Table 4.1.

Test Videos				
Video	Resolution	FPS	Colour Space	Frames
BasketBallDrive	960x540	50	YUV420p	500
	1920x1080			
	3840x2160			
CrowdRun	960x540	50	YUV420p	500
	1920x1080			
	3840x2160			
DucksTakeOff	960x540	50	YUV420p	500
	1920x1080			
	3840x2160			

Table 4.1: Videos used to validate the methods used

In this work, the evaluations are focused on the medium preset of x265 [29], which is the default quality preset in FFmpeg [13] and presenting an optimum trade-off between the encoding speed and the compression efficiency.

For the testing of intra-resolution analysis sharing as mentioned in Section 4.2, the test sequences are encoded for five different QP representations for each resolution (540p and 1080p) as mentioned in Table 4.2. Similarly, for the testing of inter-resolution analysis sharing as mentioned in Section 4.3, the test sequences are encoded for five different QP representations. When the right approaches are determined for intra-resolution and inter-resolution analysis sharing, the cVBR bitrates are used as mentioned in Table 4.3 to investigate the effect of the approach in real-time streaming applications (shown in Section 6). The motivation to select five different QP or cVBR representations is to calculate the BD-Rate, and BD-PSNR metrics [30] which gives us the proper understanding of the influence of the encoding approaches in terms of the compression efficiency. The results for 2160p encodes are calculated only for cVBR representations.

CQP representations					
Resolution	QP				
960x540	22	26	30	34	38
1920x1080	22	26	30	34	38
3840x2160	22	26	30	34	38

Table 4.2: QP considered for CQP mode test for various resolutions

Bitrate representations					
Resolution	Bitrate (in kbps)				
960x540	1000	1750	2500	3000	3500
1920x1080	3500	4500	5500	7500	9000
3840x2160	11000	13000	15000	17000	19000

Table 4.3: cVBR bitrates considered for various resolutions

Bjøntegaard Delta (BD-Rate and BD-PSNR) measurement [30] was used for evaluating the compression efficiency impact of the encoding approaches. BD-Rate calculates the percentage difference in bitrate between R-D curves for the same quality. BD-PSNR calculates the average quality difference between R-D curves for the same bitrate. A negative BD-PSNR indicates a drop in coding efficiency of the proposed approach versus a reference approach, while a positive BD-PSNR represents a coding gain. Similarly, a positive BD-Rate indicates a drop in coding efficiency of the proposed approach versus a reference approach, while a negative BD-Rate represents a coding gain.

All performance and quality data for this work are collected on a system with Intel® Core (TM) i7-7500U CPU running on Windows 10. Table 4.4 presents the test system attributes.

Test System details	
System Attribute	Value
OS Name	Windows 10 Home
Version	10.0 Build 18363
System Model	Lenovo 80YL
System Type	x64 based PC
Processor	Intel Core (TM) i7-7500U CPU @2.70Ghz (4 CPUs), 2.9GHz
Memory Type	DDR4
Memory channel	1
Memory Size	16384MB

Table 4.4: System configurations for Testing

## 4.2 Intra resolution analysis sharing in x265

In this experiment, a multi-quality encoding system that encodes each video segment at multiple quality levels is modeled and studied. Section 4.2.1 details the state-of-the-art method where the highest quality representation is the master/base representation. Section 4.2.2 describes the method proposed to improve the state-of-the-art method.

### 4.2.1 State of the art method

The highest quality representation is first encoded. The encoder analysis information is shared with the subsequent encodings with different QP. This is the same as the setup used in the approaches mentioned in [15], [16], and [17]. Figure 4.1 illustrates the flowchart of the analysis-sharing scheme. It is also imperative that in an ABR system, the bitrate tiers are as close together as possible to avoid noticeable fluctuations in quality while switching across tiers. Here we have five QP representations for 540p and 1080p encodings, respectively. For this model, the BD-Rate, BD-PSNR [30], and encoder speedup is evaluated for the overall encoding process.

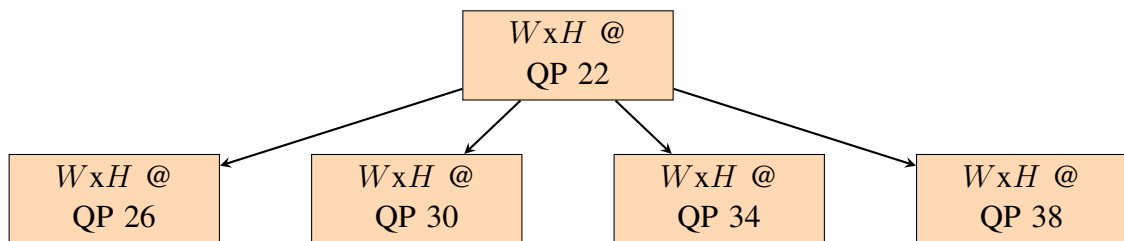


Figure 4.1: Intra resolution analysis sharing across  $W \times H$  resolution encode for CQP representation with lowest QP as master representation

The encoding scheme is evaluated for all analysis reuse levels defined in x265 as shown in A.1. From Table 4.5, we see that x265 analysis reuse level 10 gives an average speedup

of approximately 53 % with an average BD-Rate of 12 % for 540p videos. Most of the state-of-the-art methods employ this reuse level. We also observe that analysis reuse level 10 gives a similar speedup for 1080p videos but with an increase in the BD-Rate. But since we have a wide range of QPs tested, there is more variance in the CU depth and mode decisions in different representations; hence, the rise in BD-Rate is expected.

Test for CQP representations				
Resolution	Analysis level	$\Delta T$	BD-Rate	BD-PSNR
960x540	4	15.87 %	<b>1.65 %</b>	<b>-0.07 dB</b>
960x540	6	17.23 %	<b>1.65 %</b>	-0.07 dB
960x540	10	53.06 %	<b>12.27%</b>	<b>-0.46 dB</b>
1920x1080	4	11.57 %	<b>2.03 %</b>	<b>-0.06 dB</b>
1920x1080	6	12.83 %	<b>2.03 %</b>	<b>-0.06 dB</b>
1920x1080	10	49.99 %	<b>21.69 %</b>	<b>-0.47 dB</b>

Table 4.5: Measure of speedup and compression efficiency for intra-resolution analysis sharing with lowest QP (highest quality) representation as master encode

## 4.2.2 Proposed method

In the model described in the previous section, in compliance with most of the literature, the highest quality encode is the master representation. There are two key problems to address here:

- In parallel encoding systems, by this approach, the overall performance is limited by the time taken for the master encoding. Hence, using the highest quality encode as the master representation causes performance bottlenecks for multi-quality systems.
- The CU depth and mode decisions from the highest quality representation are sub-optimal as we traverse towards lower quality representations.

To mitigate the above-mentioned issues, the experiment is conducted using the median quality representation as the master representation as shown in Figure 4.2.

For the five QP representations in the test, QP 30 is the median quality representation. Hence, QP 30 representation is encoded first. The encoder analysis information is shared with the subsequent encodings- QP 22, 26, 34, and 38. Typically, QP 22 standalone representation is the slowest among all stand-alone encodings, resulting in a performance bottleneck for parallel encoding systems. But here, QP 22 encodings are expected to be paced up by using the encoder analysis information of the QP 30 representation.

Table 4.6 shows the speedup and BD-Rate for 540p and 1080p intra-resolution analysis sharing with the proposed method. Table 4.7 compares the BD-Rate and BD-PSNR for the state-of-the-art method and proposed method. There is a significant reduction in the

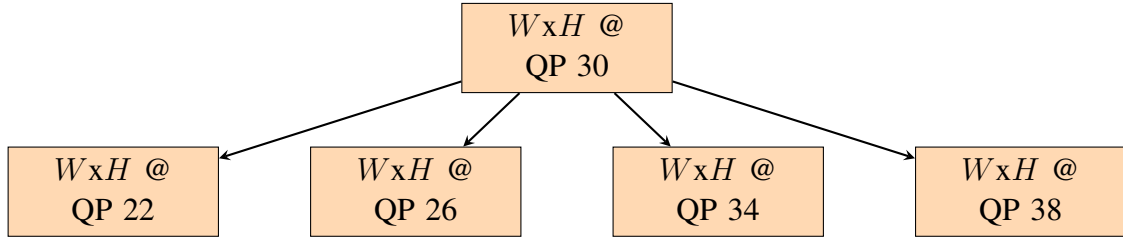


Figure 4.2: Intra resolution analysis sharing across  $W \times H$  resolution encode for CQP representation with median QP as master representation

BD-Rate for the proposed method. Hence, the median quality representation as the master representation approach is better than the existing state-of-the-art highest quality representation as the master representation approach.

Test for CQP representations				
Resolution	Analysis level	$\Delta T$	BD-Rate	BD-PSNR
960x540	4	16.94 %	0.80 %	-0.03 dB
960x540	6	18.77 %	0.80 %	-0.03 dB
960x540	10	65.60 %	6.45 %	-0.26 dB
1920x1080	4	13.91 %	1.61 %	-0.05 dB
1920x1080	6	15.07 %	1.61 %	-0.05 dB
1920x1080	10	63.91 %	8.59 %	-0.25 dB

Table 4.6: Measure of speedup and compression efficiency for intra-resolution analysis sharing with median QP representation as master encode

As mentioned earlier, the performance bottleneck of the state-of-the-art method was that the overall turnaround time in parallel encoding was bound by the speed of QP 22 encode. So, a detailed speedup analysis for every resolution tier representation is needed. Figure 4.3 shows the speedup of each CQP representation for 1080p encode with x265 analysis share mode 10 for the state-of-the-art method and the proposed method. All speeds are normalized to the QP 22 stand-alone speed. In parallel encoding, the time required to encode these five representations is the time taken by the QP 22 encode for the state-of-the-art method. For the proposed method, the time taken for QP 22 representation is the total time required for encoding the five representations, but it is observed that that time taken is decreased to a factor of 86%. It means that a factor of 14 % paces up the parallel encoding.

### 4.3 Inter-resolution analysis sharing in x265

In this experiment, a system is modeled which encodes each video segment at the highest quality in the lower resolution, and then reusing the frame-level metadata of the analysis

Resolution	Analysis level	Highest quality master		Median quality master	
		BD-Rate	BD-PSNR	BD-Rate	BD-PSNR
960x540	4	1.65 %	-0.07	0.80 %	-0.03 dB
960x540	6	1.65 %	-0.07	0.80 %	-0.03 dB
960x540	10	12.27 %	-0.46	6.45 %	-0.26 dB
1920x1080	4	2.03 %	-0.06	1.61 %	-0.05 dB
1920x1080	6	2.03 %	-0.06	1.61 %	-0.05 dB
1920x1080	10	21.69 %	-0.47	8.59 %	-0.25 dB

Table 4.7: Average improvement of BD-Rate for intra-resolution analysis sharing with median quality representation as master encode

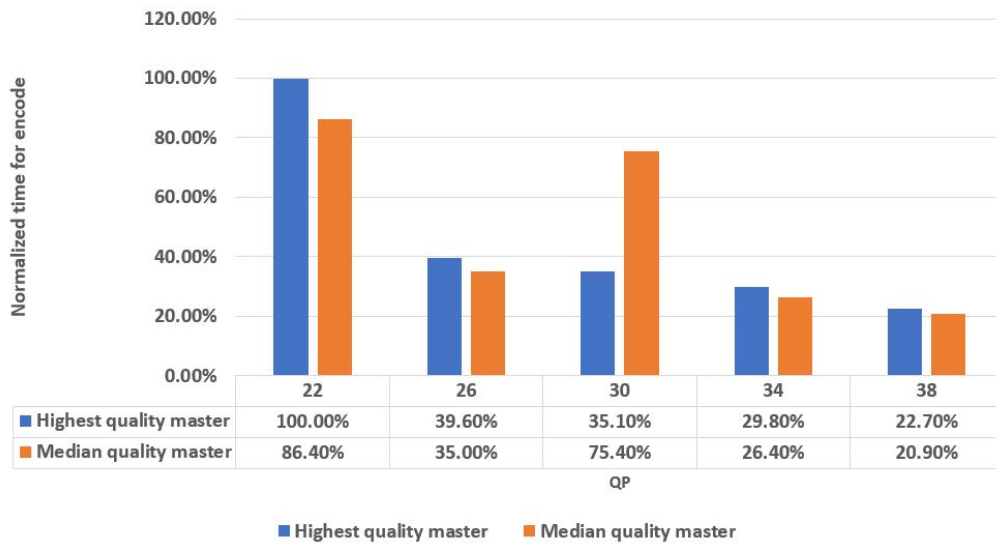


Figure 4.3: Average encode time for all representations in intra-resolution analysis sharing for 1080p videos

information, the representations in the current resolution tier are encoded. This setup is schematically represented in Figure 4.4. For this model, the BD-Rate, BD-PSNR, and overall encoder speedup are evaluated for the current resolution tier encoding process.

Test for CQP representations				
Resolution	Refinement	$\Delta T$	BD-Rate	BD-PSNR
1920x1080	no	<b>72.04 %</b>	<b>20.08 %</b>	<b>-0.62 dB</b>
1920x1080	yes	<b>28.99 %</b>	<b>1.61 %</b>	<b>-0.07 dB</b>

Table 4.8: Measure of speedup and BD-Rate for 1080p inter-resolution analysis sharing with 540p representation as the master encode and analysis reuse level 10

From Table 4.8, it is observed that, by reusing the analysis information from the highest

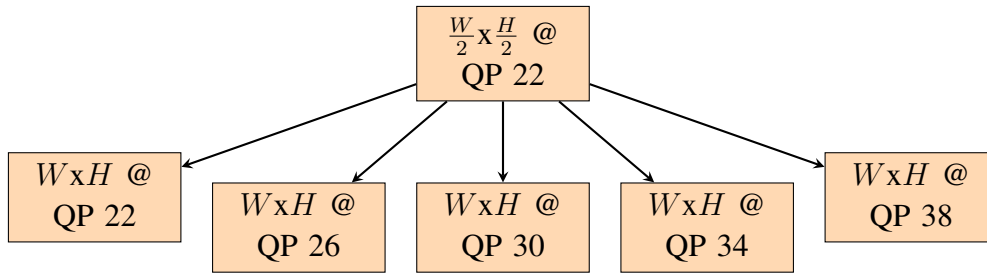


Figure 4.4: Inter resolution analysis sharing for CQP representation

quality representation of the 540p encode without analysis refinement, the 1080p resolution tier was encoded with an overall speedup of 72.04 % with BD-Rate of 20.08 % and BD-PSNR of -0.62 dB. It is also observed that, by reusing the analysis information from the highest quality representation of the 540p encode with analysis refinement, the 1080p resolution tier was encoded with an overall speedup of 28.99 % with BD-Rate of 1.61% and BD-PSNR of -0.07 dB. Hence, it is observed that refining the analysis across the resolutions is an excellent strategy to have a decent speedup and negligible BD-Rate.

# Chapter 5

## Intel SIMD optimization methods for XVC Encoding

This chapter presents the exploratory work done to understand the impact of SIMD parallelism in media processing. Section 5.1 shows various methods used for SIMD implementation and motivates the choice of the hand-written assembly method. Section 5.2 explains about NASM assembler used for compiling hand-written assembly code in this project. Section 5.3 shows the CPU cycle count improvements for kernels accelerated with Intel SSE4 and AVX2 SIMD. Section 5.4 mentions how the functions to be optimized are chosen, Section 5.4.1 and Section 5.4.2 describing the implementation of encoder cost functions and the resulting CPU cycle count improvements. Section 5.5 explains the method used to evaluate the CPU cycle count improvements for each optimized function.

### 5.1 SIMD implementation methods

There are three primary methods of utilizing SIMD instructions on Intel processors:

- writing low-level assembly code
- use of compiler-supported intrinsic functions
- compiler auto-vectorization

Generally, writing low-level assembly code that uses SIMD instructions and available registers is considered the best approach for achieving high performance. However, this method is cumbersome and error-prone. Compiler-supported intrinsic functions provide a higher level of abstraction, with an almost one-to-one mapping to assembly instructions, but without the need to deal with register allocations, instruction scheduling, type checking, and call stack maintenance. In this approach, intrinsic functions are expanded inline, eliminating function call overhead. It provides the same benefits as inline assembly, improved code readability, and fewer errors [31]. The penalty is that the overall performance boost depends on the compiler's ability to optimize across multiple intrinsic function calls.

Compiler auto-vectorization leaves everything to the compiler, relying on it to locate and automatically vectorize suitable loop structures. Therefore, the compiler's quality and the programmer's ability to write code that aids auto-vectorization becomes essential. [31] showed that state-of-the-art compilers were able to vectorize only 18-30 % of real application codes. In particular, it was noted that compilers did not perform some critical code transformations necessary for facilitating auto-vectorization. Non-unit stride memory access, data alignment, and data dependency transformations were found to be pertinent issues with compiler auto-vectorization. We choose the low-level assembly code method to perform SIMD operations in our work.

## 5.2 NASM Assembler support

The assembler support must be added to compile the hand-written assembly code to the video encoding solution. In this project, the support of the Netwide Assembler (NASM) is added to the Arowana XVC encoder solution [32]. NASM is an assembler and disassembler for the Intel x86 architecture, which can be used to write 16-bit, 32-bit (IA-32), and 64-bit (x86-64) programs. It is open-source software released under the terms of a simplified (2-clause) BSD license. The required changes are made to the solution compiling method so that NASM generates the compiled object files of the assembly code, and they get linked to the encoder solution.

## 5.3 Accelerating Arowana XVC Encoding with Intel SIMD

Figure 5.1 shows the cycle-count improvements for each of the kernels that were accelerated with SSE4 Intel SIMD. The kernels are sorted in increasing order of their cycle count gains over the corresponding C++ implementation. The detailed performance improvement for each optimized kernel gains over its corresponding C++ implementation is shown in Appendix B.

Figure 5.2 shows the cycle-count improvements for each of the kernels that were accelerated with AVX2 Intel SIMD. The detailed performance improvement for each optimized kernel gains over its corresponding C++ implementation is shown in Appendix C. The results from cycle counts indicate that at the kernel level, using Intel SIMD to accelerate XVC is advantageous.

## 5.4 Selecting the kernels to Accelerate

Over 1100+ kernels were selected from the core compute of XVC to optimize with Intel SIMD instructions for the main10 profile. These kernels were chosen based on their

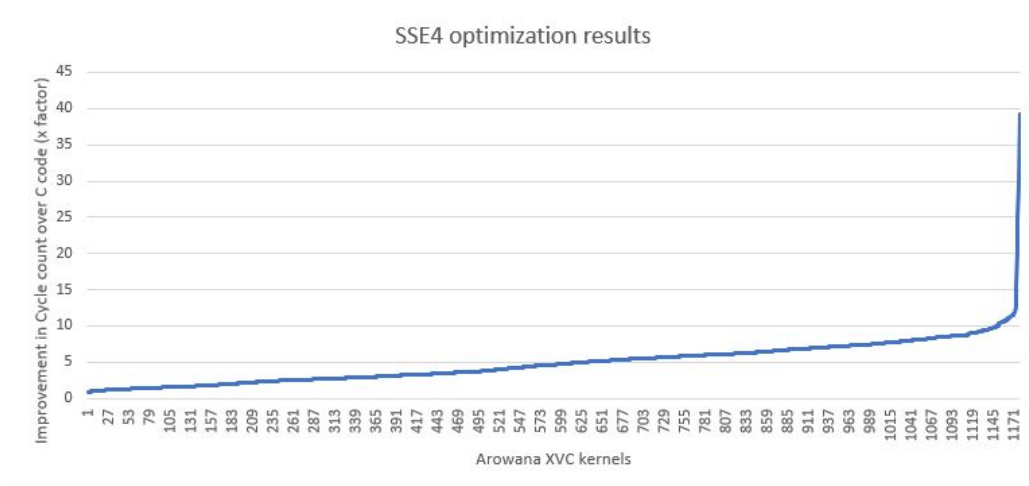


Figure 5.1: Cycle-count gains of the Intel® Streaming SIMD Extensions 4 kernels over the corresponding C++ kernels

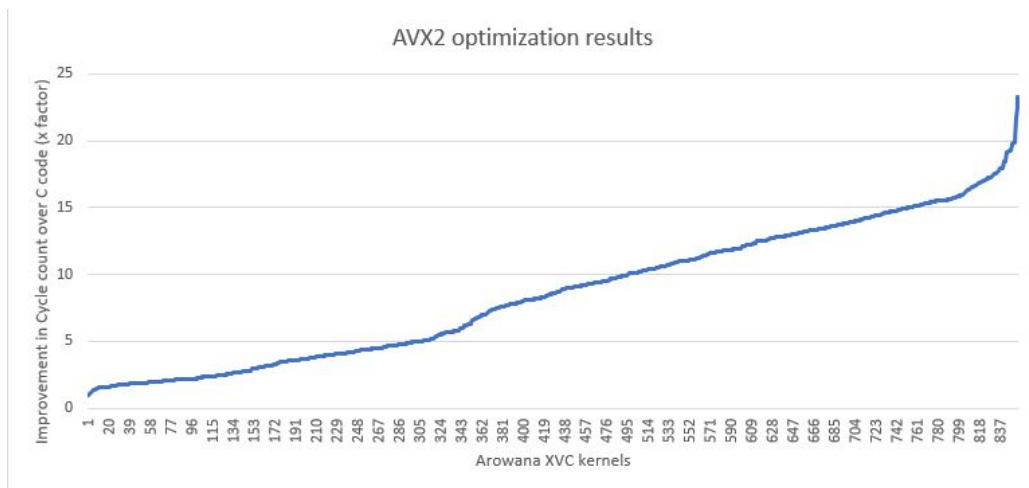


Figure 5.2: Cycle-count gains of the Intel® Advanced Vector Extensions 2 kernels over the corresponding C++ kernels

resource requirements. Some kernels may require frequent memory access, like different block-copy and block-fill kernels, while others may involve intense computation, like DCT, iDCT, and quantization kernels. There is also a third class of kernels that involves a combination of both in varying proportions. A complete list of the kernels optimized with Intel SIMD instructions are listed in Section B and Section C.

### 5.4.1 Cost functions

SAD (sum of absolute difference), SATD (sum of absolute transform difference), and DCT are some of the most complex and frequently called functions in the Arowana XVC encoder. In video coding, many cost functions are used to evaluate and choose the best coding

mode and its associated parameters. SAD and SATD are the two main cost functions to find integer and quarter-pel motion vectors in motion estimation. SAD takes around 11 % to 13 % of the total CPU cycles in the XVC encoder, and SATD takes 14 % to 15 %. These two cost functions are defined by:

$$SAD = \sum_{i,j}^{I,J} |O(i,j) - P(i,j)| \quad (5.1)$$

$$SATD = \frac{\sum_{i,j}^{I,J} |H(i,j)|}{2} \quad (5.2)$$

where  $i$  and  $j$  are the pixel indices, and their ranges are determined by block size.  $O(i,j)$  and  $P(i,j)$  is the original and predicted pixel values, respectively.  $H(i,j)$  is the Hadamard transform of the prediction error,  $O(i,j) - P(i,j)$  [33]. Because only addition and subtraction operations are involved in the cost functions, SATD can yield an accurate cost in the transform domain with relatively small complexity compared to DCT. Since both apply the same operations on multiple data, vector instructions are quite useful for reducing the required clock cycles.

## 5.4.2 SIMD implementation of cost functions

### SAD function

The C++ code for the SAD function is shown below:

```

1 template<int width, int height, typename SampleT1>
2 int ComputeSad_c(const SampleT1 *sample1, ptrdiff_t stride1,
3                 const Sample *sample2, ptrdiff_t stride2) {
4     int sum = 0;
5     for (int y = 0; y < height; y++) {
6         for (int x = 0; x < width; x++) {
7             int diff = sample1[x] - sample2[x];
8             sum += std::abs(diff);
9         }
10        sample1 += stride1;
11        sample2 += stride2;
12    }
13    return sum;
14 }

```

The corresponding x86 handwritten assembly for block sizes of width 16 is shown below:

```

1 %macro SAD_16x2_HBD_AVX2 1
2     pxor    m0, m0
3     mova   m6, [pw_1]
4     shl   r3d, 1
5     shl   r1d, 1
6 %rep %1/2
7     movu   m1, [r2]
8     movu   m2, [r2 + r3]
9     psubw  m1, [r0]

```

```

10     psubw    m2, [r0 + r1]
11     pabsw   m1, m1
12     pabsw   m2, m2
13     paddw   m1, m2
14     pmaddwd m1, m6
15     paddd   m0, m1
16     lea     r0, [r0 + 2 * r1]
17     lea     r2, [r2 + 2 * r3]
18 %endrep
19     HADD    m0, m1
20     movd    eax, xm0
21 %endmacro
22
23 INIT_YMM avx2
24 cglobal sad_16x2, 4, 4, 7
25     SAD_16x2_HBD_AVX2 2
26     RET
27 cglobal sad_16x4, 4, 4, 7
28     SAD_16x2_HBD_AVX2 4
29     RET
30 cglobal sad_16x8, 4, 4, 7
31     SAD_16x2_HBD_AVX2 8
32     RET
33 cglobal sad_16x16, 4, 4, 7
34     SAD_16x2_HBD_AVX2 16
35     RET
36 cglobal sad_16x32, 4, 4, 7
37     SAD_16x2_HBD_AVX2 32
38     RET
39 cglobal sad_16x64, 4, 4, 7
40     SAD_16x2_HBD_AVX2 64
41     RET

```

Table 5.1 shows the performance gains from the optimized kernels of the SAD function over its C++ implementation.

Speedup with SSE4 and AVX2 optimizations					
Kernel	Speedup	Kernel	Speedup	Kernel	Speedup
sad[4x4]	3.01x	sad[8x64]	2.63x	sad[32x8]	4.95x
sad[4x8]	4.41x	sad[16x2]	3.39x	sad[32x16]	4.99x
sad[4x16]	3.67x	sad[16x4]	2.44x	sad[32x32]	5.80x
sad[4x32]	5.54x	sad[16x8]	4.58x	sad[32x64]	5.54x
sad[8x4]	2.90x	sad[16x16]	6.46x	sad[64x8]	5.30x
sad[8x8]	2.40x	sad[16x32]	5.79x	sad[64x16]	5.37x
sad[8x16]	5.72x	sad[16x64]	6.27x	sad[64x32]	5.27x
sad[8x32]	2.78x	sad[32x4]	4.47x	sad[64x64]	5.14x

Table 5.1: Speedups of SAD kernels with SSE4 and AVX2 optimizations

## SATD function

The C++ code for the SATD function is shown below:

```

1  template <typename SampleT1, int w, int h>
2  // calculate satd in blocks of 8x4
3  int satd8(const SampleT1* pix1, intptr_t stride_pix1,
4           const Sample* pix2, intptr_t stride_pix2) {
5      int satd = 0;
6      for (int row = 0; row < h; row += 4)
7          for (int col = 0; col < w; col += 8)
8              satd += satd_8x4(pix1 + row * stride_pix1 + col, stride_pix1,
9                             pix2 + row * stride_pix2 + col, stride_pix2);
10     return satd;
11 }
12
13 #define HADAMARD4(d0, d1, d2, d3, s0, s1, s2, s3) { \
14     uint64_t t0 = s0 + s1; \
15     uint64_t t1 = s0 - s1; \
16     uint64_t t2 = s2 + s3; \
17     uint64_t t3 = s2 - s3; \
18     d0 = t0 + t2; \
19     d2 = t0 - t2; \
20     d1 = t1 + t3; \
21     d3 = t1 - t3; \
22 }
23
24 template <typename SampleT1>
25 static int satd_8x4(const SampleT1* pix1, intptr_t stride_pix1,
26                   const Sample* pix2, intptr_t stride_pix2) {
27     uint64_t tmp[4][4];
28     uint64_t a0, a1, a2, a3, b0, b1;
29     uint64_t sum = 0;
30
31     for (int i = 0; i < 4; i++, pix1 += stride_pix1, pix2 += stride_pix2)
32     {
33         b0 = pix1[0] - pix2[0];
34         b1 = pix1[4] - pix2[4];
35         a0 = b0 + (static_cast<uint64_t>(b1) << BITS_PER_SUM);
36         b0 = pix1[1] - pix2[1];
37         b1 = pix1[5] - pix2[5];
38         a1 = b0 + (static_cast<uint64_t>(b1) << BITS_PER_SUM);
39         b0 = pix1[2] - pix2[2];
40         b1 = pix1[6] - pix2[6];
41         a2 = b0 + (static_cast<uint64_t>(b1) << BITS_PER_SUM);
42         b0 = pix1[3] - pix2[3];
43         b1 = pix1[7] - pix2[7];
44         a3 = b0 + (static_cast<uint64_t>(b1) << BITS_PER_SUM);
45         HADAMARD4(tmp[i][0], tmp[i][1], tmp[i][2], tmp[i][3], a0, a1, a2, a3);
46     }
47     for (int i = 0; i < 4; i++) {
48         HADAMARD4(a0, a1, a2, a3, tmp[0][i], tmp[1][i], tmp[2][i], tmp[3][i]);

```

```

48     sum += abs2(a0) + abs2(a1) + abs2(a2) + abs2(a3);
49 }
50 return (static_cast<uint32_t>(sum) + (sum >> BITS_PER_SUM)) >> 1;
51 }

```

The corresponding x86 handwritten assembly for block sizes of width 16 is shown below:

```

1  cglobal calc_satd_16x4      ; function to compute satd cost for 16
   columns, 4 rows
2      ; rows 0-3
3      movu             m0, [r0]
4      movu             m4, [r2]
5      psubw           m0, m4
6      movu             m1, [r0 + r1]
7      movu             m5, [r2 + r3]
8      psubw           m1, m5
9      movu             m2, [r0 + r1 * 2]
10     movu             m4, [r2 + r3 * 2]
11     psubw           m2, m4
12     movu             m3, [r0 + r4]
13     movu             m5, [r2 + r5]
14     psubw           m3, m5
15     lea              r0, [r0 + r1 * 4]
16     lea              r2, [r2 + r3 * 4]
17     paddw           m4, m0, m1
18     psubw           m1, m0
19     paddw           m0, m2, m3
20     psubw           m3, m2
21     punpckhwd       m2, m4, m1
22     punpcklwd       m4, m1
23     punpckhwd       m1, m0, m3
24     punpcklwd       m0, m3
25     paddw           m3, m4, m0
26     psubw           m0, m4
27     paddw           m4, m2, m1
28     psubw           m1, m2
29     punpckhdq       m2, m3, m0
30     punpckldq       m3, m0
31     paddw           m0, m3, m2
32     psubw           m2, m3
33     punpckhdq       m3, m4, m1
34     punpckldq       m4, m1
35     paddw           m1, m4, m3
36     psubw           m3, m4
37     punpckhqdq      m4, m0, m1
38     punpcklqdq      m0, m1
39     pabsw           m0, m0
40     pabsw           m4, m4
41     pmaxsw          m0, m0, m4
42     punpckhqdq      m1, m2, m3
43     punpcklqdq      m2, m3
44     pabsw           m2, m2

```

```

45     pabsw          m1, m1
46     pmaxsw        m2, m1
47     pxor          m7, m7
48     mova          m1, m0
49     punpcklwd     m1, m7
50     padd          m6, m1
51     mova          m1, m0
52     punpckhwd     m1, m7
53     padd          m6, m1
54     pxor          m7, m7
55     mova          m1, m2
56     punpcklwd     m1, m7
57     padd          m6, m1
58     mova          m1, m2
59     punpckhwd     m1, m7
60     padd          m6, m1
61     ret
62
63 %macro SATD_AVX2_END 0
64     vextracti128   xm7, m6, 1
65     padd          xm6, xm7
66     pxor          xm7, xm7
67     movhlps       xm7, xm6
68     padd          xm6, xm7
69     pshufd        xm7, xm6, 1
70     padd          xm6, xm7
71     movd          eax, xm6
72 %endmacro
73
74 ; static int satd_16x4( const SampleT1* pix1, intptr_t stride_pix1,
75 ;                     const Sample* pix2, intptr_t stride_pix2,
76 ;                     int offset)
77 %macro SATD_16x4_AVX2 1
78 cglobal satd_%1_16x4, 4,6,8
79     shl          r1d, 1
80     shl          r3d, 1
81     lea          r4, [3 * r1]
82     lea          r5, [3 * r3]
83     pxor          m6, m6
84     call         calc_satd_16x4
85     SATD_AVX2_END
86     RET
87 %endmacro

```

Table 5.2 shows the performance gains from the optimized kernels of the SATD function over its C++ implementation. 3x to 10x speedup is observed for various kernel sizes using SSE4 and AVX2 SIMD extensions.

Speedup with SSE4 and AVX2 optimizations					
Kernel	Speedup	Kernel	Speedup	Kernel	Speedup
satd[8x4]	3.45x	satd[16x16]	7.32x	satd[32x64]	8.72x
satd[8x8]	3.75x	satd[16x32]	8.15x	satd[64x8]	8.43x
satd[8x16]	4.21x	satd[16x64]	8.85x	satd[64x16]	9.03x
satd[8x32]	4.01x	satd[32x4]	5.61x	satd[64x16]	9.19x
satd[8x64]	4.40x	satd[32x8]	7.83x	satd[64x32]	9.81x
satd[16x4]	5.19x	satd[32x16]	7.75x	satd[64x64]	10.22x
satd[16x8]	6.40x	satd[32x32]	8.56x		

Table 5.2: Speedups of SATD kernels with SSE4 and AVX2 optimizations

## 5.5 Method to evaluate cycle-count improvements

When handwritten x86 SIMD assembly code is implemented, two criteria need to be evaluated:

- If the primitive implemented is correct, i.e. if the outputs are the same, the same set of inputs is fed into the C++ primitive and the optimized primitive.
- If the primitive implemented is correct, the speedup is obtained from the optimized primitive with respect to the C++ primitive.

In this case, a correctness and performance measurement tool is implemented in the Arowana XVC encoder for x86 assembly kernels. To evaluate the first criteria mentioned above, the tool accepts valid arguments for a given primitive, invokes the C++ primitive and corresponding assembly kernel, and compares both output buffers. It verifies all possible corner cases for the given input type using a randomly distributed set of values. Each assembly kernel is called 100 times and checked against its C++ primitive output to ensure correctness. For the second criterion, ie to measure performance improvement, the test bench measures the difference in the clock ticks (as reported by the rdtsc instruction) between the assembly kernel and the C++ kernel for 1,000 runs and reports the average between them.

# Chapter 6

## Results and Discussion

In this chapter, the methods described in the previous chapters are evaluated in real-time streaming scenarios. In the state-of-the-art applications in the streaming industry, cVBR mode is used for video encoding. Hence, this section presents the results of the methods mentioned in Section 4 using cVBR mode in x265. The cVBR bitrates used for testing for each resolution are shown in Table 4.3. Section 6.1 shows the state-of-the-art intra-resolution analysis sharing method and discusses the results for the considered resolutions- 540p, 1080p, and 2160p. Section 6.2 discusses the proposed intra-resolution analysis sharing method and its improvement over the traditional intra-resolution analysis sharing method. Section 6.3 explains the inter-resolution analysis sharing method, the need for analysis refinement, and the associated results. Section 6.4 and Section 6.5 discuss state-of-the-art and the proposed multi-encoder structure with the scheme for encoder analysis sharing and the associated results, respectively. Section 6.6 explains the improvements of the Arowana XVC encoding speeds utilizing the SIMD extensions.

### 6.1 State of the art Intra-resolution analysis sharing in x265

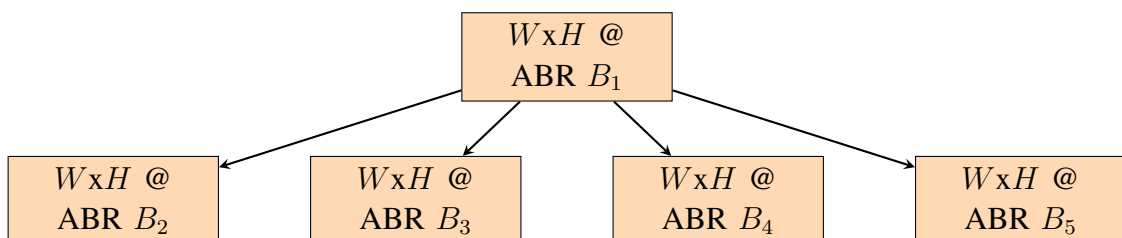


Figure 6.1: Intra resolution analysis sharing across  $W \times H$  resolution encode for ABR representation with the state of the art method ( $B_1 > B_2 > B_3 > B_4 > B_5$ )

In this model, the cVBR  $B_1$  encode instance is the master representation. The subse-

quent encodes uses the analysis information from the master representation. The results are evaluated for the test videos mentioned in Table 4.1 and cVBR bitrates shown in Table 4.3. Here, only x265 analysis reuse level 10 mentioned in Table A.1 is used since all recent literature use that analysis sharing mode.

It is observed that the results are very similar to the ones for CQP representation. As shown in Table 6.1, overall speedup for the five cVBR representations for 540p videos is 54.00% with a BD-Rate of 8.79% and BD-PSNR of  $-0.36dB$ . For 1080p videos, the overall speedup is 54.62% with a BD-Rate of 9.23% and BD-PSNR of  $-0.27dB$ . For 2160p videos, the overall speedup is 58.00% with a BD-Rate of 8.22% and BD-PSNR of  $-0.25dB$ .

Test for ABR representations			
Resolution	$\Delta T$	BD-Rate	BD-PSNR
960x540	54.00 %	8.79 %	-0.36 dB
1920x1080	54.62 %	9.23 %	-0.27 dB
3840x2160	58.00 %	8.22 %	-0.25 dB

Table 6.1: Measure of speedup and BD-Rate for ABR intra resolution analysis sharing with the state-of-the-art method

## 6.2 Proposed Intra resolution analysis sharing in x265

In this model, the cVBR  $B_3$  encode instance is the master representation. The subsequent encodes uses the analysis information from the master representation.

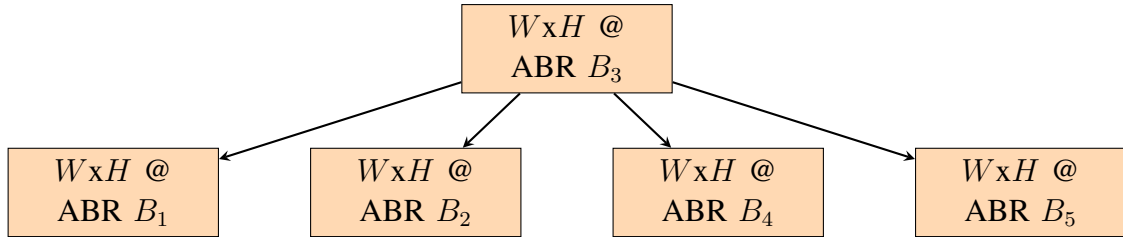


Figure 6.2: Intra resolution analysis sharing across  $W \times H$  resolution encode for ABR representation with the proposed method ( $B_1 > B_2 > B_3 > B_4 > B_5$ )

As shown in Table 6.2, overall speedup for the five cVBR representations for 540p videos is 56.14% with a BD-Rate increase of 7.75% and BD-PSNR of  $-0.27dB$ . For 1080p videos, the overall speedup is 59.15% with a BD-Rate increase of 6.47% and BD-PSNR of  $-0.18dB$ . For 2160p videos, the overall speedup is 60.09% with a BD-Rate increase of 6.01% and BD-PSNR of  $-0.17dB$ .

Test for ABR representations			
Resolution	$\Delta T$	BD-Rate	BD-PSNR
960x540	56.14 %	7.75 %	-0.27 dB
1920x1080	59.15 %	6.47 %	-0.18 dB
3840x2160	60.09 %	6.01 %	-0.17 dB

Table 6.2: Measure of speedup and BD-Rate for ABR intra resolution analysis sharing with the proposed method

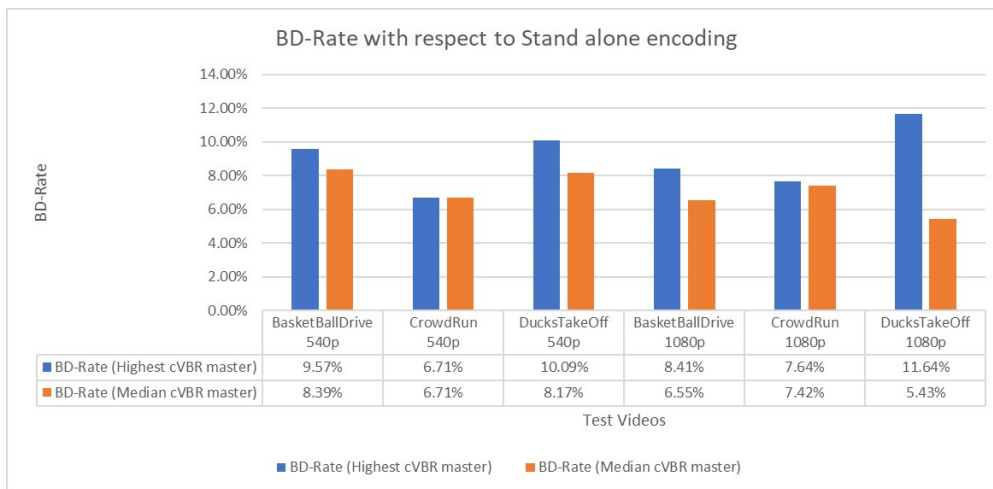


Figure 6.3: Comparison of BD-Rate for cVBR stand-alone encoding for the state-of-the-art method and the proposed method

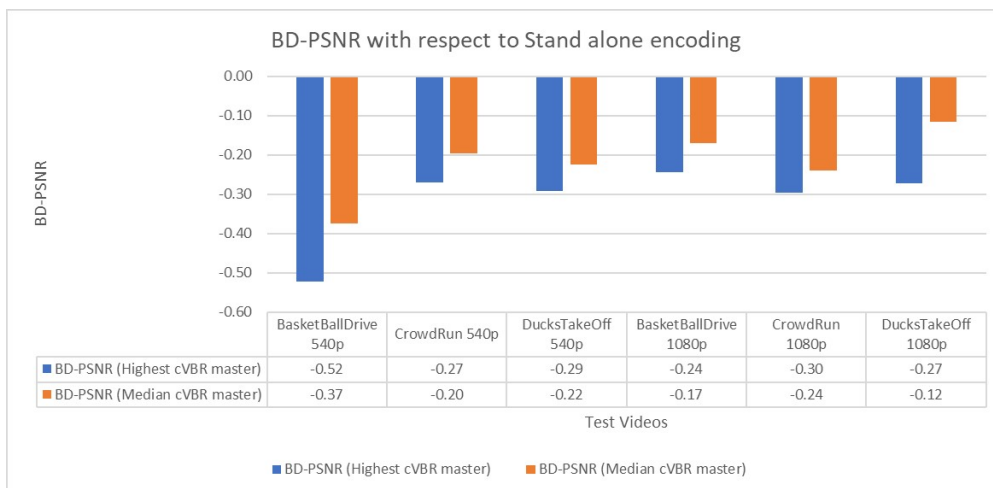


Figure 6.4: Comparison of BD-PSNR for cVBR stand-alone encoding for the state-of-the-art method and the proposed method

### 6.3 Inter-resolution analysis sharing in x265

In this model, the cVBR  $B$  encode instance for  $\frac{W}{2} \times \frac{H}{2}$  resolution is the master representation. The subsequent encodes of  $W \times H$  resolution tier use the analysis information from the master representation. The results are evaluated for x265 analysis reuse level 10 mentioned in Table A.1. Five cVBR rates are used in  $W \times H$  resolution tier to calculate the BD-Rate and BD-PSNR [30].

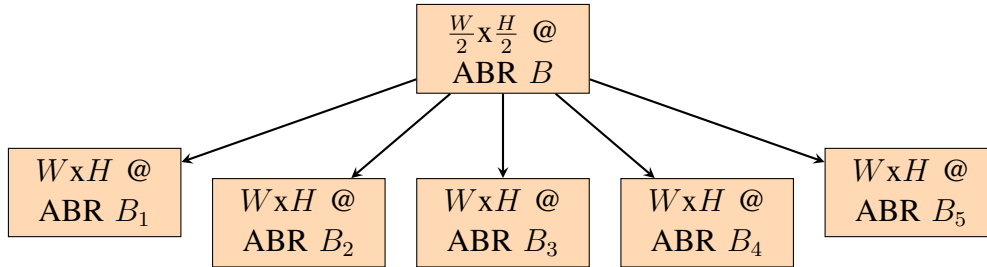


Figure 6.5: Inter resolution analysis sharing for ABR representation ( $B_1 > B_2 > B_3 > B_4 > B_5$ )

From Table 6.3 we see that, using 540p median cVBR representation as the master encode, the 1080p resolution tier has a speedup of 65.64% with a BD-Rate of 20.20% and BD-PSNR of  $-0.64dB$ . Using 1080p median cVBR representation as the master encode, the 2160p resolution tier has a speedup of 63.96% with a BD-Rate of 25.91% and BD-PSNR of  $-0.40dB$ . We notice that the BD-Rate value is too high when we use all CU analysis information without refinement. So, I use refinement options in x265 to have a reasonable BD-Rate. The analysis refinement options in x265 were explained in Section A.2 where the intra-refinement options and inter-refinement options were explained in Table A.2 and Table A.3 respectively.

Test for ABR representations			
Resolution	$\Delta T$	BD-Rate	BD-PSNR
1920x1080	65.64 %	20.20 %	-0.64 dB
3840x2160	63.96 %	25.91 %	-0.40 dB

Table 6.3: Measure of speedup and BD-Rate for 1080p and 2160p ABR inter-resolution analysis sharing with 540p median bitrate representation and 1080p median bitrate representation as master encode respectively

From Table 6.4 we see that, using 540p median cVBR representation as the master encode, the 1080p resolution tier has a speedup of 50.45% with a BD-Rate of 8.62% and BD-PSNR of  $-0.21dB$  with analysis refinement. Using 1080p median cVBR representation as the master encode, the 2160p resolution tier has a speedup of 52.82% with a BD-Rate of 7.45%

Test for ABR representations			
Resolution	$\Delta T$	BD-Rate	BD-PSNR
1920x1080	50.45 %	8.62 %	-0.21 dB
3840x2160	52.82 %	7.45 %	-0.22 dB

Table 6.4: Measure of speedup and BD-Rate for 1080p and 2160p ABR inter-resolution analysis sharing with refinement with 540p median bitrate representation and 1080p median bitrate representation as master encode respectively

and BD-PSNR of  $-0.22dB$  with analysis refinement. Figure 6.6 and Figure 6.7 shows the graphical representation of the comparison of BD-Rate and BD-PSNR for cVBR stand-alone encoding for inter-resolution with analysis refinement and without refinement.

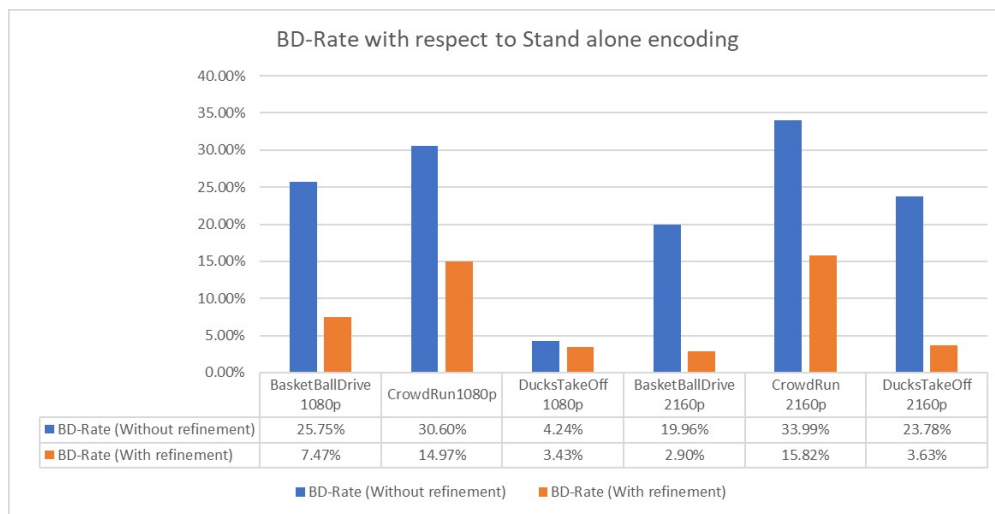


Figure 6.6: Comparison of BD-Rate for cVBR stand-alone encoding for inter-resolution with analysis refinement and without refinement

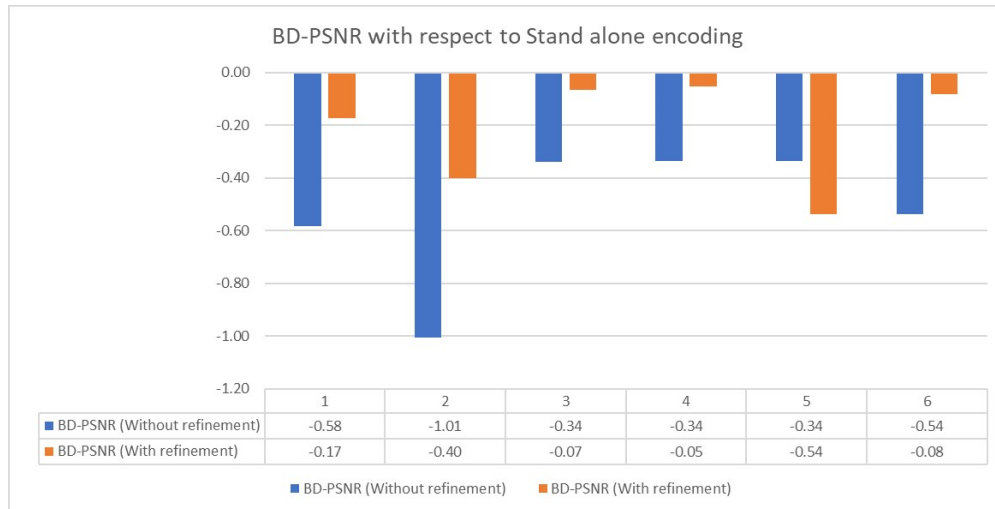


Figure 6.7: Comparison of BD-PSNR for cVBR stand-alone encoding for inter-resolution with analysis refinement and without refinement

## 6.4 State of the art multi-encoding scheme

Figure 6.8 shows the state-of-the-art multi-encoding scheme employed using the x265 HEVC encoder. The encoder analysis data from the 540p 3.5 Mbps cVBR representation is used as the master representation to encode other 540p representations. The same data is refined to encode the 1080p 9.0 Mbps representation. In other words, the highest cVBR representation of the lowest resolution tier is used to encode the remaining representations of the same tier and refined to encode the highest cVBR representation of the subsequent resolution tier.

## 6.5 Proposed multi-encoding scheme

Since an optimal intra-resolution and inter-resolution analysis sharing scheme is found, a novel multi-encoding scheme is proposed to generate cVBR bit-streams for various resolutions and bitrates for ABR streaming. In Figure 6.9, the proposed multi-encoding method is depicted with the optimal analysis-sharing scheme. The 540p 2.5 Mbps cVBR representation is the master encode representation. The encoder analysis information is shared with the other 540p resolution representations. It is also shared with the 1080p 5.5 Mbps representation, which refines the analysis data and reuses it. The analysis information from 1080p 5.5 Mbps representation encodes other 1080p resolution representations and 2160p 15 Mbps cVBR representation. The proposed method gives an average 7% less BD-Rate and 9% more speedup compared to the state-of-the-art scheme.

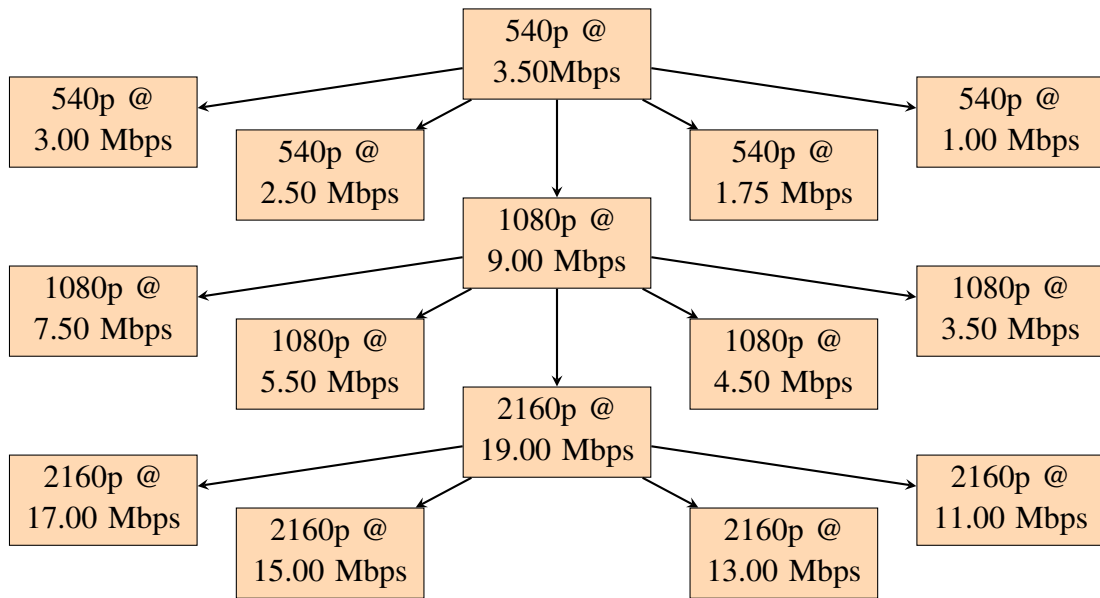


Figure 6.8: Representation of the state-of-the-art encoder analysis sharing across the resolutions and bitrates

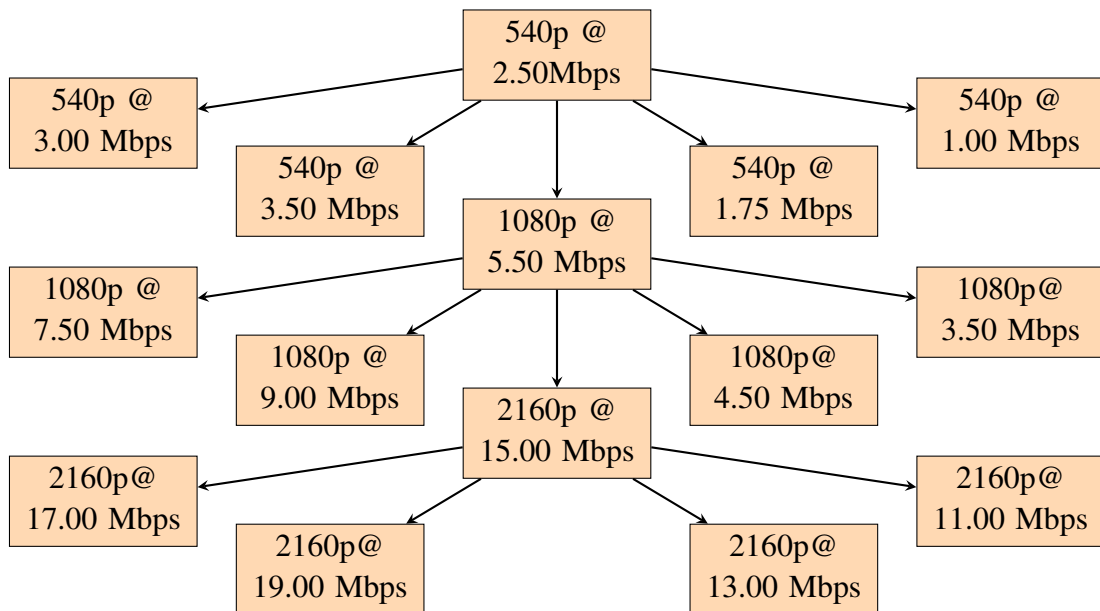


Figure 6.9: Representation of the proposed encoder analysis sharing across the resolutions and bitrates

## 6.6 Improvement in XVC encoding with SIMD optimization

The experiments are focused on all presets of the Arowana XVC encoder to represent the wide set of use cases that XVC can be used for since these presets represent a wide variety of trade-offs between compression efficiency and encoding speed (measured in frames per second). The 'slow' preset generates the most efficient encode but is the slowest; this preset is also the preferred choice for offline encoding use cases. The 'superultrafast' preset is the quickest setting of Arowana XVC but generates the encode with the lowest efficiency. The 'veryfast' preset represents an intermediate trade-off between performance and encoder efficiency. Typically, the more efficient presets employ more tools of XVC, resulting in more compute per pixel than the less efficient presets.

Figure 6.10, Figure 6.11 and Figure 6.12 shows the improvement in the encoding speed of Arowana XVC encoder for the given test videos at 540p resolution for all the presents defined in Arowana encoder. We notice that we have a net speedup of about 2.5x in some cases. This demonstrates that optimizing frequently used functions in the video encoder can boost the encoding speed significantly. The results are mainly obtained from optimizing the cost and interpolation filter functions. The critical functions like transforms are not yet optimized. The more the functions are vectorized, the speedup also increases.

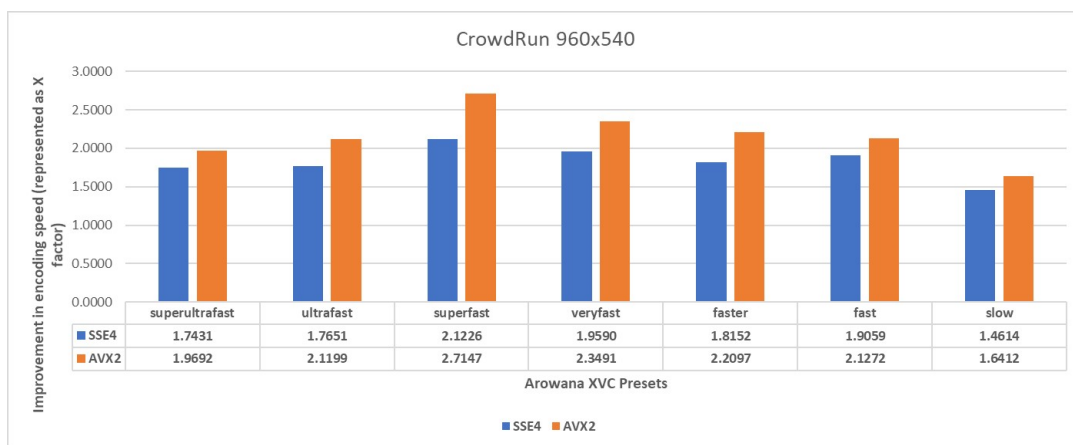


Figure 6.10: XVC encoding speedup for CrowdRun video for Arowana XVC presets (GOP length=2 seconds)

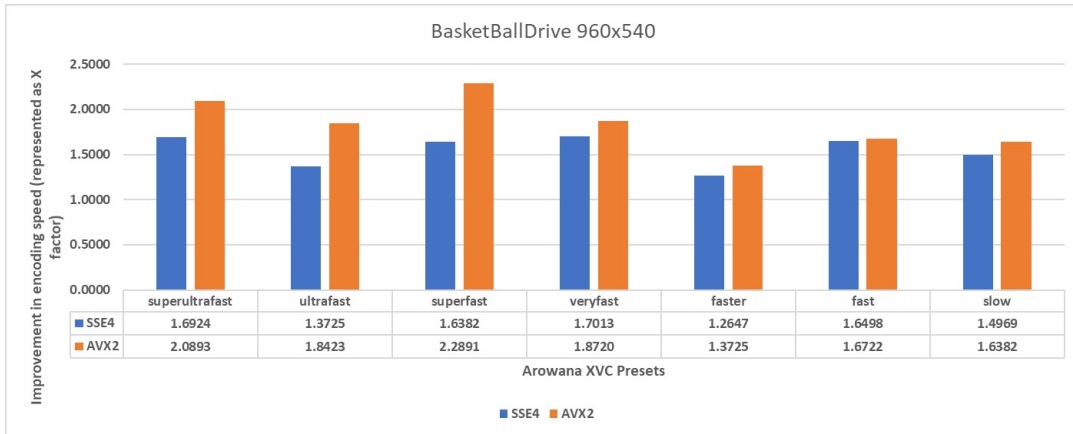


Figure 6.11: XVC encoding speedup for BasketBallDrive video for Arowana XVC presets (GOP length=2 seconds)

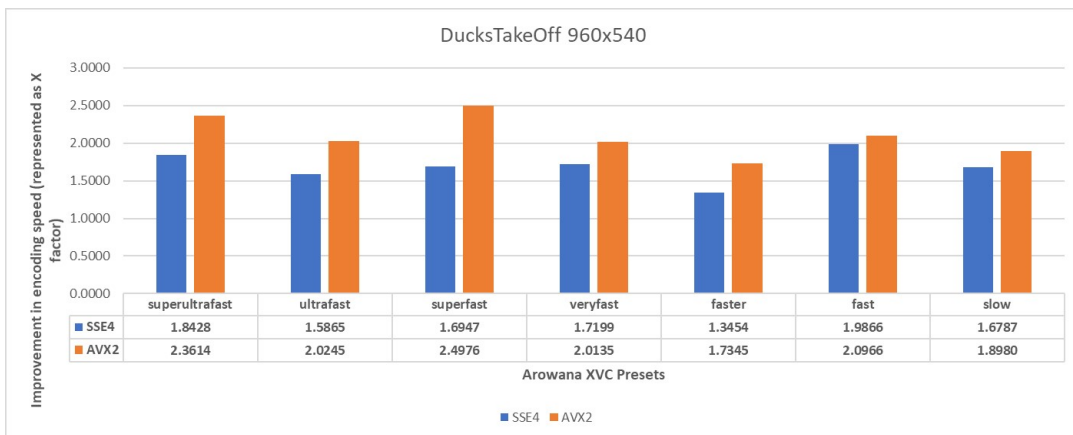


Figure 6.12: XVC encoding speedup for DucksTakeOff video for Arowana XVC presets (GOP length=2 seconds)

# Chapter 7

## Conclusions and Future Directions

This chapter concludes the project report and summarises the key findings during the project. Section 7.1 discusses the conclusions and Section 7.2 discusses the future directions of this work which haven't been explored as part of this project respectively.

### 7.1 Conclusions

The state-of-the-art intra-resolution multi-rate HEVC encoding scheme is modeled and evaluated in this project. The highest bitrate representation is used as the master representation. To mitigate the performance bottleneck in parallel encoding and improve the overall compression efficiency, a novel scheme is proposed for intra-resolution multi-rate HEVC encoding, where the median bitrate representation is used as the master representation. The state-of-the-art multi-resolution HEVC encoding scheme with inter-resolution analysis sharing is evaluated. With the updated optimized schemes, a multi-encoding scheme with multi-resolution tier multi-rate HEVC encoding scheme for ABR streaming is proposed. In the proposed scheme, the encoding instances of the same resolution tier reuse the encoder decisions of the encoding instance with median cVBR. The encoder decisions are refined and reused in the subsequent resolution tier encoding instance with median cVBR. The evaluations of the schemes were conducted on the x265 HEVC encoder. Experimental results demonstrate significant speedups with a marginal impact on coding efficiency.

In this project, the impact of SIMD extension optimizations in the encoding speeds of the next-generation video codecs is evaluated. The optimizations are implemented in the Arowana XVC encoder, where the encoding speeds were accelerated up to 2.7x by vectorizing some essential cost functions and interpolation filter functions. It is also noticed that the handwritten assembly is the best method to get the best performance boost, though it needs a lot of human effort.

## 7.2 Future Directions

In this project, the results for the parallel encoding of the various encoding instances are not considered and discussed due to hardware constraints. In the proposed model for multi-encoding discussed in Section 6.5, other representations of  $\frac{W}{4} \times \frac{H}{4}$  resolution tier can be run with a frame delay parallel to the  $\frac{W}{4} \times \frac{H}{4}$  median cVBR representation. Also, the median cVBR representation of  $\frac{W}{2} \times \frac{H}{2}$  can also be run with a frame delay parallel to the  $\frac{W}{4} \times \frac{H}{4}$  median cVBR representation. This encoding structure is possible for high-end servers with multiple CPU cores and threads. The parallel encoding approach can scale the performance benefits mentioned in the project.

In this project, only a few critical functions in the Arowana XVC encoder are optimized. There are still many vectorizable codes in Arowana, like DCT, iDCT, transpose, and other functions that can significantly boost the encoder speed across all presets. According to [28], x265 received a 5.5x speedup after implementing optimization of all generations of Intel SIMD till AVX2. Arowana being a more complex encoder can achieve a better performance boost with full-scale optimizations. The performance improvement in high-end servers can be further scaled up by AVX512 optimizations.

# Bibliography

- [1] Sandvine. *The Global Internet Phenomena Report*. May 2020. URL: <https://www.sandvine.com/phenomena>.
- [2] UltraHD Forum. *End-to-end guidelines for Phase A implementation, v1.4*. September 2017. URL: <https://ultrahdforum.org/resources/phasea-guidelinesdescription/>.
- [3] T. Fautier. “UHD Worldwide Service Deployment Update”. In: *NAB 2018, Las Vegas NV* (Apr 2018).
- [4] G. J. Sullivan et al. “Overview of the High Efficiency Video Coding (HEVC) Standard”. In: *IEEE Transactions on Circuits and Systems for Video Technology* 22.12 (2012), pp. 1649–1668.
- [5] AT & T Developer Program. *Adaptive Bitrate Video Streaming*. URL: <https://developer.att.com/video-optimizer/docs/best-practices/adaptive-bitrate-video-streaming>.
- [6] R. Lee. “Realtime MPEG video via software decompression on a PA-RISC processor”. In: Jan. 1995, pp. 186–192. DOI: 10.1109/CMPCON.1995.512384.
- [7] K. M. Patel, B. Smith, and L. A. Rowe. “The berkeley software MPEG-1 video decoder”. In: *ACM Trans. Multim. Comput. Commun. Appl.* 1 (2005), pp. 110–125.
- [8] ITU-T/ISO/IEC. *ITU-T, Recommendation H.265 (04/13), Series H: Audiovisual and Multimedia Systems, Infrastructure of audiovisual services – Coding of Moving Video, High Efficiency Video Coding*. URL: <https://www.itu.int/rec/TREC-H.265/en>.
- [9] ITU-T/ISO/IEC. *ITU-T, Recommendation H.265 (11/19), Series H: Audiovisual and Multimedia Systems, Infrastructure of audiovisual services – Coding of Moving Video, High Efficiency Video Coding*. URL: <https://www.itu.int/rec/TREC-H.265/en>.
- [10] A. Elrowayati et al. “Survey and Analysis of Digital Watermarking Algorithms on HEVC Video Coding Standard”. In: Dec. 2014. DOI: 10.13140/RG.2.1.1768.8809.
- [11] G. J. Sullivan and T. Wiegand. “Rate-distortion optimization for video compression”. In: *IEEE Signal Processing Magazine* 15.6 (1998), pp. 74–90.

- [12] HandBrake. *An OpenSource Video Transcoder*. URL: <https://handbrake.fr/>.
- [13] FFmpeg. *A complete, cross-platform solution to record, convert and stream audio and video*. URL: <http://ffmpeg.org/>.
- [14] D. Schroeder, P. Rehm, and E. Steinbach. “Block structure reuse for multi-rate high efficiency video coding”. In: *2015 IEEE International Conference on Image Processing (ICIP)*. Sep. 2015, pp. 3972–3976.
- [15] D. Schroeder, A. Ilangovan, and E. Steinbach. “Multi-rate encoding for hevc-based adaptive http streaming with multiple resolutions”. In: *2015 IEEE 17th International Workshop on Multimedia Signal Processing (MMSP)*. Oct 2015, pp. 1–6.
- [16] D. Schroeder et al. “Efficient multi-rate video encoding for HEVC-based adaptive HTTP streaming”. In: *IEEE Transactions on Circuits and Systems for Video Technology*. January 2018, pp. 143–157.
- [17] D. Nandakumar et al. “Efficient Multibitrate HEVC Encoding for Adaptive Bitrate Streaming”. In: *IEEE SMPTE Motion Imaging Journal*. 2017, pp. 36–40.
- [18] K. Goswami et al. “Adaptive Multi-Resolution Encoding for ABR Streaming”. In: *2018 25th IEEE International Conference on Image Processing (ICIP)*. 2018, pp. 1008–1012.
- [19] Divideon. *Introducing XVC- A Novel Video Compression Format with a Revolutionary Licensing Model*. URL: <https://www.divideon.com/wp-content/uploads/2017/09/Introducing-xvc-a-Divideon-whitepaper-v1.0.pdf>.
- [20] ITU-T/ISO/IEC. *H.264/14496-10 Advanced Video Coding*. URL: <https://www.itu.int/rec/T-REC-H.264>.
- [21] JVET. *JEM Software*. URL: <https://jvet.hhi.fraunhofer.de/>.
- [22] Alliance for Open Media. *AVI Video Codec*. URL: <https://aomedia.org/av1/>.
- [23] M. Flynn. “Flynn’s Taxonomy”. In: *Encyclopedia of Parallel Computing*. Ed. by D. Padua. Boston, MA: Springer US, 2011, pp. 689–697. ISBN: 978-0-387-09766-4. DOI: 10.1007/978-0-387-09766-4\_2. URL: [https://doi.org/10.1007/978-0-387-09766-4\\_2](https://doi.org/10.1007/978-0-387-09766-4_2).
- [24] C. C. Chi et al. “SIMD acceleration for HEVC decoding”. In: *Circuits and Systems for Video Technology, IEEE Transactions on* 25 (May 2015), pp. 841–855. DOI: 10.1109/TCSVT.2014.2364413.
- [25] V. Lappalainen and T. Hämäläinen. “Overview of research efforts on media ISA extensions and their usage in video coding”. In: *Circuits and Systems for Video Technology, IEEE Transactions on* 12 (Sept. 2002), pp. 660–670. DOI: 10.1109/TCSVT.2002.800865.

- [26] X. Zhou, E. Li, and Y. Chen. “Implementation of H. 264 decoder on general-purpose processors with media instructions”. In: *Electronic Imaging 2003 International Society for Optics and Photonics* 12 (2003), pp. 224–235.
- [27] Y. Chen et al. “Implementation of H.264 encoder and decoder on personal computers”. In: *Journal of Visual Communication and Image Representation* 17 (Apr. 2006), pp. 509–532. DOI: 10.1016/j.jvcir.2005.05.004.
- [28] P. K. Tiwari, V. V. Menon, and J. Murugan. *Accelerating x265 with Intel® Advanced Vector Extensions 512*. URL: <https://software.intel.com/sites/default/files/managed/d5/f6/mcw-intel-x265-avx512.pdf>.
- [29] MulticoreWare Inc. *x265 Command Line Options*. URL: <https://x265.readthedocs.io/en/default/cli.html>.
- [30] G. Bjøntegaard. “Calculation of average PSNR differences between RD-curves”. In: *Technical Report VCEG-M33, ITU-T SG16/Q6*. 2001.
- [31] S. Maleki et al. “An evaluation of vectorizing compilers”. In: *2011 International Conference on Parallel Architectures and Compilation Techniques (PACT)*. 2011, pp. 372–382.
- [32] The NASM development team. *NASM*. URL: <https://www.nasm.us/>.
- [33] K. MCCANN. “HM4 : High efficiency video coding (HEVC) test model 4 encoder description”. In: *JCTVC-F802* (2011). URL: <https://ci.nii.ac.jp/naid/20000680833/en/>.

# Appendix A

## x265 CLI Options

### A.1 Preview of x265 encoder analysis share modes

The x265 command line parameter *-analysis-save* is used to generate the corresponding encoder analysis information as a metadata file from the master/ base encodes. In the master/ base encode, an additional parameter *-analysis-save-reuse-level* defines the extent of the saved information in the metadata file as shown in Table A.1. Subsequently, the dependent representation reuses this information in the metadata file by combining the *-analysis-load* and *-analysis-load-reuse-level* parameters. The dependent representation can either be of the exact resolution as that of the master/ base, albeit targeting a different quality level, or have a different resolution from the master/ base. *-scale-factor* option is to scale up the encoder analysis data to the required resolution. Currently, x265 allows this kind of analysis sharing only across dyadic resolutions (i.e., multiples of both the width and height by a factor of two). The shared analysis data includes the encoder decisions like quad-tree structure, prediction modes (e.g., intra/inter prediction modes), motion vectors (MVs), and frame-level information, such as slice-types, reference lists, and distortion information. The choice of the analysis share level depends on the trade-off between compression efficiency and speedup. In this work, I consider only levels- 4, 6, and 10.

x265 Analysis reuse levels	
Level	Description
1	Reuse Lookahead information
2-4	Level 1 + Reuse intra/inter modes, ref's
5-6	Level 2 + Reuse rect-amp
7	Level 5 + Reuse AVC size CU refinement
8-9	Level 5 + Reuse AVC size Full CU analysis-info
10	Level 5 + Reuse Full CU analysis-info

Table A.1: x265 analysis reuse levels and their respective descriptions [29]

## A.2 Preview of x265 encoder analysis refinement modes

For multi-resolution encoding, there are specific refinement techniques used in x265. The CLI option *-refine-intra* is used to enable refinement of intra blocks in the current representation. The various values for the parameter and the respective functionality are shown in Table A.2.

Intra Refinement	
Level	Description
0	Forces both mode and depth from the reference encode
1	Evaluates all intra modes at current depth(n) and at depth (n+1) when current block size is one greater than the min-cu-size and forces modes for larger blocks.
2	In addition to the functionality of level 1, at all depths, force (i) only depth when the angular mode is chosen by the save encode. (ii) depth and mode when other intra-modes are chosen by the save encode.
3	Perform analysis of intra modes for depth reused from reference encode
4	Does not reuse any analysis information - redo analysis for the intra block

Table A.2: Intra refinement techniques in x265 [29]

The CLI option *-refine-inter* is used to enable refinement of inter blocks in the current representation. The various values for the parameter and the respective functionality are shown in Table A.3. The CLI option *-refine-mv* is used to enable the refinement of the motion vector for the scaled video. The best motion vector is evaluated based on the level selected. The various levels and the respective functionality is shown in Table A.4.

Inter Refinement	
Level	Description
0	Forces both mode and depth from the reference encode
1	Evaluates all inter modes at current depth(n) and at depth (n+1) when current block size is one greater than the min-cu-size and forces modes for larger blocks.
2	In addition to the functionality of level 1, restricts the modes evaluated when specific modes are decided as the best mode by the save encode 2Nx2N in save encode - disable re-evaluation of rect and amp SKIP in save encode - re-evaluates only SKIP, MERGE, and 2Nx2N modes.
3	Perform analysis of inter modes while reusing depths from reference encode

Table A.3: Inter refinement techniques in x265 [29]

Motion Vector Refinement	
Level	Description
1	Search around scaled MV
2	Level 1 + Search around best AMVP candidate
3	Level 2 + Search around the other AMVP candidate

Table A.4: Motion vector refinement techniques in x265 [29]

# Appendix B

## SSE4 SIMD optimization

Primitive	IPC Gain	Primitive	IPC Gain	Primitive	IPC Gain
sad_ac_p[1][8x4]	0.84	sad_ac_p[1][64x8]	1.2	sad_ac_res[1][64x16]	1.36
mean_diff_p[1][4x8]	0.9	subtract_res[32x16]	1.2	sub_weight[32x8]	1.38
subtract_pix[64x64]	0.92	sad_ac_res[0][64x8]	1.21	sad_ac_res[0][16x8]	1.4
subtract_pix[32x32]	0.95	sad_ac_p[0][16x2]	1.22	sad_ac_res[1][16x32]	1.4
subtract_res[64x32]	0.95	sad_ac_res[0][32x4]	1.22	sad_ac_res[0][8x4]	1.41
sad_ac_p[1][8x2]	0.98	subtract_pix[64x16]	1.23	sad_ac_res[1][32x8]	1.41
copy_bipred[64x32]	1.02	sub_weight[64x32]	1.23	mean_diff_p[1][8x2]	1.42
sub_weight[64x64]	1.04	sad_ac_res[0][64x64]	1.24	mean_diff_res[1][8x2]	1.43
mean_diff_p[1][4x2]	1.06	copy_bipred[32x8]	1.24	sad_ac_p[0][32x16]	1.44
sad_ac_p[0][32x8]	1.07	subtract_res[64x8]	1.25	subtract_pix[64x32]	1.44
copy_bipred[64x64]	1.07	sad_ac_res[1][8x4]	1.26	calc_sign[64x8]	1.44
subtract_pix[32x64]	1.08	subtract_res[32x32]	1.26	sad_ac_p[0][16x32]	1.45
sad_ac_res[1][64x8]	1.1	sad_ac_res[1][64x32]	1.27	sub_weight[64x8]	1.45
sad_ac_p[0][64x64]	1.1	subtract_res[32x4]	1.27	sad_ac_res[1][4x2]	1.46
copy_bipred[32x16]	1.1	sad_ac_res[1][8x8]	1.28	mean_diff_res[1][4x4]	1.46

Primitive	IPC Gain	Primitive	IPC Gain	Primitive	IPC Gain
copy_bipred[32x64]	1.1	sad_ac_res[0][32x64]	1.28	sad_ac_res[0][8x64]	1.46
subtract_pix[32x8]	1.1	subtract_pix[64x8]	1.28	sad_ac_res[1][64x64]	1.46
sad_ac_p[1][16x32]	1.11	sad_ac_res[0][16x2]	1.29	sad_ac_res[1][8x32]	1.48
mean_diff_res[1][4x2]	1.12	sad_ac_res[0][8x2]	1.3	sad_ac_res[1][32x4]	1.48
sad_ac_res[1][8x2]	1.12	sad_ac_res[0][32x32]	1.3	sad_ac_res[1][32x16]	1.48
subtract_res[64x64]	1.12	sad_ac_p[1][8x8]	1.31	sad_ac_p[1][32x32]	1.48
sad_ac_p[1][16x2]	1.14	sub_weight[32x16]	1.31	sad_ac_res[1][32x32]	1.48
sad_ac_res[1][16x2]	1.14	sad_ac_res[0][64x16]	1.32	sad_ac_p[1][32x64]	1.48
copy_bipred[64x16]	1.15	subtract_res[32x8]	1.32	sad_ac_p[1][64x64]	1.48
subtract_res[32x64]	1.15	subtract_res[64x16]	1.32	sub_weight[32x4]	1.48
copy_bipred[32x32]	1.17	calc_sign[16x2]	1.33	sad_ac_res[1][8x64]	1.49
sad_ac_res[0][64x32]	1.18	sub_weight[32x32]	1.34	sad_ac_p[0][16x16]	1.49
sad_ac_p[1][32x4]	1.19	mean_diff_p[1][16x2]	1.35	sad_ac_p[0][64x32]	1.49
copy_bipred[32x4]	1.19	sad_ac_p[1][16x16]	1.36	ang_fast_copy[8x2]	1.49
sub_weight[32x64]	1.19	sad_ac_res[0][32x8]	1.36	subtract_pix[32x16]	1.49
sad_ac_p[0][64x16]	1.5	sad_ac_p[0][8x32]	1.63	mean_diff_p[0][4x4]	1.78
sad_ac_p[1][4x2]	1.51	sad_ac_p[1][16x8]	1.63	sad_ac_res[0][4x2]	1.79
sad_ac_p[0][4x4]	1.51	calc_sign[64x32]	1.63	mean_diff_res[0][8x2]	1.79
sad_ac_res[0][4x4]	1.51	sad_ac_res[1][8x16]	1.65	sad_ac_res[1][16x16]	1.81
sad_ac_p[1][8x32]	1.52	sad_ac_p[1][8x64]	1.65	sad_ac_p[0][16x64]	1.81
sad_ac_p[0][32x64]	1.52	sad_ac_res[0][8x16]	1.66	calc_sign[32x16]	1.81
copy_bipred[64x8]	1.52	sad_ac_res[0][16x32]	1.66	sad_sp_x3[32x64]	1.83
sub_weight[64x16]	1.52	sad_ac_p[0][4x16]	1.67	copy_bipred[16x8]	1.83
sad_ac_p[1][16x4]	1.53	sad_ac_res[0][8x32]	1.67	sad_ac_p[0][8x4]	1.85
subtract_pix[4x8]	1.53	mean_diff_p[0][16x4]	1.67	sad_ac_res[0][8x8]	1.86
sad_ac_res[1][4x8]	1.54	mean_diff_res[1][16x4]	1.67	sad_ac_res[0][16x4]	1.86
sad_ac_p[0][8x2]	1.54	copy_block[1]	1.67	sad_ac_p[0][4x2]	1.87
sad_ac_p[0][64x8]	1.54	mean_diff_p[0][4x2]	1.68	sad_ac_p[1][4x4]	1.88
calc_sign[32x4]	1.54	mean_diff_p[1][4x4]	1.68	mean_diff_res[1][16x8]	1.88
sad_ac_p[0][8x16]	1.55	sad_ac_p[0][32x32]	1.68	subtract_pix[16x64]	1.88
sad_ac_p[1][16x64]	1.55	mean_diff_res[1][4x8]	1.69	sad_sp_x3[32x32]	1.89
subtract_pix[32x4]	1.55	sad_ac_p[1][4x32]	1.69	calc_sign[32x32]	1.89
sad_ac_p[0][4x32]	1.56	mean_diff_res[0][4x8]	1.7	sad_ac_res[0][4x16]	1.9
sad_ac_res[1][16x8]	1.56	sad_ac_p[0][16x8]	1.7	copy_bipred[4x2]	1.9
sad_ac_p[1][32x8]	1.56	calc_sign[16x4]	1.7	sad_sp[32x8]	1.91
sad_ac_p[1][64x32]	1.56	sad_ac_res[1][16x64]	1.71	calc_sign[16x32]	1.92
sad_ac_p[0][16x4]	1.57	copy_bipred[16x4]	1.72	calc_sign[32x8]	1.92
sad_ac_res[0][32x16]	1.57	mean_diff_res[0][4x2]	1.73	sad_ac_p[0][8x8]	1.94
sad_ac_p[1][32x16]	1.58	sad_ac_res[1][4x4]	1.73	mean_diff_res[0][8x16]	1.94
sad_ac_res[1][32x64]	1.59	sad_ac_res[0][4x32]	1.73	mean_diff_res[0][4x16]	1.95
calc_sign[32x64]	1.59	sad_ac_p[0][4x8]	1.74	sad_sp_x3[8x4]	1.95
calc_sign[64x64]	1.59	sad_ac_p[1][8x16]	1.74	sad_ac_p[1][4x8]	1.97
sad_ac_p[0][8x64]	1.6	sad_sp[8x2]	1.75	subtract_res[4x2]	1.98
sad_ac_res[0][16x16]	1.61	sad_ac_res[0][16x64]	1.76	calc_sign[64x16]	1.98
sad_ac_p[1][64x16]	1.61	copy_bipred[16x2]	1.77	subtract_res[16x64]	1.99
mean_diff_res[1][8x4]	2	mean_diff_res[0][4x4]	2.25	subtract_res[16x32]	2.44
mean_diff_p[0][8x8]	2	mean_diff_p[1][4x16]	2.25	block_zero[64x16]	2.44
subtract_res[16x8]	2	mean_diff_res[1][16x32]	2.25	sad_pp[64x32]	2.45
sad_sp_x3[64x64]	2.02	sad_sp_x3[32x16]	2.25	sad_sp[32x16]	2.46
sad_sp_x3[8x2]	2.03	mean_diff_p[1][32x4]	2.26	block_zero[64x8]	2.46
mean_diff_p[1][16x64]	2.03	subtract_res[8x32]	2.26	mean_diff_res[1][4x16]	2.47
mean_diff_res[0][16x4]	2.06	sad_ac_p[1][4x16]	2.28	sad_sp_x3[32x4]	2.47
sub_weight[4x4]	2.06	mean_diff_res[1][8x8]	2.28	chroma_hps_12[5]	2.47
mean_diff_p[1][8x8]	2.07	mean_diff_res[1][16x2]	2.28	sad_pp[64x16]	2.48
calc_sign[16x64]	2.07	subtract_pix[16x4]	2.28	mean_diff_res[0][8x64]	2.49

Primitive	IPC Gain	Primitive	IPC Gain	Primitive	IPC Gain
sad_ac_res[0][4x8]	2.09	calc_sign[16x16]	2.28	sad_pp[4x16]	2.5
sub_weight[16x8]	2.09	sad_pp[16x2]	2.32	sad_pp[8x2]	2.5
sad_sp[32x64]	2.11	sad_pp[32x8]	2.33	mean_diff_p[0][32x4]	2.5
subtract_res[4x8]	2.12	sub_weight[16x16]	2.33	subtract_pix[16x32]	2.51
sub_weight[16x64]	2.13	sad_sp_x3[8x8]	2.35	sad_sp[4x32]	2.52
subtract_res[16x4]	2.15	subtract_pix[16x8]	2.37	sad_sp_x3[16x32]	2.52
subtract_res[16x16]	2.15	sad_sp[8x4]	2.39	sad_sp[64x32]	2.52
mean_diff_p[1][16x16]	2.16	sad_sp_x3[64x8]	2.39	sad_sp_x3[16x2]	2.53
sad_sp_x3[16x64]	2.16	subtract_pix[16x16]	2.39	mean_diff_res[0][16x64]	2.53
calc_sign[16x8]	2.16	rdo_sign_reapply[4x4]	2.39	subtract_pix[4x4]	2.53
sad_sp_x3[8x64]	2.17	calc_sign[8x4]	2.39	sad_sp[4x16]	2.54
mean_diff_p[0][4x16]	2.18	sub_weight[8x8]	2.4	mean_diff_p[0][16x2]	2.54
mean_diff_p[0][8x2]	2.18	sad_pp[8x4]	2.42	sad_pp[64x8]	2.54
mean_diff_p[1][8x4]	2.19	sad_sp[16x2]	2.42	sad_sp_x3[64x16]	2.54
mean_diff_res[1][8x16]	2.2	mean_diff_res[0][32x4]	2.42	mean_diff_p[0][64x64]	2.54
mean_diff_res[1][8x64]	2.2	sad_sp_x3[64x32]	2.42	copy_bipred[16x32]	2.54
mean_diff_res[0][16x2]	2.2	chroma_vss_12[4x2]	2.42	chroma_vsp_10[4x2]	2.54
sad_sp_x3[8x16]	2.21	subtract_pix[4x2]	2.43	sad_sp[4x8]	2.55
sad_sp[8x64]	2.23	sub_weight[16x32]	2.43	sad_ac_res[1][4x16]	2.55
sad_sp_x3[8x32]	2.24	sad_ac_p[0][32x4]	2.44	mean_diff_res[1][8x32]	2.55
copy_block[2]	2.55	sad_ac_res[1][16x4]	2.7	luma_hps_12[1]	2.83
sad_sp_x3[16x4]	2.56	mean_diff_res[1][32x4]	2.7	sad_pp[4x32]	2.84
sad_pp[64x64]	2.56	chroma_vpp_10[4x2]	2.7	subtract_pix[8x8]	2.84
sad_sp[64x8]	2.57	subtract_res[8x8]	2.7	sad_sp[32x4]	2.85
chroma_vss_10[4x2]	2.57	sub_weight[8x4]	2.7	luma_hps_12[2]	2.87
subtract_res[4x4]	2.57	rdo_clipmul[4x32]	2.7	mean_diff_p[1][64x32]	2.88
mean_diff_p[0][32x64]	2.59	sad_pp[8x64]	2.71	mean_diff_p[0][8x16]	2.89
mean_diff_res[0][64x64]	2.59	mean_diff_p[0][64x8]	2.71	mean_diff_p[0][8x32]	2.89
copy_bipred[16x16]	2.6	subtract_res[8x2]	2.72	sad_sp_x3[32x8]	2.89
sad_pp[4x4]	2.61	rdo_clipmul[4x2]	2.72	chroma_hps_12[1]	2.89
mean_diff_p[1][64x16]	2.61	sad_pp[32x16]	2.73	rdo_clipmul[4x4]	2.89
sad_sp[4x2]	2.62	chroma_vss_10[4x16]	2.73	sad_sp_x3[16x16]	2.9
mean_diff_res[0][4x32]	2.62	chroma_hps_10[5]	2.74	mean_diff_res[1][16x16]	2.91
sad_sp[64x16]	2.62	sad_pp[32x4]	2.75	sad_sp[32x32]	2.91
mean_diff_p[0][16x64]	2.63	luma_hpp_10[0]	2.75	mean_diff_p[1][64x64]	2.91
mean_diff_res[1][4x32]	2.64	subtract_pix[4x32]	2.75	copy_bipred[8x2]	2.92
sad_sp_x3[16x8]	2.64	mean_diff_p[0][4x8]	2.76	chroma_hps_10[3]	2.92
sad_pp[8x16]	2.66	mean_diff_res[1][32x16]	2.76	subtract_res[4x32]	2.92
add_clip_10[8x2]	2.66	chroma_hps_10[1]	2.76	mean_diff_p[1][4x32]	2.93
mean_diff_p[0][32x16]	2.67	sad_sp[4x4]	2.77	sad_sp[16x8]	2.94
subtract_res[16x2]	2.67	sad_pp[8x32]	2.77	chroma_vps_12[4x2]	2.94
sad_ac_res[1][4x32]	2.68	sad_pp[4x2]	2.79	chroma_vps_12[8x2]	2.94
mean_diff_res[0][8x4]	2.68	rdo_clipmul[4x8]	2.8	sad_pp[16x8]	2.95
mean_diff_p[1][16x4]	2.68	ssd_ss[4x2]	2.81	rdo_sign_reapply[4x32]	2.95
rdo_sign_reapply[4x2]	2.68	sad_pp[32x32]	2.81	rdo_clipmul[16x2]	2.95
mean_diff_p[1][8x64]	2.69	add_clip_10[4x2]	2.81	mean_diff_res[1][32x8]	2.96
sad_sp[8x8]	2.7	luma_hps_12[3]	2.82	mean_diff_res[0][8x32]	2.97
mean_diff_res[0][8x8]	2.7	sub_weight[16x4]	2.82	sad_sp[8x32]	2.98
sad_sp[8x16]	2.7	mean_diff_p[0][8x4]	2.83	copy_bipred[4x4]	2.98
mean_diff_p[1][8x16]	2.7	mean_diff_p[1][16x8]	2.83	subtract_pix[4x16]	2.98

Primitive	IPC Gain	Primitive	IPC Gain	Primitive	IPC Gain
chroma_vps_10[4x2]	2.99	mean_diff_res[1][32x64]	3.16	mean_diff_res[1][64x32]	3.32
sad_pp[8x8]	3	sub_weight[4x16]	3.17	chroma_vps_12[8x4]	3.32
mean_diff_res[1][16x64]	3	mean_diff_res[0][32x64]	3.18	luma_inv_quant_10b[4x4]	3.32
chroma_vss_10[8x8]	3	chroma_vps_10[8x2]	3.18	rdo_clipmul[4x16]	3.32
sub_weight[4x8]	3	rdo_sign_reapply[4x8]	3.18	rdo_sign_reapply[4x16]	3.32
mean_diff_res[0][16x8]	3.01	rdo_clipmul[8x32]	3.18	chroma_vsp_12[8x2]	3.33
mean_diff_p[1][32x8]	3.01	mean_diff_p[0][32x32]	3.19	calc_sign[8x2]	3.33
sad_sp[16x32]	3.02	luma_inv_quant_12b[8x4]	3.19	mean_diff_res[0][64x8]	3.34
mean_diff_p[0][16x8]	3.03	sad_sp[16x64]	3.2	subtract_res[8x64]	3.34
mean_diff_p[0][64x32]	3.03	mean_diff_p[0][32x8]	3.2	add_clip_12[4x4]	3.35
copy_bipred[16x64]	3.03	mean_diff_res[0][32x32]	3.2	rdo_clipmul[32x64]	3.35
rdo_num_nonzero[8x2]	3.03	luma_inv_quant_12b[4x4]	3.2	mean_diff_res[0][32x8]	3.36
sad_sp[64x64]	3.04	rdo_clipmul[8x2]	3.2	rdo_clipmul[8x64]	3.36
subtract_pix[16x2]	3.04	mean_diff_p[1][32x32]	3.22	chroma_vss_10[8x4]	3.37
mean_diff_p[0][4x32]	3.05	mean_diff_p[1][32x64]	3.22	chroma_vss_12[8x4]	3.37
sad_sp[16x4]	3.05	subtract_pix[8x64]	3.22	satd_sp[8x4]	3.38
sad_sp[16x16]	3.05	mean_diff_p[1][16x32]	3.24	chroma_vpp_10[4x4]	3.41
block_zero[64x32]	3.05	mean_diff_p[1][64x8]	3.24	mean_diff_res[1][64x16]	3.42
mean_diff_p[0][8x64]	3.06	chroma_vss_12[4x4]	3.25	subtract_pix[8x4]	3.42
chroma_vsp_12[4x2]	3.06	chroma_vpp_12[8x2]	3.25	ang_fast_copy[8x64]	3.42
rdo_clipmul[16x4]	3.07	mean_diff_res[1][64x8]	3.27	subtract_pix[8x32]	3.43
subtract_res[8x4]	3.09	rdo_clipmul[16x32]	3.27	rdo_sign_reapply[32x32]	3.45
mean_diff_res[0][16x16]	3.1	rdo_clipmul[8x16]	3.28	chroma_hps_12[4]	3.46
mean_diff_res[0][32x16]	3.11	rdo_clipmul[32x4]	3.28	luma_inv_quant_10b[4x16]	3.46
sad_pp[16x32]	3.13	mean_diff_p[0][64x16]	3.29	chroma_vsp_12[4x4]	3.47
mean_diff_res[0][16x32]	3.14	rdo_clipmul[8x8]	3.29	subtract_pix[8x2]	3.47
mean_diff_p[1][32x16]	3.14	mean_diff_res[0][64x32]	3.31	sub_weight[4x32]	3.47
sad_pp[16x64]	3.15	luma_hps_10[4]	3.31	rdo_sign_reapply[8x64]	3.47
mean_diff_res[1][32x32]	3.15	subtract_res[8x16]	3.31	rdo_clipmul[16x8]	3.47
mean_diff_p[0][16x32]	3.16	mean_diff_p[1][8x32]	3.32	rdo_clipmul[16x64]	3.47
copy_bipred[4x8]	3.48	chroma_vpp_12[8x32]	3.65	sad_pp[16x4]	3.87
ang_fast_copy[8x32]	3.49	chroma_vsp_10[8x32]	3.65	sad_pp[32x64]	3.89
sad_pp[4x8]	3.5	add_clip_12[4x8]	3.66	add_clip_10[8x4]	3.9
luma_hps_12[4]	3.51	rdo_clipmul[32x16]	3.66	block_zero[32x16]	3.9
chroma_hps_10[2]	3.52	rdo_clipmul[32x32]	3.68	ssd_sp[4x2]	3.92
chroma_vss_10[8x2]	3.52	block_zero[64x64]	3.69	satd_sp[32x16]	3.94
rdo_clipmul[16x16]	3.52	luma_inv_quant_10b[16x4]	3.69	luma_hps_12[0]	3.94
chroma_hps_12[3]	3.53	rdo_clipmul[32x8]	3.69	chroma_vps_12[4x8]	3.94
chroma_vss_10[4x8]	3.53	satd_pp[8x4]	3.7	satd_sp[64x32]	3.98
chroma_vss_12[8x2]	3.53	chroma_vss_10[4x4]	3.7	copy_bipred[4x16]	3.98
sub_weight[8x64]	3.53	add_clip_10[4x8]	3.7	rdo_sign_reapply[8x2]	3.98
chroma_vsp_10[8x4]	3.55	luma_inv_quant_12b[4x8]	3.7	add_avg_10[8x2]	3.99
subtract_res[4x16]	3.55	satd_sp[32x64]	3.71	chroma_vps_10[8x8]	3.99
sub_weight[8x16]	3.56	chroma_vpp_10[8x4]	3.71	luma_inv_quant_12b[8x32]	4
chroma_vps_12[4x4]	3.57	mean_diff_p[0][16x16]	3.72	add_clip_12[4x16]	4.03
luma_inv_quant_12b[4x16]	3.57	chroma_vps_10[4x4]	3.73	chroma_vps_10[8x4]	4.05
add_clip_10[4x4]	3.58	luma_inv_quant_10b[8x4]	3.73	add_clip_10[8x64]	4.06
block_zero[32x8]	3.58	add_clip_12[4x2]	3.75	add_clip_12[8x64]	4.07
rdo_clipmul[64x16]	3.6	sub_weight[8x32]	3.75	chroma_vpp_10[8x16]	4.08
chroma_hps_12[2]	3.61	luma_inv_quant_10b[4x8]	3.76	satd_sp[8x64]	4.09
mean_diff_res[1][64x64]	3.62	chroma_vsp_12[4x8]	3.77	luma_hpp_12[0]	4.1
copy_block[3]	3.62	chroma_vpp_10[8x2]	3.78	chroma_vps_10[4x8]	4.12
chroma_vpp_12[4x4]	3.63	satd_pp[16x4]	3.8	chroma_vps_12[8x8]	4.12
rdo_sign_reapply[8x4]	3.63	rdo_clipmul[64x64]	3.8	chroma_vsp_12[8x8]	4.12
rdo_clipmul[64x8]	3.63	calc_sign[8x32]	3.82	chroma_vps_12[8x16]	4.12
chroma_hps_10[4]	3.64	sad_pp[16x16]	3.83	chroma_vss_10[8x32]	4.12
subtract_pix[8x16]	3.64	chroma_vpp_12[4x2]	3.84	rdo_num_nonzero[8x4]	4.16
mean_diff_res[0][64x16]	3.65	ssd_pp[4x16]	3.85	chroma_vps_10[8x16]	4.17
copy_bipred[8x4]	3.65	luma_hpp_10[3]	3.85	ssd_pp[4x4]	4.18
luma_hpp_10[1]	3.65	chroma_vsp_10[4x4]	3.85	chroma_vss_12[8x8]	4.19

Primitive	IPC Gain	Primitive	IPC Gain	Primitive	IPC Gain
chroma_vpp_12[8x4]	4.2	luma_inv_quant_10b[16x64]	4.56	rdo_sign_reapply[16x64]	4.77
chroma_vpp_12[4x8]	4.23	chroma_vsp_10[8x2]	4.57	add_avg_10[8x16]	4.79
rdo_clipmul[8x4]	4.24	chroma_vsp_10[8x16]	4.57	chroma_vss_10[8x64]	4.79
chroma_vss_12[4x8]	4.25	ang_fast_copy[16x64]	4.57	luma_inv_quant_12b[16x64]	4.8
add_clip_10[4x32]	4.25	luma_inv_quant_10b[8x32]	4.57	chroma_vpp_12[4x32]	4.82
add_avg_12[8x2]	4.26	ssd_sp[4x16]	4.58	satd_sp[8x16]	4.84
add_clip_12[4x32]	4.27	satd_sp[8x8]	4.58	satd_pp[8x32]	4.84
luma_inv_quant_10b[16x8]	4.27	luma_hpp_12[1]	4.58	luma_hps_10[1]	4.84
ssd_pp[8x2]	4.28	add_clip_12[8x32]	4.58	chroma_vsp_12[8x64]	4.84
chroma_vss_12[8x16]	4.28	chroma_vps_10[16x8]	4.59	chroma_vss_10[8x16]	4.85
chroma_vpp_12[8x8]	4.3	rdo_sign_reapply[8x32]	4.59	chroma_vps_10[16x32]	4.85
rdo_clipmul[64x32]	4.31	satd_pp[8x8]	4.6	add_clip_10[8x8]	4.86
chroma_vss_12[4x16]	4.34	satd_pp[8x16]	4.6	luma_hpp_12[2]	4.87
copy_block[4]	4.34	chroma_vss_10[16x64]	4.6	luma_inv_quant_12b[4x32]	4.87
chroma_vsp_10[4x8]	4.35	add_clip_12[8x2]	4.6	luma_hpp_12[3]	4.88
ssd_ss[4x16]	4.39	satd_pp[32x8]	4.61	luma_hps_10[3]	4.89
luma_inv_quant_12b[16x4]	4.39	add_clip_10[8x32]	4.61	satd_pp[32x16]	4.9
add_clip_12[8x4]	4.4	chroma_vpp_10[8x8]	4.63	chroma_vpp_12[8x16]	4.9
ssd_pp[4x2]	4.42	luma_inv_quant_10b[16x16]	4.63	copy_bipred[4x32]	4.92
satd_pp[64x64]	4.42	chroma_vpp_10[4x8]	4.65	ssd_ss[8x2]	4.93
calc_sign[8x8]	4.43	ssd_sp[4x4]	4.66	chroma_vsp_12[8x4]	4.93
satd_pp[32x64]	4.44	luma_vpp_10[4x16]	4.67	chroma_vsp_10[32x8]	4.95
satd_sp[64x64]	4.45	luma_hps_10[0]	4.68	ssd_sp[4x8]	4.96
chroma_vsp_10[8x8]	4.45	luma_inv_quant_10b[8x8]	4.69	luma_vps_10[4x4]	4.97
add_clip_10[4x16]	4.46	chroma_vps_12[8x32]	4.72	satd_pp[16x16]	4.99
luma_vps_12[16x8]	4.49	copy_block[5]	4.72	chroma_vss_10[16x4]	4.99
satd_pp[32x4]	4.5	ang_fast_copy[8x4]	4.72	block_zero[32x64]	4.99
ssd_ss[4x4]	4.52	rdo_sign_reapply[32x64]	4.73	chroma_vpp_12[16x32]	5.01
luma_inv_quant_12b[8x8]	4.52	chroma_vpp_10[16x2]	4.75	luma_hps_10[2]	5.02
chroma_vpp_10[4x16]	4.53	luma_vss_10[4x4]	4.75	luma_vpp_12[8x4]	5.02
chroma_vss_12[8x32]	5.03	satd_sp[64x8]	5.24	chroma_vss_10[4x32]	5.45
luma_vps_12[4x4]	5.04	chroma_vps_12[32x64]	5.26	satd_sp[8x32]	5.46
copy_sample_byte	5.05	add_avg_10[8x4]	5.27	add_avg_12[8x4]	5.46
ang_fast_copy[8x16]	5.06	luma_inv_quant_12b[16x8]	5.27	luma_vps_10[4x8]	5.46
luma_inv_quant_10b[4x32]	5.06	ssd_pp[4x8]	5.29	block_zero[32x32]	5.46
satd_pp[16x8]	5.08	chroma_vss_12[16x4]	5.29	add_avg_10[8x8]	5.47
luma_hpp_12[4]	5.09	add_avg_10[8x32]	5.32	add_clip_10[16x2]	5.48
luma_inv_quant_10b[8x64]	5.09	chroma_vps_10[8x32]	5.33	rdo_sign_reapply[16x4]	5.48
luma_inv_quant_10b[64x16]	5.09	luma_vsp_12[4x4]	5.33	chroma_vps_12[4x16]	5.51
block_zero[16x8]	5.1	add_clip_10[8x16]	5.33	add_clip_12[16x2]	5.51
satd_sp[16x32]	5.11	add_clip_12[8x16]	5.33	ang_fast_copy[64x16]	5.51
add_clip_12[8x8]	5.11	luma_inv_quant_12b[8x16]	5.34	rdo_sign_reapply[64x16]	5.52
rdo_sign_reapply[8x16]	5.11	chroma_vss_10[16x8]	5.35	luma_vss_10[16x4]	5.53
luma_vss_12[16x8]	5.12	chroma_vss_10[16x2]	5.37	luma_inv_quant_10b[32x4]	5.53
ang_fast_copy[16x32]	5.13	satd_pp[16x64]	5.39	luma_inv_quant_12b[64x16]	5.53
satd_pp[32x32]	5.14	chroma_vps_12[16x2]	5.39	chroma_vpp_12[8x64]	5.54
luma_vps_10[8x4]	5.15	copy_bipred[8x8]	5.4	chroma_vss_12[64x64]	5.55
satd_sp[32x8]	5.16	chroma_vps_10[16x4]	5.4	luma_vpp_10[16x16]	5.55
luma_inv_quant_10b[32x64]	5.16	luma_inv_quant_10b[8x16]	5.4	rdo_num_nonzero[8x8]	5.55
satd_pp[64x8]	5.17	chroma_vps_10[4x16]	5.41	chroma_vps_10[16x64]	5.56
satd_pp[64x16]	5.17	chroma_vps_10[16x2]	5.41	chroma_vpp_12[16x2]	5.57
chroma_vss_12[16x2]	5.17	chroma_vss_12[16x8]	5.41	luma_vpp_12[4x4]	5.57
luma_hpp_10[2]	5.18	luma_vpp_10[4x4]	5.41	block_zero[32x4]	5.57
chroma_vsp_10[8x64]	5.19	luma_vsp_10[8x64]	5.41	chroma_vsp_12[64x16]	5.58
chroma_vsp_12[8x16]	5.2	chroma_vsp_12[8x32]	5.42	chroma_vps_12[16x8]	5.59
satd_sp[32x4]	5.21	chroma_vpp_10[8x32]	5.43	chroma_vpp_10[64x16]	5.59
luma_vss_12[4x4]	5.21	chroma_vps_10[16x16]	5.43	luma_vps_12[4x8]	5.59
satd_pp[8x64]	5.22	chroma_vsp_12[32x4]	5.43	luma_vss_12[4x8]	5.6
satd_sp[16x16]	5.22	chroma_vss_12[8x64]	5.44	chroma_vss_12[4x32]	5.62
chroma_vpp_12[16x8]	5.22	chroma_vsp_12[16x2]	5.44	chroma_vsp_12[64x64]	5.62

Primitive	IPC Gain	Primitive	IPC Gain	Primitive	IPC Gain
satd_sp[64x16]	5.63	ang_fast_copy[32x64]	5.81	chroma_vsp_12[16x8]	5.99
chroma_vps_12[64x16]	5.63	satd_sp[16x8]	5.83	chroma_vpp_12[64x64]	5.99
ang_fast_copy[32x8]	5.64	luma_inv_quant_12b[32x32]	5.83	luma_vsp_10[8x4]	5.99
ssd_pp[8x4]	5.65	ssd_ss[4x8]	5.84	calc_sign[8x16]	5.99
chroma_vpp_12[4x16]	5.65	luma_vps_12[8x8]	5.84	luma_vsp_12[16x32]	6
luma_inv_quant_12b[32x16]	5.65	luma_vsp_12[8x32]	5.84	luma_inv_quant_12b[32x4]	6
luma_inv_quant_12b[64x32]	5.66	rdo_sign_reapply[32x8]	5.84	calc_sign[8x64]	6
rdo_sign_reapply[16x8]	5.66	rdo_sign_reapply[32x16]	5.85	chroma_vpp_12[16x64]	6.01
ssd_sp[8x2]	5.67	chroma_vps_12[8x64]	5.86	rdo_sign_reapply[16x32]	6.01
luma_inv_quant_12b[8x64]	5.67	chroma_vpp_12[32x8]	5.86	chroma_vsp_12[4x16]	6.02
luma_inv_quant_10b[16x32]	5.67	chroma_vsp_12[32x8]	5.86	chroma_vpp_10[16x4]	6.02
chroma_vsp_12[32x64]	5.68	luma_vpp_10[8x4]	5.86	chroma_vpp_12[16x4]	6.02
satd_sp[32x32]	5.69	luma_vsp_12[8x4]	5.86	chroma_vsp_12[16x64]	6.02
add_avg_10[8x64]	5.69	rdo_sign_reapply[8x8]	5.86	ssd_pp[4x32]	6.03
chroma_vps_10[8x64]	5.69	ssd_ss[4x32]	5.87	chroma_vps_12[32x4]	6.03
luma_vpp_10[8x8]	5.7	luma_vpp_10[4x8]	5.88	rdo_sign_reapply[16x16]	6.03
luma_vsp_10[8x8]	5.7	luma_inv_quant_10b[32x32]	5.89	chroma_vps_10[4x32]	6.04
luma_vpp_10[16x32]	5.7	chroma_vsp_10[32x16]	5.9	chroma_vss_10[32x4]	6.04
luma_vps_12[8x4]	5.71	luma_vpp_12[4x8]	5.9	luma_vsp_12[16x64]	6.04
ang_fast_copy[32x4]	5.71	luma_vss_10[4x8]	5.9	copy_bipred[8x16]	6.05
rdo_sign_reapply[64x64]	5.71	luma_vss_10[8x4]	5.91	chroma_vps_10[32x4]	6.05
ssd_ss[8x4]	5.73	rdo_num_nonzero[16x4]	5.91	luma_vsp_10[4x4]	6.05
chroma_vsp_10[16x2]	5.73	satd_sp[16x64]	5.92	luma_inv_quant_10b[64x8]	6.05
ang_fast_copy[16x4]	5.74	luma_vps_12[32x16]	5.92	add_clip_12[16x4]	6.07
luma_inv_quant_12b[16x32]	5.74	luma_inv_quant_10b[64x32]	5.92	chroma_vpp_12[32x32]	6.08
luma_hpp_10[4]	5.76	luma_vss_12[8x4]	5.94	chroma_vss_10[64x8]	6.08
rdo_sign_reapply[16x2]	5.77	rdo_num_nonzero[16x2]	5.94	satd_sp[16x4]	6.09
luma_vss_10[8x8]	5.78	luma_inv_quant_12b[16x16]	5.95	luma_vss_12[8x8]	6.1
chroma_vsp_10[32x4]	5.8	chroma_vpp_12[64x32]	5.96	add_clip_10[16x8]	6.1
luma_inv_quant_10b[64x64]	5.8	ang_fast_copy[16x2]	5.96	luma_vpp_12[16x4]	6.11
block_zero[4x2]	6.11	luma_vps_10[64x32]	6.32	chroma_vps_12[16x32]	6.57
chroma_vsp_10[64x32]	6.12	chroma_vsp_10[16x16]	6.33	chroma_vpp_10[16x16]	6.58
chroma_vss_12[32x8]	6.13	ssd_sp[4x32]	6.34	chroma_vps_10[64x64]	6.58
chroma_vps_12[4x32]	6.14	luma_vsp_10[32x64]	6.34	add_avg_12[8x32]	6.6
luma_vps_10[8x64]	6.14	ang_fast_copy[64x64]	6.35	chroma_vss_10[64x64]	6.61
chroma_vsp_10[4x16]	6.15	luma_vsp_10[4x8]	6.38	luma_vps_10[16x32]	6.61
chroma_vpp_10[16x64]	6.15	luma_vpp_10[32x64]	6.38	luma_vss_12[64x64]	6.61
add_avg_12[8x8]	6.17	luma_vpp_10[64x32]	6.38	chroma_vss_12[32x4]	6.62
add_avg_12[16x2]	6.17	chroma_vsp_12[16x16]	6.39	luma_vpp_12[64x8]	6.63
ang_fast_copy[64x32]	6.17	luma_vpp_12[8x8]	6.39	add_avg_12[8x16]	6.64
chroma_vsp_10[16x8]	6.18	luma_vsp_10[8x16]	6.41	add_clip_10[16x64]	6.64
ang_fast_copy[32x32]	6.19	luma_inv_quant_12b[64x8]	6.41	luma_vpp_10[8x64]	6.7
add_clip_12[32x64]	6.19	rdo_sign_reapply[32x4]	6.41	chroma_vps_10[32x32]	6.71
luma_vps_12[64x32]	6.2	chroma_vss_10[16x16]	6.43	luma_vsp_12[4x32]	6.71
luma_inv_quant_10b[32x8]	6.2	add_clip_10[16x4]	6.43	chroma_vps_12[16x16]	6.72
rdo_sign_reapply[64x8]	6.2	luma_vpp_10[4x32]	6.45	chroma_vss_10[32x8]	6.72
luma_vss_10[4x16]	6.23	luma_vsp_12[4x8]	6.46	rdo_num_nonzero[16x8]	6.73
luma_vps_12[16x4]	6.23	luma_vps_12[8x16]	6.46	luma_vsp_10[64x16]	6.76
luma_vsp_12[64x8]	6.26	chroma_vss_12[32x64]	6.47	rdo_num_nonzero[32x4]	6.77
chroma_vsp_10[16x4]	6.27	luma_vsp_10[32x32]	6.47	luma_vpp_10[8x16]	6.78
chroma_vpp_12[32x4]	6.27	chroma_vsp_10[4x32]	6.48	luma_vpp_10[64x16]	6.78
chroma_vps_10[32x8]	6.27	chroma_vsp_10[32x32]	6.48	copy_bipred[8x64]	6.79
luma_vsp_12[8x8]	6.27	satd_pp[64x32]	6.49	chroma_vpp_12[16x16]	6.79
luma_vps_10[8x8]	6.28	luma_vpp_12[8x32]	6.49	luma_vsp_12[8x64]	6.79
luma_vsp_10[16x32]	6.28	add_avg_12[8x64]	6.52	luma_vss_12[32x32]	6.79
chroma_vss_12[32x32]	6.29	luma_inv_quant_10b[32x16]	6.53	luma_vpp_12[64x32]	6.79
block_zero[16x4]	6.29	ang_fast_copy[16x16]	6.54	ssd_ss[16x8]	6.8
chroma_vsp_12[4x32]	6.3	chroma_vps_12[32x16]	6.55	luma_vsp_12[16x4]	6.81
luma_inv_quant_12b[32x8]	6.3	chroma_vpp_10[32x32]	6.56	chroma_vps_10[64x16]	6.84
add_clip_12[32x32]	6.31	luma_vsp_10[64x32]	6.56	ssd_ss[16x4]	6.85

Primitive	IPC Gain	Primitive	IPC Gain	Primitive	IPC Gain
add_clip_12[16x32]	6.85	luma_vps_12[4x32]	7.03	ssd_pp[32x4]	7.27
add_avg_12[16x8]	6.86	luma_vsp_12[64x32]	7.03	luma_vss_10[8x16]	7.27
chroma_vsp_10[64x8]	6.86	chroma_vpp_10[16x32]	7.05	ang_fast_copy[16x8]	7.27
ang_fast_copy[64x8]	6.86	luma_vps_10[4x16]	7.05	chroma_vps_10[64x8]	7.29
satd_pp[16x32]	6.87	chroma_vpp_10[8x64]	7.07	copy_bipred[8x32]	7.32
chroma_vpp_10[32x16]	6.87	luma_vsp_10[16x8]	7.07	luma_vpp_12[4x32]	7.32
chroma_vpp_10[32x8]	6.88	chroma_vsp_10[64x16]	7.08	add_clip_10[16x16]	7.33
luma_vss_12[16x4]	6.88	chroma_vsp_10[16x32]	7.11	chroma_vps_10[32x16]	7.34
luma_vps_10[32x8]	6.88	chroma_vss_12[16x32]	7.13	add_avg_10[32x64]	7.36
ssd_pp[16x2]	6.89	chroma_vss_12[32x16]	7.13	chroma_vpp_10[32x4]	7.36
chroma_vps_12[64x8]	6.89	chroma_vss_12[16x64]	7.14	luma_vps_10[16x4]	7.36
luma_vss_10[32x4]	6.9	add_clip_10[64x64]	7.14	luma_vpp_10[16x8]	7.36
chroma_vps_12[32x8]	6.91	luma_inv_quant_12b[32x64]	7.14	luma_vpp_10[32x32]	7.36
luma_vps_10[4x32]	6.92	luma_vps_12[64x16]	7.15	add_avg_12[32x64]	7.37
chroma_vps_12[32x32]	6.93	add_clip_12[16x8]	7.15	chroma_vpp_10[64x32]	7.37
luma_vss_12[8x16]	6.93	chroma_vsp_12[16x32]	7.16	add_avg_12[16x4]	7.38
rdo_sign_reapply[64x32]	6.93	chroma_vss_10[32x32]	7.16	luma_vss_10[8x32]	7.38
chroma_vpp_12[32x16]	6.94	chroma_vss_12[64x16]	7.16	chroma_vsp_12[32x32]	7.39
luma_vps_12[4x16]	6.95	luma_vpp_12[4x16]	7.16	luma_vss_12[4x16]	7.39
luma_vss_10[8x64]	6.96	luma_vss_10[16x8]	7.17	luma_vss_10[16x64]	7.39
luma_vsp_10[16x4]	6.96	luma_vss_12[16x64]	7.17	chroma_vss_10[16x32]	7.42
add_clip_10[16x32]	6.96	add_clip_12[16x64]	7.17	chroma_vpp_12[64x8]	7.42
luma_vps_12[64x64]	6.99	luma_vps_10[8x16]	7.18	luma_vsp_12[16x8]	7.42
ang_fast_copy[32x16]	6.99	luma_vpp_12[8x16]	7.19	luma_vss_10[16x32]	7.44
chroma_vss_10[32x64]	7	add_avg_10[16x2]	7.2	luma_vss_10[64x32]	7.44
rdo_num_nonzero[8x16]	7	luma_vsp_12[8x16]	7.2	chroma_vpp_10[32x64]	7.45
add_avg_10[16x32]	7.01	luma_vps_10[16x16]	7.24	chroma_vpp_10[64x8]	7.45
chroma_vss_12[64x8]	7.01	ssd_sp[8x8]	7.25	luma_vsp_10[8x32]	7.45
luma_vpp_10[32x16]	7.01	chroma_vsp_12[32x16]	7.25	luma_vps_10[16x8]	7.46
luma_vss_10[32x16]	7.01	luma_vpp_12[16x8]	7.26	luma_vps_10[64x16]	7.47
ssd_sp[8x4]	7.48	luma_vps_12[16x16]	7.77	luma_vps_12[64x8]	8.09
add_avg_10[16x4]	7.48	ssd_ss[8x16]	7.79	chroma_vsp_10[16x64]	8.1
luma_vpp_10[16x4]	7.48	add_avg_12[32x4]	7.79	luma_vss_12[32x4]	8.1
chroma_vps_12[16x64]	7.49	chroma_vpp_12[64x16]	7.79	add_clip_12[16x16]	8.1
luma_vps_12[8x32]	7.5	add_clip_12[32x4]	7.79	luma_vss_12[64x16]	8.16
luma_vps_12[16x32]	7.51	ssd_sp[16x8]	7.8	luma_vss_10[32x8]	8.17
chroma_vps_10[64x32]	7.53	luma_vss_12[8x32]	7.84	add_avg_10[16x16]	8.18
ssd_sp[16x2]	7.54	luma_vpp_12[32x4]	7.85	add_avg_10[64x64]	8.18
add_clip_10[32x64]	7.54	ssd_ss[32x4]	7.87	luma_vps_12[32x8]	8.18
luma_vps_12[16x64]	7.57	luma_vsp_10[16x16]	7.87	luma_vsp_10[64x8]	8.21
luma_vps_10[8x32]	7.58	add_clip_10[32x16]	7.88	luma_vsp_12[32x64]	8.24
chroma_vss_10[64x32]	7.59	rdo_num_nonzero[8x32]	7.88	rdo_num_nonzero[8x64]	8.25
chroma_vsp_12[64x8]	7.62	chroma_vss_10[32x16]	7.9	chroma_vpp_10[4x32]	8.26
luma_vps_10[32x4]	7.62	add_avg_12[16x64]	7.91	luma_vsp_12[32x4]	8.28
luma_vsp_12[32x8]	7.64	chroma_vsp_12[16x4]	7.93	ssd_pp[16x4]	8.3
ssd_sp[32x4]	7.65	chroma_vpp_10[16x8]	7.93	ssd_sp[32x8]	8.3
luma_inv_quant_12b[64x64]	7.65	add_avg_10[16x8]	7.96	ssd_ss[16x2]	8.33
rdo_num_nonzero[32x8]	7.66	chroma_vpp_12[32x64]	7.96	add_avg_12[16x32]	8.33
luma_vss_12[4x32]	7.68	chroma_vss_10[64x16]	8	luma_vss_10[4x32]	8.35
luma_vss_12[32x8]	7.68	chroma_vps_12[64x32]	8	luma_vpp_12[32x8]	8.37
luma_vsp_12[32x16]	7.68	chroma_vsp_10[32x64]	8.01	ssd_pp[16x16]	8.38
luma_vpp_12[64x16]	7.68	add_avg_10[16x64]	8.02	luma_vsp_12[32x32]	8.38
ssd_sp[16x4]	7.69	add_avg_10[32x16]	8.03	luma_vps_10[32x32]	8.41
luma_vss_12[8x64]	7.69	luma_vsp_10[32x4]	8.03	luma_vss_12[16x32]	8.42
luma_vpp_12[16x64]	7.69	add_clip_10[32x8]	8.05	luma_vss_10[64x64]	8.44
ssd_ss[8x8]	7.7	rdo_num_nonzero[16x16]	8.05	add_avg_12[64x16]	8.45
luma_vsp_12[4x16]	7.7	luma_vpp_12[16x16]	8.06	luma_vps_10[64x8]	8.46
luma_vpp_12[16x32]	7.74	luma_vpp_12[32x64]	8.06	chroma_vss_12[16x16]	8.47
luma_vsp_10[32x16]	7.76	luma_vpp_10[32x4]	8.08	add_clip_12[32x8]	8.48
add_clip_10[32x32]	7.76	luma_vpp_10[8x32]	8.09	ssd_pp[16x8]	8.49

Primitive	IPC Gain	Primitive	IPC Gain	Primitive	IPC Gain
chroma_vss_12[64x32]	8.49	luma_vss_12[32x64]	8.74	rdo_num_nonzero[32x32]	9.62
chroma_vps_12[64x64]	8.49	add_clip_12[64x16]	8.77	ang_fast_copy[8x8]	9.65
luma_vps_10[32x64]	8.49	luma_vss_12[32x16]	8.83	add_clip_12[64x8]	9.7
block_zero[16x32]	8.5	add_avg_12[32x16]	8.89	luma_vss_10[32x32]	9.71
luma_vpp_10[32x8]	8.51	luma_vpp_10[64x8]	8.93	add_clip_10[64x8]	9.75
chroma_vpp_10[64x64]	8.52	luma_vpp_12[32x32]	8.98	rdo_num_nonzero[64x32]	9.77
ssd_pp[32x8]	8.53	luma_vss_12[64x8]	9.02	block_zero[8x2]	9.86
ssd_sp[8x16]	8.55	rdo_num_nonzero[16x64]	9.02	add_clip_12[64x64]	9.88
ssd_ss[32x8]	8.55	luma_vsp_10[16x64]	9.03	add_avg_12[32x8]	9.9
block_zero[16x16]	8.55	luma_vss_10[16x16]	9.09	add_avg_12[64x32]	9.9
add_clip_10[32x4]	8.55	luma_vpp_12[32x16]	9.09	add_avg_10[32x4]	10.06
ssd_ss[8x32]	8.59	add_avg_10[32x8]	9.12	block_zero[16x2]	10.39
luma_vss_10[64x16]	8.59	luma_vpp_12[8x64]	9.12	add_avg_12[64x8]	10.43
chroma_vsp_12[64x32]	8.6	add_avg_10[32x32]	9.13	luma_vps_10[64x64]	10.45
luma_vsp_10[4x32]	8.61	chroma_vps_12[16x4]	9.14	luma_vps_10[16x64]	10.48
block_zero[8x8]	8.62	luma_vsp_10[4x16]	9.2	add_avg_10[64x16]	10.51
block_zero[16x64]	8.62	luma_vsp_12[16x16]	9.2	rdo_num_nonzero[64x16]	10.56
chroma_vps_10[32x64]	8.63	luma_vsp_12[64x16]	9.2	rdo_num_nonzero[32x64]	10.58
add_avg_12[16x16]	8.65	luma_vss_12[64x32]	9.24	ssd_sp[32x16]	10.65
ssd_ss[16x16]	8.66	luma_vss_10[64x8]	9.26	luma_vsp_12[64x64]	10.73
ssd_pp[32x16]	8.67	ssd_pp[8x16]	9.28	add_avg_12[32x32]	10.82
rdo_num_nonzero[16x32]	8.67	rdo_num_nonzero[32x16]	9.4	add_avg_10[64x8]	10.87
luma_vss_12[16x16]	8.68	add_clip_10[64x16]	9.42	luma_vps_10[32x16]	10.99
ssd_pp[8x8]	8.69	ssd_sp[16x16]	9.46	add_avg_10[64x32]	11.13
add_clip_12[32x16]	8.69	luma_vpp_10[16x64]	9.46	luma_vpp_12[64x64]	11.13
add_clip_10[64x32]	8.69	add_avg_12[64x64]	9.5	block_zero[8x16]	11.16
ssd_sp[8x32]	8.71	luma_vps_12[32x4]	9.51	luma_vsp_10[64x64]	11.22
luma_vss_10[32x64]	8.72	luma_vps_12[32x64]	9.51	block_zero[8x32]	11.39
ssd_pp[8x32]	8.73	chroma_vsp_10[64x64]	9.6	luma_vps_12[8x64]	11.44
luma_vpp_10[64x64]	8.73	rdo_num_nonzero[64x8]	9.6	luma_vps_12[32x32]	11.46
luma_vsp_10[32x8]	11.6	block_zero[4x4]	15.31	block_zero[4x32]	29.09
block_zero[8x64]	11.85	block_zero[8x4]	20.03	block_zero[4x8]	39.21
add_clip_12[64x32]	12.56	block_zero[4x16]	24.86		

# Appendix C

## AVX2 SIMD optimization

Primitive	IPC Gain	Primitive	IPC Gain	Primitive	IPC Gain
dst4[2]	1.02	sad_ac_p[0][8x4]	1.75	sad_ac_res[0][64x32]	1.96
dst4[1]	1.04	sad_ac_p[0][16x4]	1.77	subtract_res[32x64]	1.97
sad_ac_p[1][8x2]	1.22	sad_ac_res[1][64x16]	1.77	sad_ac_res[1][32x32]	1.99
mean_diff_res[1][8x2]	1.24	sad_ac_p[0][32x4]	1.79	sad_ac_res[1][8x16]	2
sad_ac_res[1][16x2]	1.26	copy_bipred[32x4]	1.79	sad_ac_res[1][64x64]	2
sad_ac_res[0][8x4]	1.35	subtract_res[32x16]	1.79	subtract_pix[32x8]	2
sad_ac_p[0][8x2]	1.4	sad_ac_res[1][64x8]	1.81	sub_weight[32x16]	2
copy_bipred[16x2]	1.44	subtract_res[32x4]	1.81	sad_ac_p[1][16x8]	2.02
sad_ac_res[1][8x2]	1.48	sad_ac_p[0][64x8]	1.83	sad_ac_p[0][8x16]	2.03
sad_ac_p[1][16x2]	1.49	sad_ac_p[1][8x4]	1.85	sad_ac_p[0][32x32]	2.04
mean_diff_p[1][8x2]	1.53	sad_ac_p[1][32x8]	1.85	sad_ac_p[1][32x16]	2.07
mean_diff_res[1][16x2]	1.56	sad_ac_res[0][16x4]	1.87	subtract_pix[64x8]	2.07
subtract_pix[32x16]	1.57	sad_ac_res[1][32x16]	1.87	sad_ac_res[0][32x64]	2.08
subtract_pix[64x16]	1.58	copy_bipred[32x32]	1.87	subtract_res[32x32]	2.08
sad_ac_p[1][32x4]	1.59	subtract_pix[32x32]	1.87	sub_weight[32x8]	2.09
sad_ac_res[1][8x8]	1.62	subtract_res[64x8]	1.88	sad_ac_p[0][64x16]	2.11

Primitive	IPC Gain	Primitive	IPC Gain	Primitive	IPC Gain
sad_ac_p[0][16x2]	1.62	sad_ac_res[0][8x2]	1.91	sad_ac_p[1][32x64]	2.12
sad_ac_p[1][16x4]	1.62	sad_ac_res[1][8x4]	1.91	subtract_res[32x8]	2.12
sad_ac_p[0][32x64]	1.62	sad_ac_p[0][16x8]	1.91	sad_ac_res[1][32x64]	2.13
copy_bipred[64x64]	1.62	sad_ac_p[1][64x8]	1.91	sub_weight[64x32]	2.13
subtract_pix[32x4]	1.62	sad_ac_res[1][64x32]	1.91	sad_ac_res[1][32x8]	2.14
copy_bipred[32x16]	1.63	subtract_pix[32x64]	1.91	sub_weight[64x16]	2.14
sad_ac_p[1][64x64]	1.65	sad_ac_res[1][16x16]	1.92	sad_ac_res[0][32x8]	2.15
sub_weight[32x4]	1.67	sad_ac_res[0][32x4]	1.92	sad_ac_res[0][8x32]	2.17
sad_ac_res[0][16x2]	1.68	sad_ac_res[0][64x64]	1.92	sad_ac_res[1][16x32]	2.17
sad_ac_p[0][64x32]	1.69	sad_ac_p[1][8x32]	1.93	sad_ac_p[0][32x16]	2.17
sad_ac_p[0][64x64]	1.72	sad_ac_res[0][8x16]	1.94	sad_ac_res[1][32x4]	2.18
mean_diff_p[1][16x2]	1.74	sad_ac_res[0][16x64]	1.94	sad_ac_res[0][64x8]	2.18
sad_ac_res[1][16x4]	1.74	copy_bipred[16x4]	1.95	subtract_pix[64x64]	2.18
copy_bipred[64x16]	1.74	sad_ac_p[1][64x16]	1.96	sad_ac_p[0][8x32]	2.19
sad_ac_p[1][64x32]	2.19	sad_ac_p[0][8x64]	2.48	subtract_res[16x4]	2.96
sub_weight[32x64]	2.19	sad_ac_p[0][16x64]	2.49	sad_ac_p[0][32x8]	2.98
sad_ac_p[1][8x16]	2.21	sad_ac_p[0][16x16]	2.5	calc_sign[16x2]	2.99
sad_ac_res[0][16x16]	2.21	sub_weight[16x4]	2.5	mean_diff_res[1][16x32]	3
sad_ac_res[0][32x16]	2.21	subtract_pix[16x2]	2.52	sub_weight[16x16]	3
subtract_pix[64x32]	2.21	mean_diff_p[1][8x4]	2.53	mean_diff_res[0][16x2]	3.03
sub_weight[64x8]	2.21	subtract_pix[16x4]	2.53	calc_sign[32x32]	3.06
subtract_res[64x64]	2.22	mean_diff_p[0][8x2]	2.54	mean_diff_res[1][8x16]	3.07
sad_pp[16x2]	2.23	sad_ac_p[1][8x64]	2.57	mean_diff_res[0][8x8]	3.08
sad_ac_res[0][32x32]	2.23	mean_diff_res[1][16x4]	2.57	mean_diff_p[1][8x8]	3.11
sad_ac_res[1][16x8]	2.25	sad_ac_res[0][16x8]	2.59	calc_sign[32x8]	3.11
sad_ac_p[1][32x32]	2.26	sad_ac_p[1][16x32]	2.59	struct_ssd_block_s_4	3.12
sad_ac_res[0][8x8]	2.27	copy_bipred[32x8]	2.61	sad_sp_x3[16x8]	3.14
sub_weight[32x32]	2.31	sub_weight[64x64]	2.64	calc_sign[16x4]	3.14
copy_bipred[64x8]	2.33	sad_ac_res[1][16x64]	2.65	copy_bipred[16x16]	3.17
subtract_res[16x2]	2.34	struct_ssd_block_p_4	2.65	mean_diff_p[0][16x2]	3.2
subtract_res[64x32]	2.34	sad_ac_p[0][8x8]	2.66	sad_sp_x3[64x32]	3.2
mean_diff_res[0][8x2]	2.37	mean_diff_res[1][8x4]	2.68	sad_sp_x4[16x4]	3.21
sad_ac_res[1][8x32]	2.37	sad_sp_x4[64x64]	2.69	mean_diff_res[0][16x4]	3.21
subtract_res[64x16]	2.37	mean_diff_res[1][8x8]	2.71	sad_pp[16x4]	3.23
sad_sp_x4[16x2]	2.38	copy_bipred[32x64]	2.72	subtract_pix[16x64]	3.24
sad_ac_p[1][16x16]	2.38	sad_ac_res[1][8x64]	2.74	subtract_res[16x64]	3.26
sad_ac_res[0][64x16]	2.38	sad_sp_x4[32x64]	2.75	calc_sign[64x16]	3.3
copy_bipred[64x32]	2.38	mean_diff_p[0][8x4]	2.76	mean_diff_p[1][16x4]	3.34
subtract_pix[16x8]	2.39	calc_sign[32x16]	2.77	sad_sp_x4[32x4]	3.41
sad_sp_x3[16x2]	2.4	mean_diff_res[0][8x4]	2.79	mean_diff_p[1][8x16]	3.42
sad_ac_p[1][8x8]	2.41	mean_diff_p[0][8x8]	2.8	sad_sp[16x4]	3.45
sad_ac_res[0][16x32]	2.41	copy_bipred[16x8]	2.8	mean_diff_res[1][16x8]	3.45
sad_ac_p[0][16x32]	2.44	sad_ac_p[1][16x64]	2.83	mean_diff_p[0][16x8]	3.47
sad_ac_res[0][8x64]	2.45	calc_sign[32x4]	2.83	sad_sp_x3[32x4]	3.47

Primitive	IPC Gain	Primitive	IPC Gain	Primitive	IPC Gain
sad_sp_x3[32x64]	3.48	luma_inv_quant_10b[8x4]	3.84	mean_diff_p[0][8x16]	4.19
sad_sp_x4[32x16]	3.52	mean_diff_res[0][8x32]	3.87	subtract_res[16x32]	4.19
sub_weight[16x32]	3.53	sad_sp_x4[64x8]	3.88	mean_diff_res[1][64x16]	4.2
mean_diff_p[1][16x16]	3.55	block_zero[64x8]	3.9	mean_diff_p[0][8x32]	4.22
sub_weight[16x64]	3.55	mean_diff_res[1][8x32]	3.92	copy_bipred[16x64]	4.23
sad_sp_x4[16x8]	3.56	mean_diff_res[0][32x8]	3.92	sad_sp_x3[16x16]	4.25
mean_diff_p[0][64x16]	3.57	rdo_clipmul[8x4]	3.93	block_zero[64x64]	4.29
sad_sp_x4[32x8]	3.58	calc_sign[64x64]	3.94	mean_diff_p[0][8x64]	4.3
subtract_pix[16x16]	3.59	sub_weight[16x8]	3.97	mean_diff_p[1][64x32]	4.31
sad_sp_x3[16x4]	3.6	ang_fast_copy[16x2]	3.98	mean_diff_res[0][16x64]	4.34
subtract_pix[16x32]	3.61	rdo_clipmul[8x64]	3.99	mean_diff_res[0][16x8]	4.35
calc_sign[32x64]	3.61	sad_sp_x3[64x8]	4	mean_diff_res[0][64x64]	4.35
mean_diff_res[0][8x16]	3.62	mean_diff_res[0][64x32]	4	mean_diff_p[1][16x64]	4.38
calc_sign[16x8]	3.63	rdo_clipmul[16x64]	4	mean_diff_p[1][8x32]	4.4
mean_diff_p[1][16x8]	3.65	sad_pp[32x4]	4.02	rdo_clipmul[64x32]	4.4
mean_diff_res[1][32x4]	3.67	mean_diff_res[1][16x16]	4.03	mean_diff_res[0][32x64]	4.41
sad_sp_x3[32x16]	3.67	mean_diff_res[0][32x4]	4.05	rdo_clipmul[8x8]	4.41
mean_diff_p[1][32x4]	3.68	sad_sp_x4[64x32]	4.05	rdo_num_nonzero[16x2]	4.42
calc_sign[64x8]	3.69	sad_pp[16x8]	4.06	copy_bipred[16x32]	4.43
luma_inv_quant_12b[8x4]	3.7	sad_sp_x4[32x32]	4.06	sad_sp[64x32]	4.44
sad_sp_x3[16x64]	3.71	mean_diff_p[0][64x64]	4.08	mean_diff_res[0][32x16]	4.45
subtract_res[16x8]	3.71	calc_sign[16x32]	4.08	rdo_clipmul[32x16]	4.46
rdo_clipmul[8x2]	3.71	sad_sp[32x4]	4.09	sad_sp_x3[32x32]	4.47
sad_sp_x4[16x64]	3.75	mean_diff_res[1][8x64]	4.11	sad_sp[32x8]	4.49
calc_sign[64x32]	3.75	sad_sp_x4[16x16]	4.12	sad_sp_x3[64x64]	4.5
calc_sign[16x64]	3.76	mean_diff_res[1][32x8]	4.12	mean_diff_p[1][32x8]	4.51
subtract_res[16x16]	3.77	mean_diff_res[0][16x16]	4.13	rdo_clipmul[16x2]	4.51
calc_sign[16x16]	3.78	sad_sp_x3[32x8]	4.16	rdo_clipmul[16x4]	4.52
copy_block[3]	3.83	mean_diff_res[0][8x64]	4.17	sad_pp[64x64]	4.53
mean_diff_p[0][16x4]	3.84	mean_diff_p[1][64x64]	4.18	block_zero[64x16]	4.53
mean_diff_res[1][32x16]	4.57	rdo_clipmul[16x16]	4.99	struct_ssd_block_s_8	5.7
mean_diff_p[0][64x32]	4.57	mean_diff_p[0][32x32]	5.02	luma_inv_quant_12b[16x8]	5.7
mean_diff_res[0][32x32]	4.59	mean_diff_p[1][32x32]	5.02	struct_ssd_block_p_8	5.72
sad_sp[64x8]	4.6	rdo_clipmul[64x16]	5.02	ang_fast_copy[64x8]	5.72
sad_sp_x4[16x32]	4.66	mean_diff_res[0][64x8]	5.03	sad_sp[32x32]	5.73
sad_sp_x3[64x16]	4.66	rdo_clipmul[32x64]	5.03	rdo_clipmul[8x32]	5.76
mean_diff_p[0][32x4]	4.68	mean_diff_p[0][32x16]	5.04	sad_pp[16x16]	5.77
mean_diff_p[0][16x64]	4.7	luma_inv_quant_10b[8x8]	5.07	satd_pp[16x4]	5.78
luma_inv_quant_12b[8x8]	4.71	rdo_clipmul[8x16]	5.08	sad_pp[32x32]	5.79
mean_diff_p[1][8x64]	4.72	sad_sp[16x16]	5.1	sad_sp[64x64]	5.79
sad_pp[64x32]	4.72	rdo_clipmul[64x64]	5.11	mean_diff_p[1][32x64]	5.81
rdo_clipmul[16x8]	4.72	sad_sp[64x16]	5.12	rdo_num_nonzero[16x4]	6.02
mean_diff_p[0][32x8]	4.73	mean_diff_res[1][64x8]	5.13	mean_diff_res[1][64x32]	6.03
sad_sp[16x2]	4.74	luma_hpp_12[0]	5.14	rdo_sign_reapply[16x4]	6.04
sad_sp_x3[16x32]	4.75	luma_hpp_10[0]	5.17	luma_inv_quant_10b[16x4]	6.08
mean_diff_p[0][16x32]	4.75	sad_pp[64x8]	5.2	sad_pp[32x64]	6.16
sad_pp[32x8]	4.75	mean_diff_p[0][32x64]	5.23	sad_sp[32x64]	6.21
mean_diff_res[0][64x16]	4.75	mean_diff_p[1][64x8]	5.33	luma_inv_quant_12b[32x4]	6.24
mean_diff_p[0][16x16]	4.76	sad_sp[16x8]	5.37	sad_sp[16x32]	6.31
mean_diff_res[1][32x32]	4.78	luma_inv_quant_10b[8x16]	5.37	ang_fast_copy[16x64]	6.34
mean_diff_res[1][32x64]	4.82	mean_diff_res[0][16x32]	5.44	sad_pp[16x32]	6.35
block_zero[64x32]	4.83	luma_inv_quant_12b[8x16]	5.46	rdo_clipmul[32x32]	6.37
mean_diff_p[1][64x16]	4.85	sad_pp[64x16]	5.53	luma_vsp_10[32x4]	6.56
mean_diff_res[1][16x64]	4.89	sad_pp[32x16]	5.54	luma_vss_10[4x4]	6.57
mean_diff_res[1][64x64]	4.9	rdo_clipmul[32x8]	5.55	copy_block[4]	6.71
mean_diff_p[1][16x32]	4.92	ssd_sp[16x2]	5.62	luma_inv_quant_12b[16x4]	6.73
mean_diff_p[1][32x16]	4.94	rdo_sign_reapply[16x2]	5.63	add_clip_12[16x2]	6.74
sad_sp_x4[64x16]	4.95	luma_vsp_12[4x4]	5.67	luma_vss_12[4x4]	6.78
rdo_clipmul[32x4]	4.95	mean_diff_p[0][64x8]	5.68	sad_pp[16x64]	6.8
rdo_clipmul[16x32]	4.96	rdo_clipmul[64x8]	5.69	rdo_sign_reapply[64x32]	6.9

Primitive	IPC Gain	Primitive	IPC Gain	Primitive	IPC Gain
luma_inv_quant_12b[8x32]	6.95	luma_inv_quant_12b[32x32]	7.8	luma_inv_quant_12b[8x64]	8.4
luma_inv_quant_10b[8x32]	6.97	add_avg_12[16x2]	7.84	copy_block[5]	8.43
ssd_sp[16x4]	7	luma_vss_10[8x4]	7.84	luma_vss_10[4x8]	8.49
luma_vps_12[4x8]	7	luma_vps_10[4x16]	7.87	luma_inv_quant_12b[16x16]	8.49
ssd_pp[32x4]	7.02	luma_vsp_10[4x4]	7.88	luma_inv_quant_10b[32x16]	8.51
luma_vpp_10[4x4]	7.15	luma_inv_quant_10b[64x64]	7.93	chroma_vss_12[16x2]	8.64
luma_vpp_12[4x4]	7.17	add_avg_10[16x2]	7.95	luma_inv_quant_12b[16x64]	8.65
satd_pp[32x4]	7.21	luma_vsp_12[8x4]	7.97	luma_inv_quant_12b[32x16]	8.66
sad_sp[32x16]	7.26	block_zero[32x16]	7.98	luma_inv_quant_10b[32x32]	8.66
luma_vsp_10[4x8]	7.32	luma_inv_quant_10b[16x32]	8.06	luma_inv_quant_10b[16x64]	8.69
luma_vpp_12[4x16]	7.42	luma_vsp_10[4x16]	8.08	luma_inv_quant_12b[16x32]	8.71
luma_vpp_12[4x32]	7.42	luma_inv_quant_10b[64x32]	8.09	chroma_vpp_10[16x4]	8.74
block_zero[32x8]	7.42	luma_vps_10[8x4]	8.11	luma_vss_10[4x32]	8.76
rdo_sign_reapply[64x64]	7.43	satd_pp[16x8]	8.12	rdo_sign_reapply[64x16]	8.84
satd_pp[64x8]	7.48	rdo_sign_reapply[32x4]	8.12	luma_hpp_12[1]	8.88
luma_inv_quant_10b[16x8]	7.48	luma_vsp_12[4x16]	8.13	satd_sp[64x16]	8.91
satd_pp[32x8]	7.52	ssd_pp[16x2]	8.14	luma_vss_12[4x8]	8.96
rdo_sign_reapply[16x64]	7.55	rdo_sign_reapply[32x32]	8.14	luma_vss_12[8x8]	8.96
luma_vss_12[32x4]	7.57	ssd_ss[16x2]	8.15	luma_vsp_12[4x8]	8.98
chroma_hps_10[2]	7.61	luma_vpp_10[4x8]	8.17	chroma_vss_10[16x2]	8.99
sad_sp[16x64]	7.65	ssd_pp[16x8]	8.18	luma_inv_quant_10b[64x16]	9.01
block_zero[32x4]	7.65	rdo_sign_reapply[32x8]	8.18	satd_sp[16x4]	9.02
luma_vsp_12[16x4]	7.71	chroma_vps_10[16x2]	8.23	luma_inv_quant_10b[32x64]	9.04
rdo_sign_reapply[16x16]	7.72	chroma_hps_10[5]	8.24	rdo_sign_reapply[16x8]	9.04
luma_vps_12[4x4]	7.74	satd_sp[32x4]	8.25	ang_fast_copy[16x16]	9.06
add_clip_10[16x2]	7.75	add_clip_12[16x32]	8.34	luma_vss_10[8x8]	9.09
luma_inv_quant_10b[8x64]	7.76	rdo_sign_reapply[32x64]	8.34	add_clip_10[16x4]	9.09
luma_inv_quant_10b[64x8]	7.77	satd_sp[32x64]	8.35	add_clip_10[16x64]	9.1
luma_vps_10[4x8]	7.79	luma_inv_quant_10b[16x16]	8.35	block_zero[32x64]	9.11
luma_vps_10[4x4]	7.8	luma_vpp_12[8x4]	8.4	luma_vsp_10[8x16]	9.13
chroma_vss_10[32x4]	9.15	chroma_vsp_10[16x2]	9.7	luma_vpp_12[4x8]	10.33
luma_inv_quant_12b[64x16]	9.16	luma_inv_quant_12b[64x8]	9.73	luma_vps_12[16x4]	10.33
luma_vss_12[4x32]	9.21	luma_vps_12[16x64]	9.75	add_clip_10[16x8]	10.33
luma_vss_12[8x4]	9.22	ang_fast_copy[16x4]	9.75	add_clip_12[64x8]	10.38
luma_vss_12[4x16]	9.23	luma_inv_quant_12b[64x64]	9.76	luma_vsp_10[4x32]	10.39
luma_vpp_12[16x8]	9.23	satd_pp[32x32]	9.79	satd_sp[32x8]	10.4
luma_inv_quant_12b[32x64]	9.24	satd_pp[32x16]	9.81	luma_vss_12[16x4]	10.4
luma_vps_10[32x4]	9.25	luma_vps_10[16x4]	9.81	chroma_vpp_10[64x32]	10.41
luma_vpp_10[8x4]	9.29	ang_fast_copy[32x64]	9.81	luma_vpp_12[32x4]	10.44
luma_vsp_10[16x4]	9.29	ssd_pp[16x4]	9.89	satd_pp[16x64]	10.46
luma_vps_10[4x32]	9.3	luma_inv_quant_10b[32x8]	9.9	luma_vpp_10[16x64]	10.5
block_zero[16x2]	9.3	rdo_sign_reapply[32x16]	9.92	luma_hpp_10[1]	10.51
luma_inv_quant_12b[64x32]	9.3	luma_vpp_10[4x32]	9.97	luma_vpp_12[32x8]	10.52
add_avg_12[16x4]	9.32	luma_vps_10[8x8]	9.97	luma_vss_10[8x64]	10.53
luma_vps_12[4x16]	9.39	luma_vps_12[32x32]	10.01	add_avg_10[32x16]	10.61
ang_fast_copy[16x32]	9.39	luma_vps_12[32x64]	10.01	luma_vss_10[8x16]	10.61
ang_fast_copy[32x32]	9.39	add_clip_12[16x64]	10.1	luma_vpp_12[16x4]	10.61
add_avg_10[16x4]	9.42	luma_vpp_10[4x16]	10.11	luma_hps_10[1]	10.65
luma_vps_12[4x32]	9.43	luma_vps_12[8x4]	10.11	ang_fast_copy[32x4]	10.66
luma_vsp_10[16x8]	9.44	chroma_vps_10[16x4]	10.12	satd_sp[64x64]	10.67
satd_sp[64x8]	9.45	luma_vsp_12[32x8]	10.12	luma_vpp_12[64x32]	10.68
block_zero[32x32]	9.47	luma_vsp_10[8x4]	10.13	luma_vss_10[16x64]	10.7
luma_vss_10[4x16]	9.51	luma_vsp_12[32x32]	10.13	luma_vpp_10[16x4]	10.75
rdo_num_nonzero[32x4]	9.51	ang_fast_copy[64x32]	10.16	satd_sp[16x16]	10.76
rdo_sign_reapply[16x32]	9.52	luma_vss_10[32x8]	10.21	luma_vsp_10[64x16]	10.81
luma_vpp_10[32x64]	9.55	rdo_num_nonzero[16x16]	10.23	chroma_vps_10[32x4]	10.85
rdo_sign_reapply[64x8]	9.55	luma_vss_10[32x4]	10.24	luma_vss_10[16x4]	10.85
luma_inv_quant_10b[32x4]	9.59	luma_vpp_10[32x4]	10.27	luma_vpp_10[16x8]	10.85
chroma_vpp_10[16x2]	9.62	ang_fast_copy[32x16]	10.3	satd_pp[16x16]	10.89
add_clip_10[16x32]	9.68	satd_pp[64x64]	10.32	ssd_ss[16x4]	10.9

Primitive	IPC Gain	Primitive	IPC Gain	Primitive	IPC Gain
rdo_num_nonzero[16x8]	10.94	chroma_vps_10[32x32]	11.58	ssd_ss[32x4]	12.13
satd_sp[32x16]	11	chroma_vpp_12[16x2]	11.59	luma_vsp_10[64x32]	12.15
chroma_hps_10[3]	11	luma_hps_10[4]	11.6	luma_vpp_10[8x8]	12.17
luma_vsp_10[16x64]	11	chroma_vsp_10[32x16]	11.63	add_clip_10[16x16]	12.21
ang_fast_copy[64x16]	11.01	luma_vsp_12[16x64]	11.64	chroma_vss_12[16x16]	12.24
ssd_sp[16x8]	11.04	satd_pp[32x64]	11.66	chroma_vpp_12[32x64]	12.26
satd_sp[16x32]	11.04	luma_vps_10[32x32]	11.68	luma_vss_12[8x32]	12.27
chroma_vpp_12[16x4]	11.04	luma_vsp_12[8x8]	11.69	ssd_pp[32x32]	12.28
luma_vsp_12[32x4]	11.04	luma_vps_10[8x32]	11.71	luma_vpp_12[32x64]	12.28
luma_vsp_12[8x64]	11.05	ssd_pp[32x8]	11.72	add_avg_12[16x8]	12.3
luma_inv_quant_12b[32x8]	11.05	chroma_vss_12[16x4]	11.75	chroma_vss_10[16x4]	12.33
satd_pp[16x32]	11.08	luma_vps_12[16x32]	11.75	luma_vsp_10[8x8]	12.38
luma_vps_10[32x64]	11.08	luma_vps_10[16x64]	11.79	ssd_sp[64x16]	12.48
luma_vsp_10[16x16]	11.1	rdo_num_nonzero[32x8]	11.8	luma_vps_12[64x64]	12.5
ang_fast_copy[64x64]	11.1	rdo_num_nonzero[64x8]	11.8	chroma_vsp_10[16x32]	12.51
satd_pp[64x32]	11.17	luma_vps_12[32x4]	11.81	luma_vss_12[16x64]	12.51
chroma_vpp_12[64x16]	11.17	add_avg_10[16x8]	11.82	ssd_sp[32x4]	12.53
satd_pp[64x16]	11.18	chroma_vsp_10[16x4]	11.82	chroma_vpp_12[32x8]	12.53
chroma_vpp_12[64x32]	11.2	luma_vps_12[32x8]	11.82	block_zero[16x32]	12.53
add_clip_12[16x4]	11.2	block_zero[16x16]	11.85	luma_vss_12[32x8]	12.55
satd_sp[16x8]	11.23	luma_vss_12[16x16]	11.87	satd_sp[16x64]	12.58
luma_vps_10[64x32]	11.3	luma_vss_12[64x64]	11.88	luma_vss_10[64x8]	12.58
luma_vps_10[64x64]	11.35	luma_vss_12[8x64]	11.89	chroma_vpp_12[16x16]	12.64
luma_vss_12[32x16]	11.42	chroma_vpp_10[32x64]	11.9	add_clip_12[32x16]	12.64
luma_vsp_12[4x32]	11.43	add_clip_12[16x16]	11.91	chroma_vsp_10[32x4]	12.68
luma_vsp_12[16x8]	11.44	add_avg_12[32x4]	11.92	chroma_vpp_10[16x64]	12.69
add_clip_12[16x8]	11.47	luma_vss_12[8x16]	11.93	luma_vss_12[16x8]	12.72
chroma_hps_10[4]	11.48	luma_vss_10[16x8]	11.93	chroma_vss_12[32x4]	12.73
add_clip_10[64x16]	11.48	chroma_vps_10[64x16]	11.95	luma_vpp_12[16x16]	12.74
add_clip_10[32x4]	11.52	add_clip_12[64x32]	12.1	luma_vps_12[8x32]	12.78
luma_vss_10[32x16]	12.8	luma_vps_12[64x32]	13.27	luma_vps_12[16x16]	13.76
satd_sp[64x32]	12.81	luma_hpp_12[3]	13.3	luma_vps_12[16x8]	13.78
luma_hpp_12[2]	12.82	chroma_vsp_10[32x32]	13.31	luma_vsp_10[32x16]	13.81
luma_vss_12[16x32]	12.83	luma_vps_10[32x8]	13.31	add_avg_10[16x64]	13.84
chroma_vps_10[16x64]	12.84	luma_vss_10[32x64]	13.31	chroma_vpp_12[32x4]	13.84
add_clip_10[32x64]	12.84	luma_vpp_12[8x8]	13.32	luma_vss_12[64x32]	13.84
ang_fast_copy[16x8]	12.86	satd_sp[32x32]	13.34	ssd_pp[16x32]	13.87
chroma_vsp_10[32x64]	12.87	luma_vps_10[8x16]	13.37	luma_vsp_12[16x32]	13.87
add_clip_12[32x32]	12.87	luma_vss_10[64x16]	13.37	luma_vss_10[64x64]	13.91
add_avg_12[16x32]	12.89	luma_vps_12[8x64]	13.41	luma_vsp_10[32x8]	13.94
add_avg_12[64x64]	12.93	luma_vss_10[64x32]	13.41	luma_vsp_10[64x8]	13.94
chroma_vss_10[16x16]	12.95	chroma_vss_12[64x64]	13.43	chroma_vsp_10[16x8]	13.95
chroma_vss_12[64x8]	12.97	rdo_num_nonzero[16x32]	13.44	luma_vss_12[64x8]	13.95
ssd_sp[32x8]	12.98	chroma_vss_10[64x64]	13.46	chroma_vpp_12[16x8]	14.01
add_clip_12[32x4]	12.98	luma_vpp_12[16x32]	13.46	luma_vpp_12[32x32]	14.01
luma_vss_10[16x32]	13	chroma_vss_12[64x32]	13.47	chroma_vsp_10[32x8]	14.07
luma_vps_10[16x16]	13.03	luma_vpp_10[32x32]	13.49	luma_vsp_10[8x32]	14.09
luma_vps_12[8x8]	13.04	luma_vss_12[32x32]	13.52	luma_vsp_12[16x16]	14.09
chroma_vpp_10[64x64]	13.05	block_zero[16x64]	13.56	add_clip_10[32x8]	14.1
luma_vss_12[64x16]	13.05	luma_vss_10[8x32]	13.57	ssd_pp[64x64]	14.16
luma_vsp_12[8x16]	13.07	luma_vps_10[16x8]	13.61	chroma_vpp_10[16x8]	14.19
luma_vss_10[16x16]	13.1	luma_vps_12[32x16]	13.62	chroma_vpp_10[32x16]	14.2
luma_vpp_10[64x8]	13.13	block_zero[16x8]	13.63	ssd_pp[32x16]	14.21
ssd_ss[16x8]	13.14	luma_vsp_10[32x32]	13.64	chroma_vps_10[16x32]	14.23
add_avg_10[32x4]	13.14	luma_vpp_12[8x16]	13.65	luma_vsp_12[8x32]	14.23
luma_hpp_10[2]	13.15	ang_fast_copy[32x8]	13.68	luma_vps_12[64x16]	14.25
add_clip_10[32x32]	13.22	chroma_vsp_10[64x64]	13.69	ssd_ss[32x16]	14.26
chroma_vsp_10[16x64]	13.24	chroma_vsp_10[16x16]	13.72	luma_vpp_10[64x16]	14.33
luma_vps_10[32x16]	13.26	chroma_vss_10[16x8]	13.73	chroma_vss_10[64x16]	14.34
chroma_vps_10[64x64]	13.27	luma_vps_10[8x64]	13.74	luma_vpp_10[8x32]	14.35

Primitive	IPC Gain	Primitive	IPC Gain	Primitive	IPC Gain
luma_vsp_12[64x32]	14.35	luma_vpp_10[32x8]	14.98	add_clip_10[64x64]	15.52
ssd_ss[32x8]	14.41	luma_hps_10[3]	15.01	add_clip_12[32x8]	15.54
luma_vpp_10[16x16]	14.43	luma_hpp_10[4]	15.01	ssd_ss[32x32]	15.56
ssd_sp[32x16]	14.44	chroma_vps_10[32x8]	15.02	chroma_vps_10[16x16]	15.56
chroma_vps_10[16x8]	14.44	add_clip_10[64x8]	15.07	chroma_vss_10[32x16]	15.58
chroma_vpp_10[32x4]	14.45	chroma_vpp_12[32x32]	15.09	chroma_vss_12[32x64]	15.58
luma_vpp_12[8x32]	14.49	luma_vsp_12[64x64]	15.09	chroma_vpp_12[32x16]	15.59
luma_vps_10[64x16]	14.55	chroma_vss_12[32x32]	15.1	chroma_vsp_10[64x16]	15.59
add_avg_12[32x8]	14.56	chroma_vps_10[32x16]	15.13	ssd_sp[32x32]	15.61
luma_hpp_10[3]	14.59	ssd_sp[16x16]	15.16	luma_hpp_12[4]	15.66
chroma_vss_10[32x8]	14.6	luma_hps_10[2]	15.16	ssd_ss[64x32]	15.68
add_avg_12[16x16]	14.61	luma_vpp_10[8x16]	15.18	chroma_vsp_10[64x32]	15.68
ssd_pp[16x16]	14.66	chroma_vss_10[32x64]	15.19	luma_vpp_10[32x16]	15.7
add_avg_12[32x32]	14.66	chroma_vss_12[64x16]	15.24	chroma_vpp_10[32x8]	15.72
luma_vsp_12[64x8]	14.66	chroma_vps_10[32x64]	15.27	ssd_sp[64x32]	15.75
chroma_vss_12[16x8]	14.7	luma_vsp_10[32x64]	15.29	rdo_num_nonzero[16x64]	15.77
add_clip_12[32x64]	14.71	ssd_ss[64x16]	15.33	chroma_vps_10[64x8]	15.83
luma_vsp_12[32x16]	14.72	chroma_vpp_10[16x32]	15.33	add_avg_10[32x32]	15.86
luma_vps_10[64x8]	14.74	ssd_ss[16x16]	15.38	rdo_num_nonzero[32x16]	15.89
luma_vpp_12[64x16]	14.74	ssd_sp[64x8]	15.39	chroma_vss_10[64x8]	15.94
chroma_vss_10[64x32]	14.75	ssd_pp[64x16]	15.39	luma_vpp_10[16x32]	15.94
chroma_vpp_12[64x64]	14.76	luma_vpp_10[64x64]	15.39	luma_vsp_12[64x16]	15.94
luma_vpp_12[32x16]	14.8	luma_vsp_10[16x32]	15.4	chroma_vpp_10[32x32]	16.05
chroma_vpp_12[16x64]	14.84	add_avg_12[32x16]	15.41	add_clip_12[64x64]	16.12
luma_vpp_10[8x64]	14.87	add_avg_10[16x16]	15.43	add_avg_12[16x64]	16.14
luma_vps_10[16x32]	14.89	chroma_vss_12[32x8]	15.44	ssd_pp[64x32]	16.27
luma_vps_12[64x8]	14.91	chroma_vpp_10[64x16]	15.44	ssd_sp[32x64]	16.35
chroma_vpp_10[64x8]	14.97	chroma_vsp_10[64x8]	15.5	ssd_pp[64x8]	16.38
chroma_vpp_12[64x8]	14.97	chroma_vpp_10[16x16]	15.52	add_avg_10[16x32]	16.42
add_clip_10[32x16]	14.97	add_clip_12[64x16]	15.52	luma_vss_10[32x32]	16.48
luma_vsp_12[32x64]	16.57	ssd_sp[16x64]	17.14	rdo_num_nonzero[64x32]	17.96
chroma_vss_10[32x32]	16.58	ssd_pp[16x64]	17.21	chroma_vss_12[16x64]	18.43
ssd_sp[16x32]	16.66	luma_vsp_10[8x64]	17.23	add_avg_12[64x8]	18.44
add_avg_10[32x8]	16.68	add_avg_12[64x16]	17.25	chroma_vps_10[64x32]	18.49
chroma_vpp_12[16x32]	16.73	ssd_ss[16x64]	17.31	add_avg_10[64x64]	19.13
chroma_vss_12[32x16]	16.75	rdo_num_nonzero[64x16]	17.44	chroma_vss_10[16x32]	19.2
ssd_pp[32x64]	16.83	add_avg_10[64x8]	17.51	rdo_num_nonzero[32x64]	19.28
luma_vss_12[32x64]	16.84	luma_vpp_12[8x64]	17.57	add_avg_10[64x32]	19.31
luma_vpp_12[64x8]	16.92	luma_vsp_10[64x64]	17.59	luma_vpp_12[16x64]	19.67
add_avg_10[32x64]	16.97	rdo_num_nonzero[32x32]	17.62	block_zero[16x4]	19.78
add_clip_10[64x32]	16.98	luma_vpp_12[64x64]	17.71	ssd_ss[16x32]	19.84
luma_vps_12[8x16]	17.02	add_avg_12[32x64]	17.91	rdo_num_nonzero[64x64]	19.85
chroma_vss_12[16x32]	17.05	chroma_vss_10[16x64]	17.94	ssd_ss[32x64]	21.72
add_avg_12[64x32]	17.11	add_avg_10[64x16]	17.96	luma_vpp_10[64x32]	22.48
ssd_ss[64x8]	23.33				





